PETROLOGY AND GEOCHEMISTRY OF SOME ARCHEAN METAMORPHIC ROCKS NEAR YELLOWKNIFE DISTRICT OF MACKENZIE

A thesis

submitted to the

School of Graduate Studies

University of Ottawa

in partial fulfilment

of the requirements for the Degree of

DOCTOR OF PHILOSOPHY

in Geology

by

Dayananda Choudari Kamineni

April 1973

"Because of their antiquity, as well as metamorphic state, Archean suites were considered by most geologists as unsuitable for petrological and geochemical investigations"

- Glikson (1970)

ABSTRACT

Archean meta greywacke and meta argillite of the Yellowknife Supergroup show a range of metamorphic grade from greenschist to hornblende-hornfels facies. They contain various combinations and proportions of the minerals, cordierite, biotite, garnet, gedrite, sillimanite, andalusite, muscovite and cummingtonite at higher grades; and biotite, chlorite and muscovite in the lower grades. East of Sparrow Lake, three metamorphic isograds can be located, namely the cordierite, gedrite and sillimanite isograds.

The character of the mineral assemblages suggests that metamorphism is of the low pressure type.

A considerable amount of mineral growth occurred during an early period of regional deformation and metamorphism. However, an increase in amounts and decrease in grain size of cordierite toward the Sparrow Lake Granite Pluton indicates that this mineral grew in response to contact as well as regional metamorphism. The sillimanite isograd lies close to the Sparrow Lake Pluton and is parallel to its contact, which suggests that this mineral developed due to a contact effect.

Information on the chemical composition of the rocks indicates that different mineral assemblages developed depending upon the original bulk composition and the physical conditions of metamorphism. The cordierite-gedrite-bearing rocks formed in potash-poor lower horizons of the greywacke beds. Different mineral assemblages define different areas in a compositional field obtained by plotting K_2O versus $(MgO + FeO + MnO) \;/\; ((Al_2O_3 - (Na_2O + 2CaO))$.

The chemical composition of biotite, cordierite, gedrite, cummingtonite, plagioclase, andalusite and garnet does not vary greatly, presumably due to a limited range in original rock composition. The observed compositional variation in biotite and cordierite may be related to differences in mineral paragenesis rather than metamorphic grade. The garnets are compositionally zoned with Mn concentrated at the centres and Fe at the rims. In gedrite most of the Mg is evidently present in the M_2 site along with Al.

The partitioning of Fe, Mg and Mn between coexisting cordierite, biotite, and gedrite shows a regular trend indicating that exchange equilibrium with reference to these elements was established during metamorphism. The distribution of Fe, Mg, and

Mn between garnet rims and other ferromagnesian minerals is dependent on the Ca content of the garnet.

TABLE OF CONTENTS

LIST OF FIGURES

LIST OF TABLES

LIST OF PLATES

INTRODUCTION

The Yellowknife-Beaulieu region which lies northeast of the town of Yellowknife is part of the Slave structural Province of the Canadian Shield. The area is underlain by different lithological units of Precambrian age. Major rock units of the area consist of metasediments, metavolcanics, granitic rocks and diabase; the granitic rocks comprise about fifty percent, the metasediments about thirty percent of the total.

Location, Accessibility and Physiography

The study area lies within the Yellowknife-Beaulieu area, about 50 km northeast of Yellowknife. The area covers about 100 square miles and lies within an area that is bounded by latitudes $62^{o}30'$ and $62^{o}45'$ and longitudes $113^{o}00'$ and $113^{o}45'$ (Fig. 1).

Access to the area is achieved by light aircraft. Recently a road has been constructed from Yellowknife to Tibbit Lake, immediately south of the study area.

The average surface elevation of the Yellowknife-Beaulieu area is about 1300 feet above sea level. Areas of high ground are in general underlain

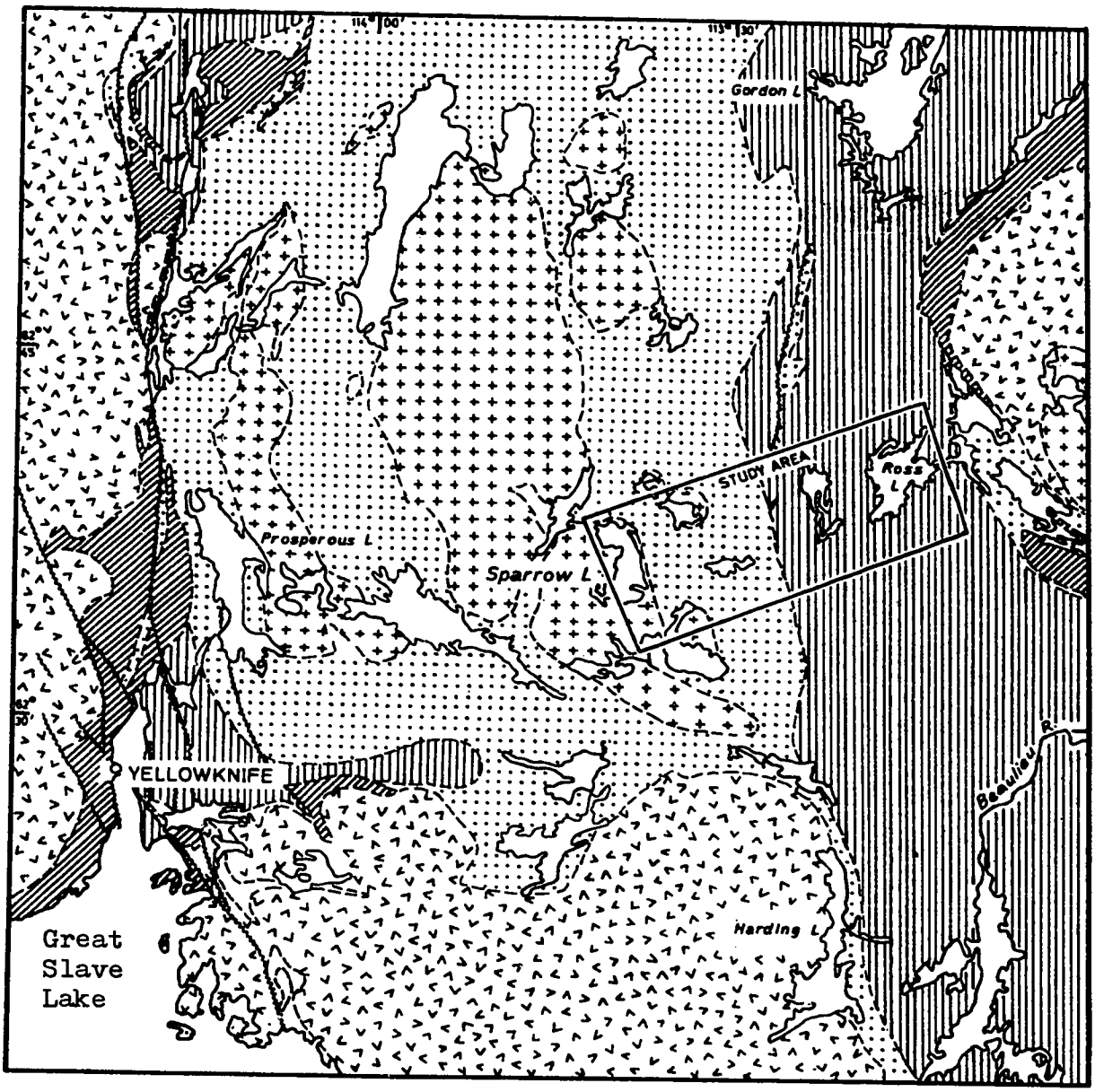

Figure 1. Location Map, Geology compiled by Y.O. Fortier, 1946 and R. Kretz, 1967.

by granitic or volcanic rocks, and the maximum relief is about 300 feet.

Bed rock is well exposed in most of the area, especially where the terrain is rugged. Exposure is poor in the low lying areas due to swamps and glacial debris.

Almost all the hills have a rounded outline, imposed by the Pleistocene glaciation. Several glacial features such as striae, drumlins and roches moutonnées are commonly observed. Numerous lakes of various sizes occur throughout the area, most being connected by rivers and streams that drain ultimately into Great Slave Lake. Drainage in the Yellowknife-Beaulieu region is dominated by the Cameron and Beaulieu river systems.

Geological Setting

On the basis of geological investigations, mainly by the Geological Survey of Canada, several rock units have been defined. The oldest rocks consist of a volcanic and sedimentary succession (Henderson and Jolliffe, 1941; Jolliffe, 1942, 1946). These two lithological units together were originally known as the Point Lake-Wilson Island Group (Stockwell, 1933) but were later renamed the Yellowknife Group (Henderson, 1938; Jolliffe, 1938; Lord, 1939);

recently the Yellowknife Group was raised to Supergroup status (Henderson, 1970).

All the rocks of the Supergroup have been complexly folded. According to Henderson (1943) and Fortier (1946), folds developed in two phases; the first was characterized by the formation of upright isoclinal folds and the second by the wrapping of these folds about near vertical fold axes.

A wide spectrum of intrusive rocks ranging from granite to gabbro occur, granites and granodiorites of batholithic dimensions being the most abundant. Other varieties such as syenites, diorites and gabbros occur as smaller bodies. Diabase dykes with north-south and east-west trends comprise the youngest rocks in the region. Some alkaline intrusives such as nepheline syenites occur near Caribou Lake (A. Davidson, personal communication); they may be of Proterozoic age.

Chronologically, the Slave Province compares with the Superior Province of the Shield in that both regions were affected by the Kenoran Orogeny (Stockwell, 1964). Evidence for a prior orogeny is found in the presence of granitic pebbles in a

conglomerate that lies at the boundary of volcanics and the sediments of the Yellowknife Supergroup (Stockwell, 1933; Jolliffe, 1942).

Previous Work

Since the early part of this century the Precambrian Geology around Yellowknife has attracted several workers, mainly due to the gold, uranium, and rare mineral potential of the area.

Systematic geological mapping was undertaken by the Geological Survey of Canada, and a compilation map on the Beaulieu River Area was published in 1941.

Many aspects of the area have been investigated by various workers. The greenstone belt at Yellowknife was extensively examined by Henderson and Brown (1952) from a structural and mineralization view point, whilst Baragar (1966) and Boyle (1961) studied the geology and geochemistry from different angles. Metamorphism and mineralization were studied by Folinsbee (1941). Sedimentological investigations were carried out by Henderson (1970). The pegmatites were examined by Hutchinson (1955) and Kretz (1967). In addition, some radiometric dating was done by the University of Alberta isotopic research group (see Folinsbee et al. 1968; Green and Baadsgaard, 1971).

Recent and current projects in the area include the preparation of a cross-country airborne spectrometric profile (Darnley et al. 1970), colour aerial photography (Slany, 1971), geological mapping to revise the Yellowknife and Hearne Lake map sheets (Henderson et al. 1971) and granite studies (Davidson, 1971).

Problems

From the previous geological mapping various metasedimentary belts were identified (Henderson, 1938, 1943, Jolliffe, 1942). These consist of argillites and slates, in which cordierite and andalusite become present at higher grades of metamorphism. Early workers considered that these minerals were products of thermal metamorphism associated with the granitic intrusion. However, the work of Davidson (1967) in the Benjamin Lake Area to the east indicates that the rocks have undergone regional as well as contact metamorphism.

On the basis of geological and geochronological work, Folinsbee et al. (1968) and Green and Baadsgaard (1971) proposed an island arc model starting with an oceanic crustal basement; however unequivocal evidence for this is lacking, as the

boundary between the Ross Lake granodiorite and the adjacent volcanic rocks is not an intrusive contact; also the detailed sedimentological work by Henderson (1970) suggests a sialic crust in the area.

Scope of the Present Work

In the metasedimentary rocks, at higher grades, only the isograd for cordierite had been delineated by previous workers (Henderson and Jolliffe, 1941). The aim of the present work was to delineate other zones such as garnet, gedrite and cummingtonite, whose occurrences have been pointed out by Kretz (1967, and oral communication).

Although several aspects of the geology had been studied in detail very little geochemical work on the metasedimentary rocks had been done when the present study was initiated. In view of this an attempt was made to collect geochemical data and to explain mineral assemblages in terms of differences in bulk composition, oxidation state of iron, and metamorphic grade. Special attention was directed towards the origin of the cordierite-gedrite-bearing rocks.

The extensive development of cordierite provides an opportunity to study chemical equilibria between

this mineral and the other coexisting phases such as biotite, garnet and gedrite. In the subsequent chapters some chemical reactions are suggested to explain the development of these minerals; some criteria regarding equilibrium in metamorphic rocks are also discussed.

Method of Investigation

Systematic geological mapping and sample collection in the study area (Fig. 2) was carried out during the summer of 1969. Aerial photographs were used, outcrops being located by pace and compass traverses tied to recognizable points on the photographs. Landmarks such as lakes proved helpful in locating the outcrops. Traverses were run approximately at half mile intervals in most cases. A few additional samples were collected in the northern part of the study area during the 1971 field season, while the writer was working for the Geological Survey of Canada.

Four hundred samples were collected, and about three hundred thin sections were examined to identify the mineral assemblages and to locate the metamorphic zones. Textural relations that indicate the paragenetic relations were recorded. Several samples free of inhomogeneities and retrograde

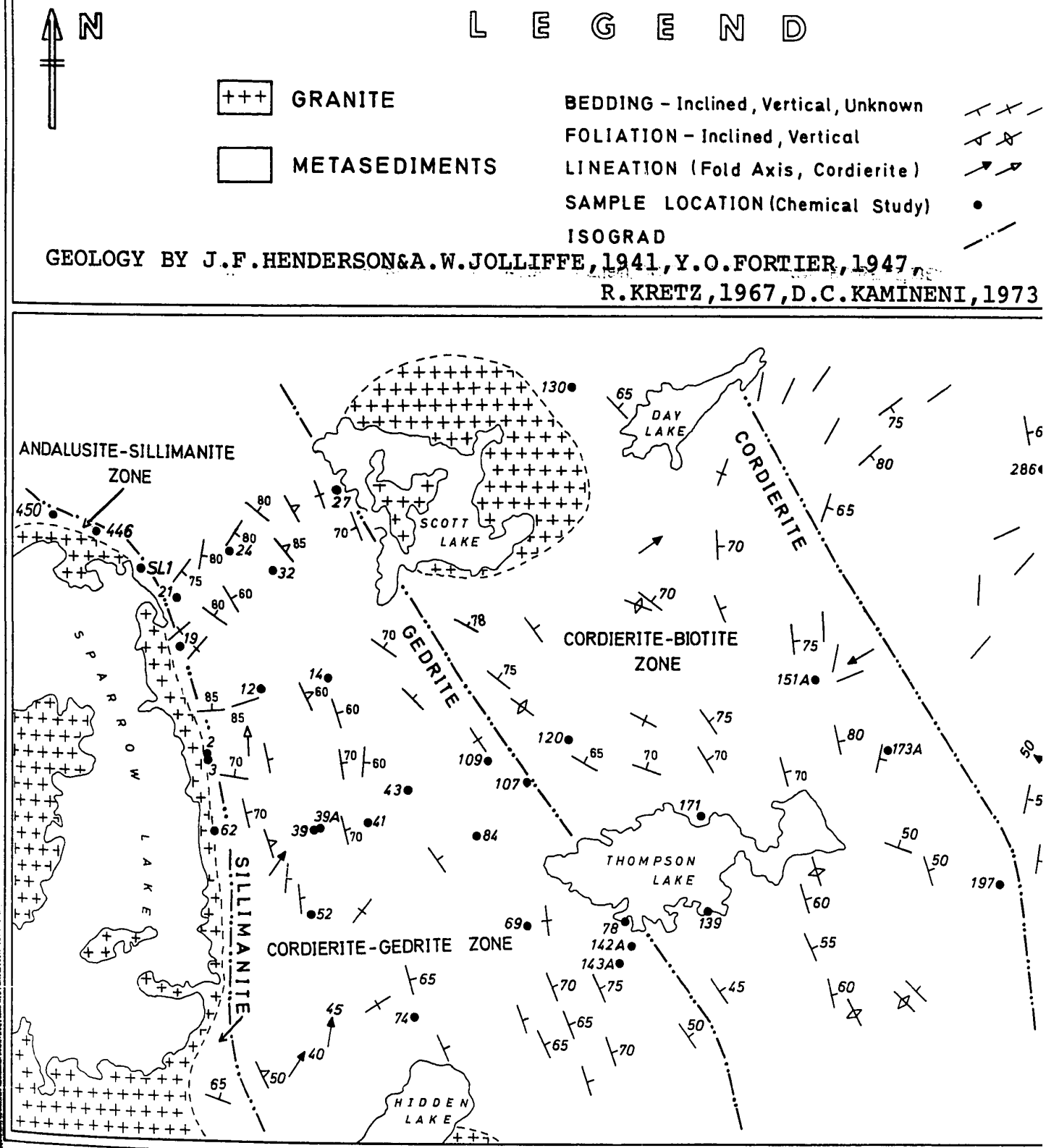

Figure 2. Geological M

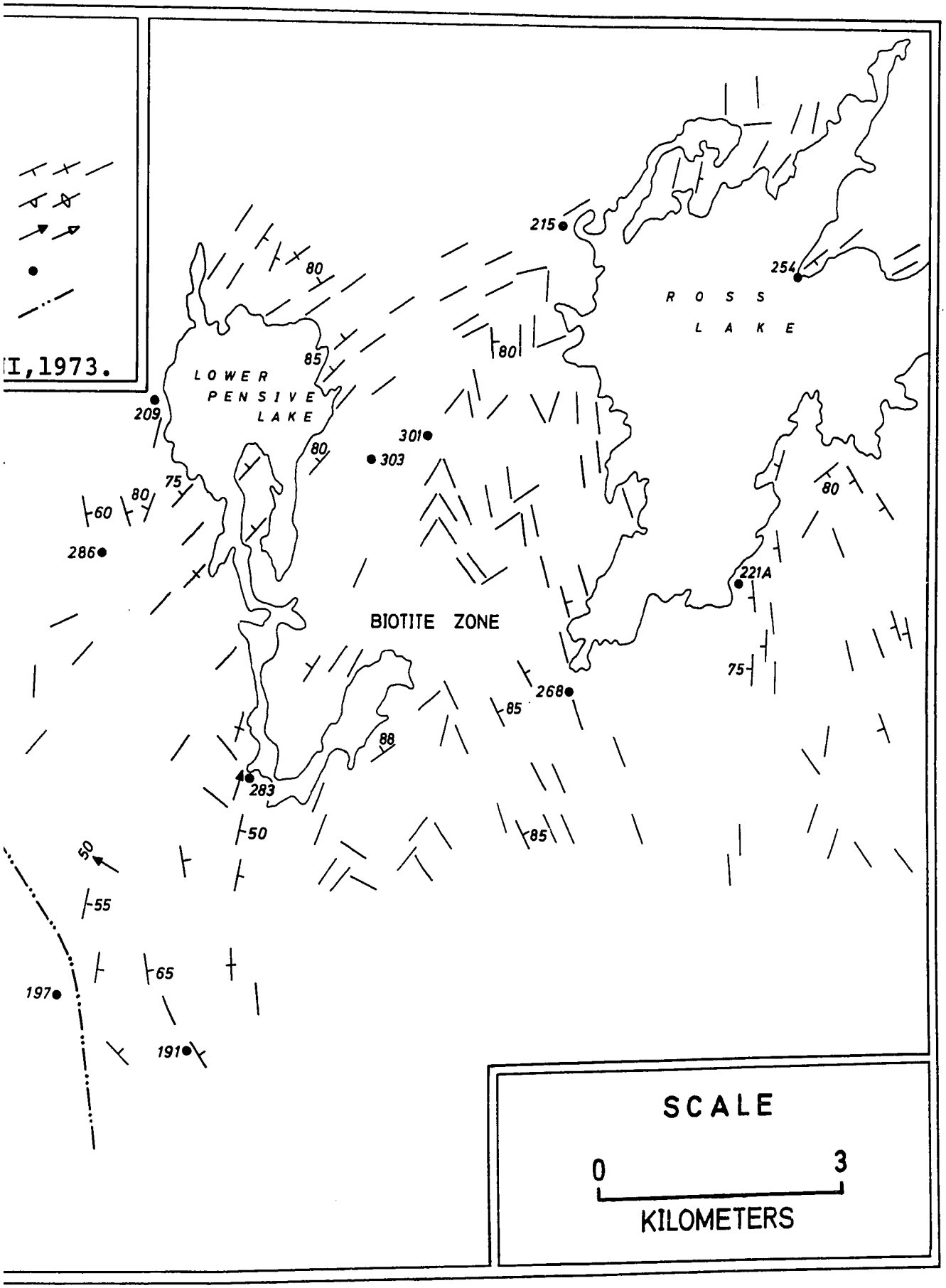
I, 1973.
LOWER PENSIVE LAKE
ROSS LAKE
BIOTITE ZONE
215
254
209
301
303
286
221A
268
283
197
191
80
85
75
60
50
55
65
88
SCALE
0
3
KILOMETERS

cal Map

phenomena were chosen for chemical study.

Mineral separation was carried out on the selected samples and the separation techniques as well as the analytical procedure used for both rock and mineral analyses are described in the appendices.

Regional Stratigraphy

Although the lithology in Archean terranes may be simple, the age relations are not as straight forward as those of the younger geological systems. Stratigraphic relationships in these areas are often obscured by polyphase deformation, and by metamorphism and magmatism. One of the main problems lies in the recognition of the basement rocks. The general geological succession on the basis of previous work, mainly by the Geological Survey of Canada is given in Table 1.

The Yellowknife Supergroup comprises meta-volcanics at the base, which are well exposed near Yellowknife town and Cameron River. According to Baragar (1966) the geochemical trends of these lavas are those of tholeiitic magma, the deviations towards calc-alkaline trends being explained by contamination of crustal material during ascent. Near Yellowknife town, a variable degree of meta-morphism is observed in these rocks, ranging from

Table 1: Geological Succession

Post-Kenoran	Diabase dykes and sills		Medium to coarse grained, augite, plagioclase and occassionally olivine diabase
Kenoran	Intrusive rocks: Granite, granodiorite, gabbro and pegmatite		Massive muscovite-biotite-granite, biotite-epidote-perthitic microcline-plagioclase-granodiorite. May contain hornblende, simple and complex pegmatites.
Pre-Kenoran Yellowknife Supergroup	Metasediments	Most altered	Gedrite, cordierite, andalusite, and garnet schists and hornfelses.
		Least altered	Greywacke, argillite and impure quartzite.
	Felsic volcanics		Cummingtonite schists, sericite and chlorite schists.
	Other sediments		Conglomerate with mafic volcanic pebbles, impure limestone with skarn minerals, forsterite marble.
	Meta volcanics		Spillitic basalt, (greenstones) metamorphosed to greenschist to amphibolite facies; may also contain at the base or within iron formations.
	Ross Lake Granodiorite?		Foliated muscovite-biotite-perthitic microcline-plagioclase gneiss

greenschist facies to amphibolite facies (Boyle, 1961). Within the metavolcanics, and at the contact of volcanics-granodiorite, iron formation containing quartz-grunerite-magnetite and probably some minnesotaite, may be found in some localities (personal observation, 1971).

The upper part of the volcanic succession, east of Ross Lake (Fig. 1), contains felsic volcanics (Henderson et al. (1971), and is noted to comprise sericitic and cummingtonite schists (personal observation, 1971). The felsic volcanics are followed by a thick succession of sediments that are widely distributed in the Slave Province. McGlynn and Henderson (1970) subdivided the meta-sedimentary rocks into three units: 1 conglomerates, 2. greywacke-mudstone and 3. other sediments. Beds of the greywacke-mudstone subdivision of the Super-group are most abundant and these are the only type that are found in the study area. The greywacke-mudstone sequence exhibits the characteristics of a typical turbidite cycle of Bouoma (Henderson, 1970). Several primary features such as graded bedding, flute casts, load balls and slump structures can be seen.

The granitic rocks which form a major litho-

logical unit can be broadly subdivided into granodiorites and granites. The former are essentially concentrated in the regions lying to the southeast and southwest of Yellowknife town, and near Ross Lake, immediately to the east of study area (Fig. 1). On the basis of petrological and field observations, Baragar (1966) considered the Ross Lake granodiorite as the basement to the Yellowknife Supergroup.

The muscovite-biotite granitic rocks which are unanimously considered to have been intruded during the late Kenoran Orogeny, form another important unit of the granitic suite. These granites, near Sparrow Lake (Fig. 2) are composed of quartz, plagioclase, potash feldspar, biotite, muscovite and apatite. A series of samples collected by Kretz (1967) showed this pluton to be homogeneous with respect to mineral constituents. However, modal variations in mineralogy at the contact and away from it, were noted by him. Near the contact, depletion in potash feldspar and an increase of muscovite, which is probably a reflection of differences in water pressure, are recorded. In addition, the presence of tourmaline is also noted at the contact.

Petrographically, the Sparrow Lake pluton contains discrete grains of plagioclase (An_{10}),

potash feldspar and quartz. The size of these mineral grains range from 2 to 4 mm in diameter, with potash feldspar grains reaching a size up to 10 mm (Kretz, 1967). The potash feldspar grains show perthitic texture in some cases and 'cross-hathed' twins in most cases. Plagioclase possesses albite twins. Aggregates of muscovite and biotite, ranging in size from 1 to 2 mm in greatest dimension, are found throughout the rock. Chlorite may be observed replacing biotite. In plagioclase and muscovite crystals near the margin of the pluton, Kretz (1967) has reported some signs of strain, indicated by bent albite twin planes and cleavage planes of muscovite.

Another important lithological unit in the area is pegmatite. Pegmatite bodies are found in granitic plutons as well as metasedimentary rocks. In the latter case, however, they occur only in higher grade metamorphic rocks. In most cases, the mineralogy of the pegmatite is simple consisting of quartz, albite, potash feldspar and muscovite, while some contain notable amounts of beryllium, lithium and niobium-tantalum minerals (Kretz, 1967).

Swarms of post-orogenic diabase dykes cut the Yellowknife-Beaulieu region. In many instances, these are associated with faults. The dykes contain

plagioclase (An_{65}) and augite intergrown in a sub-ophitic texture. Olivine is occasionally present. Whole rock K-Ar dates of four sets of dykes by Burwash et al. (1963) and Leech (1966) fall into different groups indicating several periods of dyke intrusion.

Acknowledgments

The author is indebted to Dr. Ralph Kretz for introducing him to the Yellowknife-Beaulieu region, supervision of the thesis and for constant encouragement throughout the study. Drs. A.J. Baer, W.K. Fyson and D.D. Hogarth kindly read the thesis and offered valuable suggestions.

Thanks are also due to my colleagues A. Carrara, T. Rivers, and especially to R. Divi for helpful suggestions. A.S. Wong and N.Miles helped in the X-ray work. E.R. Rambaldi assisted with the chemical analysis, particularly in the initial stages.

The author is thankful to Dr. M.I. Corlett for her patient supervision of the probe work and to Dr. M.G. Townsend of the Mines Branch for providing the Mössbauer spectra on gedrite and cummingtonite.

Thanks are also due to S. Meunier for typing the thesis and E.W. Hearn for helpful suggestions in the drafting, and for taking photographs.

The author is grateful to Dr. J.B. Henderson of the Geological Survey of Canada for providing the opportunity to work in several parts of the Yellowknife-Beaulieu region and also for generously donating many samples for the study.

Teddy Blondin of Yellowknife and Lyle Hartwig of Hamilton gave helpful assistance in the field.

Finally, financial assistance from the National Research Council of Canada and the Geological Survey of Canada in the form of grants to Dr. Ralph Kretz is gratefully acknowledged. Further thanks are due to the Ontario Ministry of Education and the National Research Council of Canada for the awards of a Graduate Fellowship (1970-1971) and a bursary (1971-1972), respectively.

METAMORPHISM

Introduction

The Yellowknife sedimentary rocks are variously metamorphosed, and on the basis of difference in the intensity of metamorphism, two broad mappable units can be delineated in the field. These units may be termed as i) less or least altered rocks and ii) more altered rocks.

The less altered rocks constitute alternating beds of greywacke and slate or argillite, with a general greyish to rusty appearance on the outcrop. Bedding in these rocks is fairly continuous, and locally can be traced for distances up to several hundred feet. Slaty cleavage is well developed in the argillite horizons. Grain size of these rocks varies from fine to medium.

The appearance of cordierite marks the onsets of the higher grade of metamorhism. Cordierite in these rocks occurs in the form of nodules, and on the weathered surface these nodules form both resistant 'knots' as well as weathered-out pits. The size of the cordierite nodules varies from 4 mm to 3 cm in diameter. The bigger nodules are generally elongated, and sometimes these cordierites were

observed to be oriented oblique to the bedding (plate 1). As noted by Fortier (1946), the cordierite is flattened to a northwest trending cleavage (Plate 2). Bedding in these rocks is preserved even in the highest grades (Plate 4).

Mineral Assemblages

Microscopically, the less altered rocks contain a fine pelitic matrix composed mainly of white mica and chlorite. Within this matrix, porphyroblasts of biotite, quartz and feldspar are inequidimensional in shape and appear to be aligned. Other minerals such as tourmaline, apatite, ilmenite, pyrite and pyrrhotite are sporadically distributed, while cummingtonite is present in certain layers. On the basis of this study the following mineral associations are observed in the lower grade rocks:

a. quartz-chlorite-white mica-oligoclase
b. quartz-chlorite-white mica-biotite-oligoclase
c. quartz-biotite-cummingtonite-oligoclase

Assemblage a, was observed only in a few samples which were obtained near Ross Lake. Rocks of this nature have been described by Henderson (1943) as more common near Gordon Lake, north of the study area. Near Ross Lake, biotite-free rocks are sporadically distributed, and no meaningful biotite isograd can be drawn.

On the basis of mineral assemblages, the metamorphic conditions in the lower grades may be considered as those of the greenschist facies, perhaps towards the upper part of the facies as indicated by the occurrence of biotite and cummingtonite. Magnesium-iron amphiboles are not usually observed under these conditions and cummingtonite is recorded for the first time in such an environment. However, Salotti (1962) described an occurrence of anthophyllite near the greenschist facies - epidote amphibolite facies boundary.

Cordierite is abundantly present in the high grade rocks. Several other minerals such as biotite, garnet, gedrite, cummingtonite, actinolite, andalusite and sillimanite coexist with cordierite in different combinations to give rise to various mineral assemblages. Despite these various combinations a certain degree of zonation is observed with reference to some minerals. On the basis of the first appearance of minerals, from east to west, towards the Sparrow Lake granite pluton, three metamorphic zones may be separated; the cordierite-biotite zone, the cordierite-gedrite zone, and the andalusite-sillimanite zone (Fig. 2). The eastern boundary of the cordierite-biotite zone corresponds to that of the knotted quartz-

mica schist and hornfels zone of Henderson and Jolliffe (1941) or the cordierite isograd of Fortier (1947). However, the present study modifies the location of the eastern limit of this line. The following mineral associations are found in the cordierite-biotite zone:

a. quartz-cordierite-biotite-chlorite-white mica-oligoclase
b. quartz-biotite-cordierite-oligoclase
c. quartz-cordierite-biotite-muscovite-oligoclase
d. quartz-cordierite-biotite-actinolite-oligoclase
e. quartz-cummingtonite-biotite-oligoclase to andesine
f. quartz-cummingtonite-actinolite-biotite-oligoclase
g. quartz-biotite-oligoclase

Among these assemblages, cordierite-biotite-oligoclase is commonly found. Garnet was found, coexisting with cordierite-biotite, in only two samples.

The cordierite-gedrite zone lies between the cordierite-biotite zone and the andalusite-sillimanite zone. Garnet and gedrite occur together in these rocks; however, gedrite occurs more sporadically than garnet. The irregular occurrence of garnet leads to the development of different mineral assemblages. Minerals in this zone, like in the other zones, differ from layer to layer implying that original compositional differences played a prominent role in their paragenesis. The following mineral

associations are found in the cordierite-gedrite zone:

a. quartz-cordierite-biotite-oligoclase
b. quartz-cordierite-muscovite-biotite-oligoclase
c. quartz-cordierite-biotite-garnet-oligoclase
d. quartz-cordierite-biotite-gedrite-garnet-oligoclase
e. quartz-cordierite-biotite-cummingtonite-garnet-oligoclase
f. quartz-biotite-oligoclase

In the andalusite-sillimanite zone adjacent to the Sparrow Lake granite, andalusite is more widely developed than sillimanite. It occurs as crystals, 1 to 3 mm in size, and is associated with sillimanite. Two other types of andalusite are recorded in the Slave Province. (Folinsbee, 1941; Davidson, 1967; and personal observation, 1969, 1971). A chiastolitic variety is found in the lower grade rocks, and a pink variety, (Folinsbee, 1942) is found in quartz veins.

Near Sparrow Lake, sillimanite occurs essentially in the form of fibrolite. Three modes of occurrence of fibrolite are observed in thin section: i. as wispy needles around andalusite crystals, giving the impression of a polymorphic transition, ii. intergrown with biotite crystals, analogous to the epitaxial growth described by Chinner (1961), iii. as inclusions in cordierite and quartz, and also along cordierite crystal boundaries. Bigger chunky

crystals of sillimanite were found elsewhere in the Slave Province by Folinsbee (1947), Jolliffe (1938) and Davidson (1967).

The following mineral associations are found in the andalusite-sillimanite zone:

a. quartz-garnet-biotite-oligoclase
b. quartz-cordierite-biotite-muscovite-andalusite-oligoclase
c. quartz-cordierite-biotite-muscovite-andalusite-sillimanite-oligoclase
d. quartz-biotite-oligoclase

Ilmenite, pyrrhotite, magnetite tourmaline and apatite were present in all the zones, pyrite and graphite was found only in the lower grade rocks.

In addition to the assemblages described above, some other assemblages are present in the siliceous concretions that are present in all the three zones. These concretions occur in different forms within the metasediments, assuming the form of i. concordant layers ii. discordant layers iii. ellipsoidal-lenses, and iv. thin layers along fault planes. Minerals such as cummingtonite, biotite, oligoclase, andesine and ilmenite are commonly found in these concretions. Gedrite is occasionally developed at the margins of the concretions. The following associations are observed in the concretions:

a. quartz-cummingtonite-andesine-ilmenite
b. quartz-cummingtonite-biotite-epidote-andesine-ilmenite
c. quartz-cummingtonite- biotite-garnet-ilmenite

Mineral-Forming Reactions

The occurrence of some of the metamorphic minerals can be explained in terms of metamorphic reactions. The first mineral that may be considered in this connection is biotite.

Formation of Biotite:

The development of biotite in metamorphic rocks has been discussed by Ramberg (1952), Chinner (1960), Ernst (1963), McNamara (1965, 1966), Brown (1967) and others. Ramberg (1952) pointed out that the biotite-generating reaction is one involving muscovite and aluminium-poor chlorite to give an aluminium-rich chlorite and biotite. This has been criticized by Chinner (1960) and McNamara (1965, 1966) on the evidence that chlorites in the biotite zone are no richer in aluminium than the chlorites from the chlorite zone. Although Brown (1967) analysed chlorites of the two zones and found no significant differences in aluminium, iron and magnesium, he then concluded that iron-magnesium muscovite and chlorite must be the reactants in the biotite-generating reaction. This conclusion may be valid, since the studies of

Lambert (1959) and Ernst (1963) reveal that phengitic mica is one of the common varieties of muscovite at lower grades.

Phengitic mica in the study area was identified by X-ray diffraction work. As identification in thin section is impossible due to the very fine-grained nature of these rocks, diffractograms were obtained for concentrated white mica fractions. The phengitic reflections reported by Ernst (1963) between 34^{o} and 37^{o} were detected.

Although several workers discussed the biotite-forming reactions, no attention has been given to the source of titanium in biotites. It is well known that biotites commonly contain a considerable concentration of titanium. Neither chlorite nor ordinary muscovite contain sufficient titanium to account for the amounts present in biotites. On the other hand, phengite is capable of containing a fair amount of titanium (see Ernst, 1963; Brown, 1967). It is quite reasonable therefore to postulate that phengitic mica is one of the phases participating in the biotite-forming reaction. In this process chlorite would become enriched in aluminium while phengite would become enriched in the muscovite

component. A reaction combining these characteristics is written below:

$$10KAl_2(Mg,Fe)_{0.5}Si_{3.5}O_{10}(OH)_2 + 8(Mg,Fe)_5Al_2Si_3O_{10}(OH)_8 =$$

Phengite Al-poor chlorite

$$4KAl_3Si_3O_{10}(OH)_2 + 3(Mg,Fe)_9Al_6Si_5O_{20}(OH)_{16} +$$

Muscovite Al-rich chlorite

$$6K(Mg,Fe)_3AlSi_3O_{10}(OH)_2 + 14SiO_2 + 8H_2O$$

Biotite Quartz

The titanium associated with aluminium in phengite would supply the titanium commonly present in biotites. Thus this reaction may explain the formation of biotite in the lower grade rocks.

Formation of Cordierite

Near the cordierite isograd, cordierite coexists with chlorite, muscovite and white mica. The development of cordierite in this vicinity could be simply explained by the breakdown of muscovite and chlorite. This is supported by the depletion of chlorite and muscovite in rocks above the isograd, compared to the lower grade rocks.

$$4(Mg,Fe)_9Al_6Si_5O_{20}(OH)_{16} + 6KAl_3Si_3O_{10}(OH)_2 + 25SiO_2 =$$

Chlorite Muscovite Quartz

$$9(Mg,Fe)_2Al_4Si5O_{18} + 6K(Mg,Fe)_3AlSi_3O_{10}(OH)_2 + 32H_2O$$

Cordierite — Biotite

This reaction for the Mg-end members was experimentally investigated by Seifert (1970).

The association of cordierite with garnet and gedrite can also be accounted for in terms of metamorphic reactions in which chlorite and muscovite form the reactants. Obviously the Mg/Fe and Al/Si ratios must differ in these chlorites. The following two reactions are proposed to explain two important mineral assemblages.

$$2(Mg,Fe)_9Al_6Si_5O_{20}(OH)_{16} + 2KAl_3Si_3O_{10}(OH)_2 + 11SiO_2 =$$

Chlorite — Muscovite — Quartz

$$3(Mg,Fe)_2Al_4Si_5O_{18} + 2(Mg,Fe)_3Al_2Si_3O_{12} +$$

Cordierite — Garnet

$$K(Mg,Fe)_3AlSi_3O_{10}(OH)_2 + 16H_2O$$

Biotite

$$3(Mg,Fe)_9Al_6Si_5O_{20}(OH)_{16} + KAl_3Si_3O_{10}(OH)_2 + 20SiO_2 =$$

Chlorite — Muscovite — Quartz

$$2(Mg,Fe)_6Al_2Si_7O_{22}(OH)_2 + 3(Mg,Fe)_2Al_4Si_5O_{18} +$$

Gedrite — Cordierite

$$2(Mg,Fe)_3Al_2Si_3O_{12} + K(Mg,Fe)_3AlSi_3O_{10}(OH)_2 + 22H_2O$$

Garnet — Biotite

As no chlorite or muscovite is found in these assemblages, these reactions would necessarily have consumed all of the chlorite and muscovite.

However, the textures observed in thin sections suggest other kinds of reactions relating the minerals in the gedrite and garnet-bearing rocks. In the garnet-cordierite rocks as well as the gedrite-cordierite rocks, some garnet is observed to be enclosed in cordierite. These garnets have corroded edges and irregular shape, indicating signs of break-down. Similarly, gedrite in these rocks is enclosed by cordierite as well as biotite. Biotitization of gedrite is clearly observed by replacement of gedrite along cleavages and relicts of gedrite grains enclosed in biotite. Some of these replacement textures are illustrated in plates 5 and 6. On the basis of these textures two reactions may be proposed:

1) $4(Mg,Fe)_3Al_2Si_3O_{12} + 2KAl_3Si_3O_{10}(OH)_2 + 3SiO_2 =$

Garnet — Muscovite — Quartz

$3(Mg,Fe)_2Al_4Si_5O_{18} + 2K(Mg,Fe)_3AlSi_3O_{10}(OH)_2$

Cordierite — Biotite

2) $5(Mg,Fe)_3Al_2Si_3O_{12} + 2(Mg,Fe)_6Al_2Si_7O_{22}(OH)_2 +$

Garnet — Gedrite

$$5KAl_3Si_3O_{10}(OH)_2 + SiO_2 = 6(Mg,Fe)_2Al_4Si_5O_{18} +$$

Muscovite Cordierite

$$5K(Mg,Fe)_3AlSi_3O_{10}(OH)_2 + 2H_2O$$

Muscovite is absent in both these assemblages.

Development of Andalusite and Sillimanite

Davidson and Heywood (1969) noted the presence of andalusite around granite plugs in the Benjamin Lake area, about 70 miles east of the study area, and concluded that andalusite is formed by the breakdown of cordierite and muscovite in the aureole. In the study area both cordierite and muscovite are observed in the andalusite-sillimanite zone. As muscovite is found to pseudomorph cordierite and also cut across S_2 foliation, it is interpreted as a late-formed mineral, most probably by the influx of potash associated with the intrusion of the Sparrow Lake granite. Therefore, it appears that the only feasible process that might have operated was the production of muscovite from cordierite followed by a complex reaction of the type described in Figure 3. Obviously this implies that either a lowering of temperature or a raise in humidity was associated with the influx of potash. Complex processes of this sort were reported elsewhere; for example in New Hampshire, Green (1963) in order to account for the observation

that muscovite rims are developed on andalusite but never on sillimanite, suggested that "the stability field of sillimanite was not entered until after both the production of andalusite and its partial muscovitization".

An examination of the andalusite-bearing rocks of the study area reveals that sillimanite is present in most of the assemblages. The fibrolite crystals reconcile with the textures described on page 21. Biotite surrounds cordierite crystals while muscovite encloses irregular grains of andalusite. The contacts between oligoclase and biotite are corroded as has been described by Tozer (1955). On the basis of the textures, it is inferred that a complex reaction of the type described by Carmichael (1969) for the kyanite $\rightleftharpoons$ sillimanite transition was operative. Carmichael showed that metamorphic reactions proceed by an exchange of ions, and further showed that aluminium has a limited mobility.

Following the above-mentioned textural observations, a model for the reaction mechanism is presented below:

i. $9Al_2SiO_5 + 6(Mg,Fe)^{+} + 12SiO_2 + 2K^{+} + 9H_2O \rightleftharpoons$

Andalusite Quartz

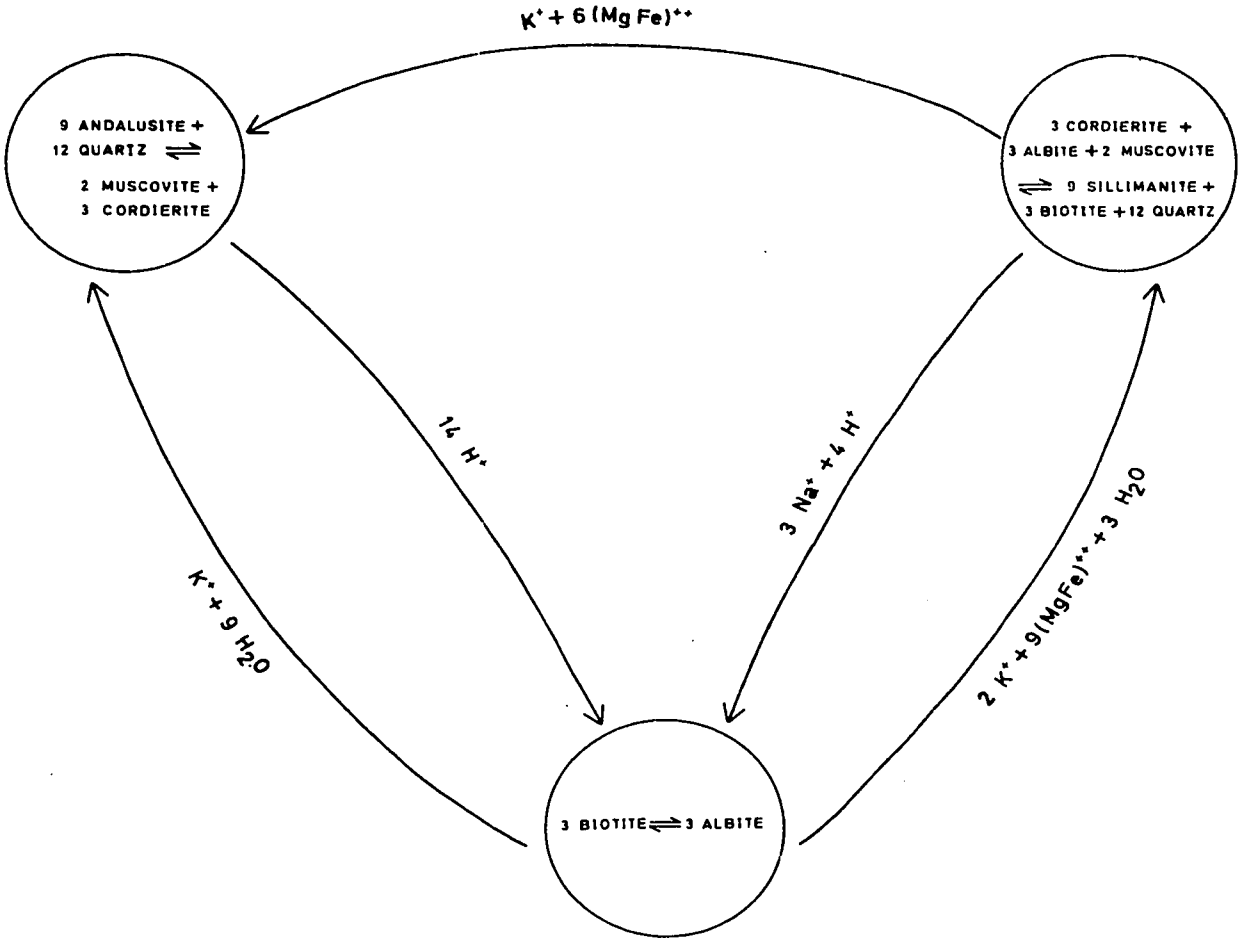

Figure 3. Mechanism of the reaction at the Sillimanite Isograd

$$2KAlSi_3O_{10}(OH)_2 + 3(Mg,Fe)_2Al_4Si_5O_{18} + 14H^+$$

Muscovite Cordierite

ii. $$3(Mg,Fe)_2Al_4Si_5O_{18} + 3NaAlSi_3O_8 + 2KAl_3Si_3O_{10}(OH)_2 +$$

Cordierite Albite Muscovite

$$3(Mg,Fe)^{++} + 3H_2O \rightleftharpoons 9Al_2SiO_5 + 3(Mg,Fe)_3AlSi_3O_{10}(OH)_2 +$$

Sillimanite Biotite

$$12SiO_2 + 3Na^+ + 4H^+$$

iii. $$3K(Mg,Fe)_3AlSi_3O_{10}(OH)_2 + 3Na^+ + 18H^+ \rightleftharpoons$$

Biotite

$$3NaAlSi_3O_8 + 9(Mg,Fe)^{++} + 3K^+ + 12H_2O$$

Albite

Combining the above three reactions, we get the transition 9 andalusite $\rightleftharpoons$ 9 sillimanite. The model may be schematically presented as shown in Figure 3.

Mineral Fabrics and Mineral Growth

Introduction

Metamorphic zones associated with granite or migmatitic complexes have been reported from many parts of the world. In this regard, notable information comes from New Hampshire (Billings, 1937) the Central Alps (Wenk, 1962) and the Central Pyrenees (Zwart, 1963). From the symmetrical arrangement of isograds around granitic plutons, it is argued (Billings, 1937; White and Billings, 1951)

that the plutons are the immediate cause of metamorphism. However, such interpretations are less conclusive if we consider that the heat necessary to drive the endothermic dehydration reactions is not adequately supplied by the plutons (Turner, 1968).

A more reasonable hypothesis (Lyons, 1955; Zwart, 1963; and Turner, 1968) is that the plutons, instead of being the cause of, are considered to be culmination products of metamorphism. The whole process is considered as a continuous process of deformation, metamorphism and magmatism.

In the study area, the parallel and concordant arrangement of isograds with respect to the eastern boundary of the Sparrow Lake granitic pluton (Fig. 2) suggests that the pluton had some influence on the arrangement of the isograds. However, deformational structures of minerals, indicate that most of the minerals grew under dynamo-thermal (regional metamorphic) conditions. Therefore, in an attempt to understand the events of mineral growth under varying metamorphic conditions (regional and contact), mineral fabrics were studied in detail. Criteria used to infer the relationships of mineral growth and deformational phases are those used by Johnson (1962, 1963), Zwart

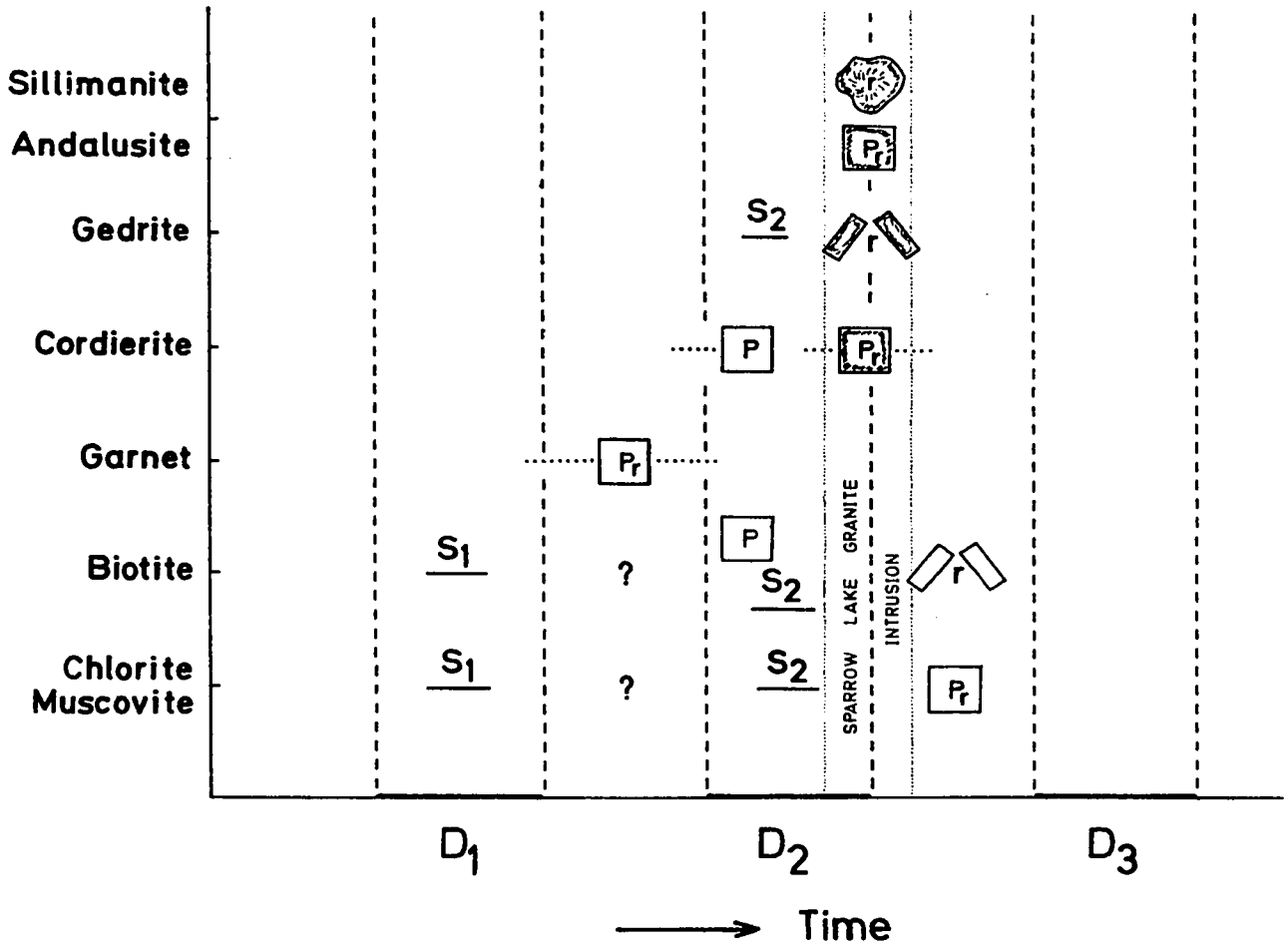

Figure 4. Time relations between mineral growth and deformational phases, P porphyroblast, r random.

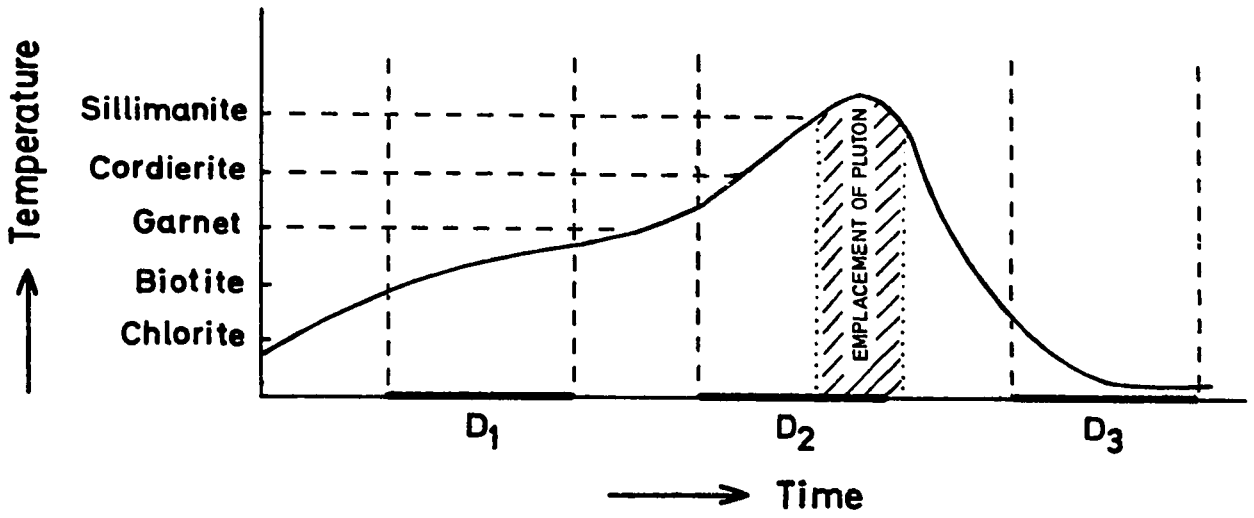

Figure 5. Graph showing relation between temperature changes and deformational events

(1960, 1963), and Spry (1969). The main results are given in Figures 4 and 5, and the following is an explanation in detail.

Mineral Growth and Deformational Phases

In the lower grade rocks, aligned chlorite and phengitic mica form a planar fabric S_1, which in most of the cases is parallel and in a few cases is inclined to the bedding S_o. Presumably the latter cases represent the hinges of the isoclinal tight folds F_1 bending S_o (Henderson, 1943; Fortier, 1947). Another planar fabric S_2, in rocks of higher grade, in which biotite crystals are aligned crosses S_1 at variable angles (Fig. 6). S_2 is steeply dipping to vertical and parallel to the axial surfaces of the mesoscopic folds F_2 bending S_1 parallel to S_o. As shown by Fortier (1946) this foliation (his late cleavage) trends northwesterly in a wide region, well beyond the map area. The third fabric, a crenulation cleavage S_3, cutting S_2 nearly at right angles, is seen in a few cases only. Possibly, the crenulations (F_3) represent the effects of the last phase of deformation. Thus, two main phases (D_1 and D_2) and a third less intense phase (D_3) of deformation can be inferred from the minor structures and textures

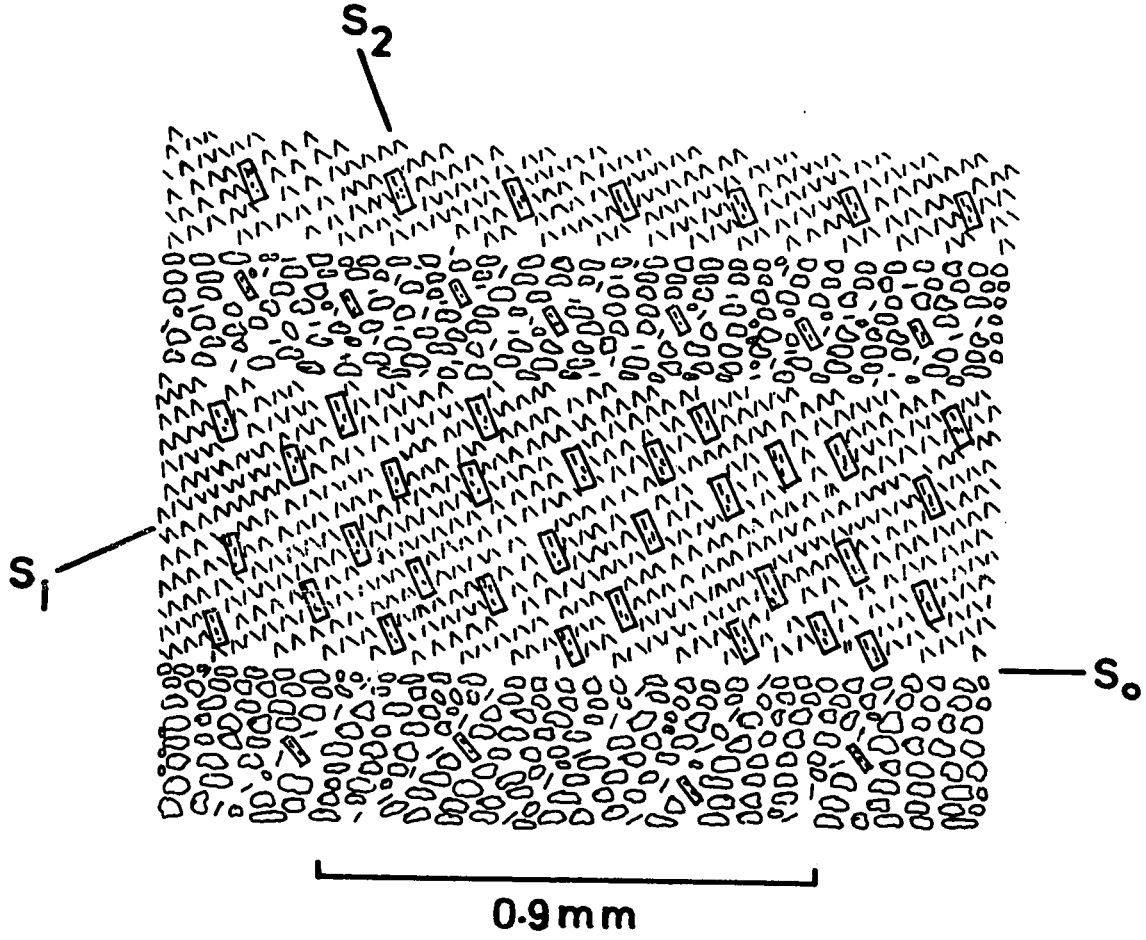

Figure 6. Fabric relations in low grade layered pelitic rock (idealized sketch from the thin section). Bedding S_o, F_2 crenulations bending platy minerals (chlorite, muscovite and biotite) originally aligned parallel to S_1 schistosity. Larger prismatic crystals of biotite are aligned parallel to the axial surface, S_2 of the crenulations. Pelitic (dashes) and psmmitic layers define bedding S_o. (Loc. - 215, Fig. 2).

in the rocks.

Chlorite, white mica and biotite crystals lie in both S_1 and S_2 foliations, hence it is assumed that growth of these crystals was during D_1 and D_2 phases of deformation. Additionally, chlorite crystals transect S_2 foliation and are evidently later than the D_2 deformation. As the chlorite crystals were not seen in juxtaposition to F_3 crenulations, growth in relation to D_3 is not known. Biotite porphyroblasts are elongated parallel to S_2 foliation, which is warped around them (Plate 7). Apparently, porphyroblasts grew before the end of D_2. Possibly, to account for the aligned cleavage in the porphyroblasts parallel to S_2 outside, it is considered that the porphyroblasts grew in the early stages of D_2, and were later flattened in S_2 during late D_2. The early kinematic porphyroblastic and the later, synkinematic fabric-forming biotite crystals show compositional differences in terms of Mg, Fe, Ti and Al (Kamineni and Carrara, 1973). Some chlorite and muscovite crystals grew across S_2 during post D_2 time. Biotite lying in foliation is bent by F_3 crenulations.

In some garnet crystals, fine quartz inclusions form an internal fabric, which is at an angle to the

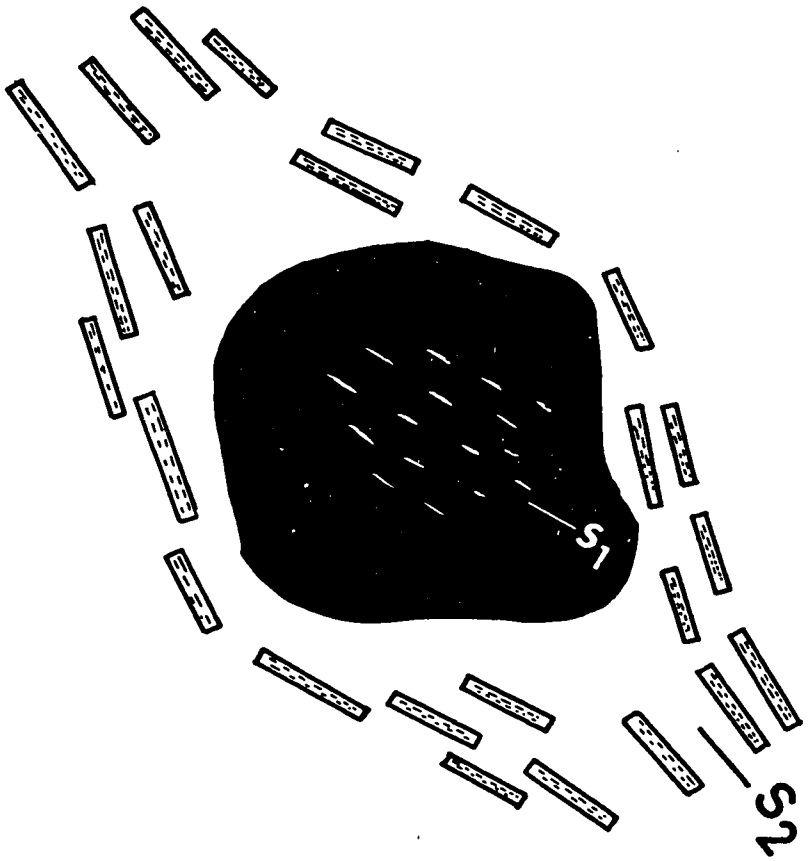

Figure 7. Garnet crystal enclosing fine S_1 quartz fabric. Coarse S_2 Coarse S_2 biotite schistosity outside the crystal is inclined to S_1. The growth time of the garnet crystal is inferred as post D_1 and pre D_2. (Loc. - 142A, Fig. 2).

coarse biotite external foliation S_2 (Fig. 7). Because the grains are of comparable 'size' of the biotites aligned along S_2, it is not apparent whether or not S_2 is warped about the garnets in most cases. The garnet crystals are considered to have grown and included S_1 during or post D_1, but pre D_2 deformation. Other garnet grains with internal fractures (extension) at nearly right angles to the outside S_2, could have grown during pre or early D_2.

Two kinds of cordierite porphyroblasts are distinguished: inequidimentional and nearly equidementional. The latter variety are described separately under the next heading below, as they are considered to have developed in response to the heat supplied by the Sparrow Lake granitic pluton, and not due to the regional metamorphism accompanying deformation. Cordierite porphyroblasts near the cordierite isograd are elongated along the S_2 biotite schistosity, which warps around them (Plate 7). Apparently, cordierite growth was before the end of D_2 deformation. In most examples, cordierite penetrates between biotite crystals aligned along S_2, indicating growth after the foliation was developed. The elongation and penetration along S_2

and the deflection of S_2 about the cordierite porphyroblasts (Plate 8) are consistent with growth at an early stage of D_2 deformation.

Mineral Growth Influenced by Sparrow Lake Pluton

The proximity and close parallelism of the sillimanite isograd (Fig. 2) to the eastern boundary of the Sparrow Lake pluton suggests that this isograd was influenced by the presence of the pluton. Textural evidence support this suggestions; firstly, the rocks exhibit typical hornfelsic texture; secondly, random fibrolite and andalusite porphyroblasts cut across S_2 biotite schistosity, indicating their growth to be late- or post D_2. Pegmatite veins, considered to be the offshoots of the Sparrow Lake pluton, are folded gently with their axial planes paralleling the S_2 axial-surface schistosity of tight D_2 folds in the nearby metasediments. Intrusion of the pluton thus appears to have been during the waning stages of D_2 deformation. Therefore, closeness in timing of the sillimanite growth and intrusion of the pluton (late D_2), and the close proximity and parallelism between the pluton's eastern boundary and sillimanite isograd, strongly suggest that it is a reflection of the conditions imposed by the emplacement of the pluton. Whether any of these aluminosilicates crystallized

before the emplacement of the pluton is not known.

Nearly equidimentional cordierite porphyroblasts, like fibrolite, cut across or enclose S_2 schistosity and appear to have grown during late or post D_2 (Fig. 8a). Additionally, their spatial density seems to increase towards the pluton, suggesting that perhaps more crystals were nucleated as larger amounts of reactants breakdown with progressive 'metamorphism' near the pluton. Such a difference in nucleation rate should reflect difference in crystal sizes with reference to the closeness of the pluton.

To determine whether a difference in crystal size exists, size measurements on cordierite crystals were carried out in five rock samples, collected from different distances from the pluton (Table 2). Slabs of 10 x 15 cms size and 2 cms thick were cut and polished if necessary, to outline the cordierite crystal shapes. The slabs were further sliced gradually to get the maximum 'diameters' of each crystal. The measurements were then averaged for all the crystals in each of the slab. This procedure is similar to a method used by Kretz (1966).

Table 2, indicates that although there is not a direct relationship between distance on the map and

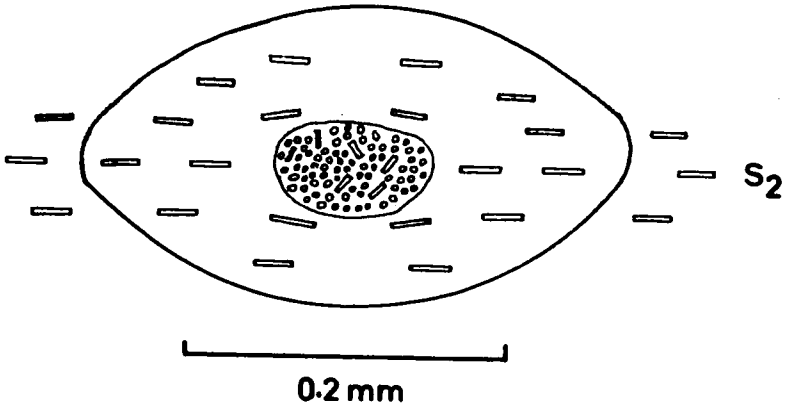

Figure 8a. Zoned cordierite crystal in semi-pelitic rock. The outer zone, enclosing S_2 schistosity (aligned biotite and gedrite crystals), suggests its growth during late or post D_2. The inner zone contains finer quartz and biotite inclusions. Its growth time is inferred as pre D_2. (Loc. - 32, Fig. 2).

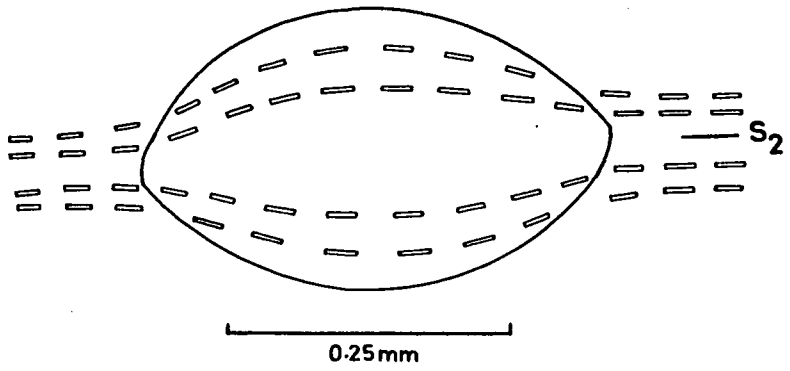

Figure 8b. Flattened cordierite porphyroblast aligned parallel to and enclosing S_2 biotite schistosity. Its growth time is inferred as early D_2. Idealized sketch drawn from the thin section. (Loc. - 69, Fig. 2).

Table 2: Size Analyses of Cordierites

Sample No.	No. of Crystals	Mean size in cms.	Standard Deviation	Distance from Granite (Km)
197	11	2.64 x 3.55	0.55, 0.66	10.05
171	12	1.63 x 2.34	0.35, 0.56	7.20
		Gedrite isograd		
142	15	2.23 x 3.10	0.48, 0.36	5.50
32	25	0.30 x 0.48	0.03, 0.05	0.80
		Sillimanite isograd		
62	22	0.33 x 0.49	0.11, 0.02	0.05

mean size of cordierite crystals, in general the size does decrease towards the pluton. Evidently, the crystals near the pluton grew for a relatively short period of time while crystals away from the pluton grew under more uniform temperature for a longer time, and to larger sizes. The standard deviations from the mean size increase with increase in size of the cordierite crystals outward from the pluton (Table 2). Since the nucleation rate was high near the pluton, the sizes of the crystals does not vary much, as most of them remain small, while away from the pluton, the nucleation rate is low so that earlier nucleated crystals tend to grow to a larger size than the later ones. This resulted in a greater variability in the sizes of the crystals away from the pluton, and hence the higher standard deviations than near the pluton. It is evident that the size relationships are compatible with at least some cordierite growth in response to the heat supplied by the pluton.

To test whether there exists a relation between the amount of garnet and nearness to the pluton, a similar study was carried out on garnetiferous rocks. A fragment of a rock of known weight was disintegrated

by a series of heating (to 300°C) and cooling (under cold water) operations. Garnet was separated from these powdered rocks by means of methelene iodide, and this operation was repeated to ensure complete recovery of the garnet fractions. The garnet recovered by this procedure was weighed, and the weight percentage of the garnet calculated by taking the weight of the rock into consideration. The results are presented in Table 3.

Table 3 shows that although the sample farthest from the pluton contains the least amount, the variation in weight percent of garnet from the pluton is somewhat irregular. Thus the study suggests that the paragenesis of garnet is largely controlled by bulk compositional differences and that more extensive sampling would be necessary to relate the amount of garnet to distance from pluton.

A few gedrite crystals lying parallel to S_2 biotite schistosity (Fig. 8a) are observed in two thin sections. However, in the majority of the cases, they are randomly oriented and cut across the S_2 foliation (Plate 6), indicating that the crystals grew during late or post D_2 phase of deformation. This time of growth and the presence of gedrite-bearing rocks very near the pluton, up to the alumino-

Table 3: Weight Percent of Garnet

Sample No.	Wt Percent of Garnet	Mineral Assemblage	Distance from the Contact (Km)
2	1.25	Garnet-Biotite	0.05
19	1.52	Garnet-Biotite-Cordierite	0.05
21	0.65	Garnet-Cordierite-Biotite-Gedrite	0.10
32	1.72	Garnet-Cordierite-Biotite-Gedrite	0.80
14	0.70	Garnet-Cordierite-Biotite-Gedrite	1.56
89	0.51	Garnet-Cordierite-Biotite	4.10

silicate zone, suggests that the paragenesis of this mineral was influenced by the heat supplied by the granitic pluton. This is also supported by the field and petrographic observation that the gedrite crystals are more closely spaced towards the pluton. Cummingtonite has a similar textural relation, with reference to S_2, to that of gedrite, but the influence of the granite pluton in its formation is considered to be minimal as this mineral extends much below the cordierite isograd (Plates 3 and 10).

Discussion

In the study area, most metamorphic minerals grew under dynamothermal conditions existing during regional metamorphism of the sediments. This is strongly supported by the alignment of minerals, to form S_1 and S_2 schistosities. Some of the minerals like garnet and chlorite porphyroblasts grew in the "static" intervals between two phases of deformation.

Relations between mineral growth and structural events (D_1, D_2 and D_3) suggests that the regional metamorphism is one of a progressive nature with respect to time. This is particularly evident from the growth of chlorite and biotite during D_1, growth of garnet during post D_1 and pre D_2, and growth of

cordierite during early D_2. Such progressive growth of these minerals indicates a rise of temperature with time during regional metamorphism (Fig. 5). The three phases of deformation D_1, D_2 and D_3 are separated 'arbitrarily' for the sake of better visualisation of 'structural-time' events. In fact, very little is known about the continuity or relative duration of the three phases of deformation.

Growth of sillimanite indicates that the maximum temperatures were attained during late, and probably until a little after, D_2, when the Sparrow Lake pluton intruded the sediments. That the pluton transmitted a great amount of heat, thus raising the temperature of the sediments, is evident from the closeness of the sillimanite isograd to the pluton's edge, and also the increasing occurrence of cordierite (Table 2) and gedrite towards the pluton.

Though the pluton imposed "contact metamorphic conditions" on the sediments around it, it is considered only as a culminating feature of the regional metamorphic process. Similar time relations between granite intrusion and regional metamorphism in other Archean terrains are widely noted (Anhaeusser et al. 1969). Whether pluton had any direct influence on the crystal

in the surrounding rocks would depend on the temperature of the rocks prior to the intrusion. Obviously, if the temperature of the sediments is already as high as or higher than the temperature of the pluton, no 'contact effect' of the pluton would be seen in the sediments. This does not seem to be the case in the study area, where it is possible to see the influence of the pluton on the growth of certain minerals.

Most of the mineral growth in the study area was completed by the end of or after the D_2 phase. The waning stages of metamorphism are indicated by growth of random chlorite and muscovite across the S_2 schistosity. The temperature of the sediments must have been dropped considerably by the time the rocks were deformed during the D_3 phase, when the micas were only crenulated.

Physical Conditions of Metamorphism

Some conclusions regarding the physical conditions during metamorphsim can be estimated by comparison with the pressure-temperature conditions obtained for synthesis of index minerals. Although the experimental conditions and the compositions of the synthetic phases are different from the natural systems, a

fairly close approximation can be achieved.

Information for this purpose can be obtained from the P-T stability limits of end-member minerals and also from some univariant reactions.

Most of the maximum stability fields for end-members of the minerals encountered have been investigated experimentally; i.e. muscovite (Yoder and Eugster, 1955; Segnit and Kennedy, 1961); biotite (Eugster and Wones, 1962); chlorite (Turnock, 1960; Nelson and Roy, 1958; Yoder 1952 and Segnit, 1963); garnet (Yoder and Chinner, 1960a, b; Chinner, 1960); and cordierite (Schairer, 1965; Schreyer and Schairer, 1962). The stability limits of the aluminosilicate polymorphs have been studied by several workers but the information used in this study is that of Richardson et al. (1965).

Information on the minimum stability of these minerals is less complete. However, in a few cases such information is available; Kennedy (1959) and Kerrick (1968) have studied the synthesis of andalusite quartz from pyrophyllite; and the breakdwon of mont-morillonite to chlorite + quartz has been investigated by Fawcett and Yoder (1962). The lower stability limits of Mg-cordierite have been obtained from the reaction pyrophyllite + quartz breaking down to Mg-cordierite

(Schreyer and Yoder, 1964).

In addition, information is also available on the reactions: muscovite + quartz (Evans, 1965; Velde, 1966; Segnit and Kennedy, 1961 and Winkler, 1967), chlorite + quartz (Fawcett and Yoder, 1966; Akella and Winkler, 1966; and Hsu, 1968) and Mg-Al chlorite + quartz (Seifert, 1969).

Three reactions involving the breakdown of chlorite are important in inferring the temperature of metamorphism. One of these is:

muscovite + Mg-Al chlorite + quartz $\rightleftharpoons$ phlogopite + cordierite + water (Seifert, 1969).

This reaction fixes the conditions at the cordierite isograd. The system investigated by Seifert was iron free and with the addition of iron the equilibrium temperature would probably be lowered. The equilibrium temperatures of this reaction were found to be $495 \pm 10^{o}C$ at 1Kb P_{H_2O}; $525 \pm 10^{o}C$ at 2Kb P_{H_2O} and $610 \pm 15^{o}C$ at 5Kb P_{H_2O}.

Another relevant reaction that was experimentally investigated by Akella and Winkler (1967) is:

Mg-Fe, Al chlorite + quartz $\rightleftharpoons$ gedrite + cordierite + water

The chlorite used in this study is very close to the natural chlorite and the equilibrium temperature of

the reaction was found to be of $562 \pm 8^{o}C$ at 1Kb P_{H_2O}. In the same work the upper stability of gedrite was determined where gedrite in presence of quartz breaks down to hypersthene + cordierite + water at $755 \pm 15^{o}C$ and 4Kb P_{H_2O}. Since gedrite is obviously stable in the presence of quartz in the study area, the upper limit of metamorphic conditions could be expected to be below the breakdown temperature of gedrite + quartz.

The third reaction is based on the work of Hsu (1968) in which the Fe and Mn end-members of chlorite in the presence of quartz breakdown to almandine and spessartine respectively. On the basis of this work, the almandine-spessartine garnet could be considered to form at about $500^{o}C$ and 1 to $4Kb_{H_2O}$. This temperature should be increased by the presence of other components in solid-solution with spessartine-almandine. Garlick and Epstein (1967), on the basis of oxygen isotpic ratios indicated that the garnet crystallizes at temperature greater than $475^{o}C$, from which it can be inferred that the minimum temperature of crystallization is around $500^{o}C$.

Metamorphic conditions could also be derived from the assemblage staurolite-garnet-cordierite-andalusite-biotite which was located by the author

on the northern side of Prelude Lake, immediately west of the study area (see Henderson et al. 1971). Richardson (1969) in his work on the system Fe-Al-Si-O-H showed that cordierite-staurolite-quartz can coexist with andalusite-sillimanite under a pressure of 1.5Kb to 3Kb P_{H_2O} and a temperature range of 530 to 680°C. Garlick and Epstein (1967) also gave an apparent stability range to staurolite from 525 to 620°C, based on oxygen isotopic ratios.

The presence of muscovite with quartz in these rocks, indicates that the temperatures must have been below the second sillimanite isograd. The stablity of muscovite + quartz has been determined by several workers, the results of Segnit and Kennedy (1961), Evans (1965), Velde (1966) and Winkler (1967) being relevant to this work. Segnit and Kennedy (1961) report that muscovite + quartz breakdwon to K-feldspar andalusite water at 665°C and 1Kb water pressure. These values are much higher than those of Evans (1965) who has obtained an equilibrium temperature of 550°C at 1Kb P_{H_2O}. In view of this discrepency Winkler (1967) conducted experiments reversibly for very long durations, and hence his results are probably better. Winkler placed the stability of

muscovite + quartz at 580 ± 10°C / 0.5Kb, 600 ± 10°C / 1Kb, 630 ± 10°C / 2Kb and 690 ± 10°C / 4Kb, water pressure. From this it can be stated that the temperatures during metamorphism was certainly below 700°C. Some inferences regarding pressures during metamorphism can be obtained from the stability fields of aluminosilicates and the muscovite + quartz breakdown curve. Since no K-feldspar is observed in the lower as well as highest grades, and at the highest grades both andalusite and sillimanite are present with cordierite, biotite and muscovite, the pressure can be ascertained from the intersection of the muscovite + quartz breakdown curve with that of andalusite-sillimanite boundary. These pressures should certainly be higher than at the intersection point due to the negative slope of the andalusite-sillimanite boundary curve. From this the minimum confining pressures should not be less than 3.8Kb.

In conclusion, metamorphic temperatures in the higher grades ranged from 450 to 600°C. The hornblende-hornfels facies metamorphism (Turner, 1968) which coincides with the appearance of cordierite commenced at approximately 500°C. The other minerals,

Explanation of Figure 9

aa: Stability fields of aluminosilicates (Richardson et al. 1969)

bb: Field in which garnet-biotite and cordierite coexist (Hirchberg and Winkler, 1968)

c: Mn chlorite+quartz $\rightleftharpoons$ spessartine + fluid (Hsu, 1968)

d: Muscovite+chlorite+quartz $\rightleftharpoons$ phlogopite cordierite water (Seifert, 1970)

e: Chlorite+muscovite $\rightleftharpoons$ cordierite+biotite + Al_2SiO_5 (Hirchberg and Winkler, 1968)

f: Fe chlorite+quartz $\rightleftharpoons$ almandine+fluid (Hsu, 1968)

g: Mg,Fe-Al chlorite+quartz $\rightleftharpoons$ gedrite+cordierite water (Akella and Winkler, 1966)

h: Muscovite+quartz $\rightleftharpoons$ K-feldspar + Al_2SiO_5 + water (Winkler, 1967)

i: Gedrite+quartz $\rightleftharpoons$ hypersthene + cordierite+ water (Akella and Winkler, 1966)

j: Low-pressure metamorphic trend (Miyashiro, 1972)

k: Metamorphic trend inferred in the study area

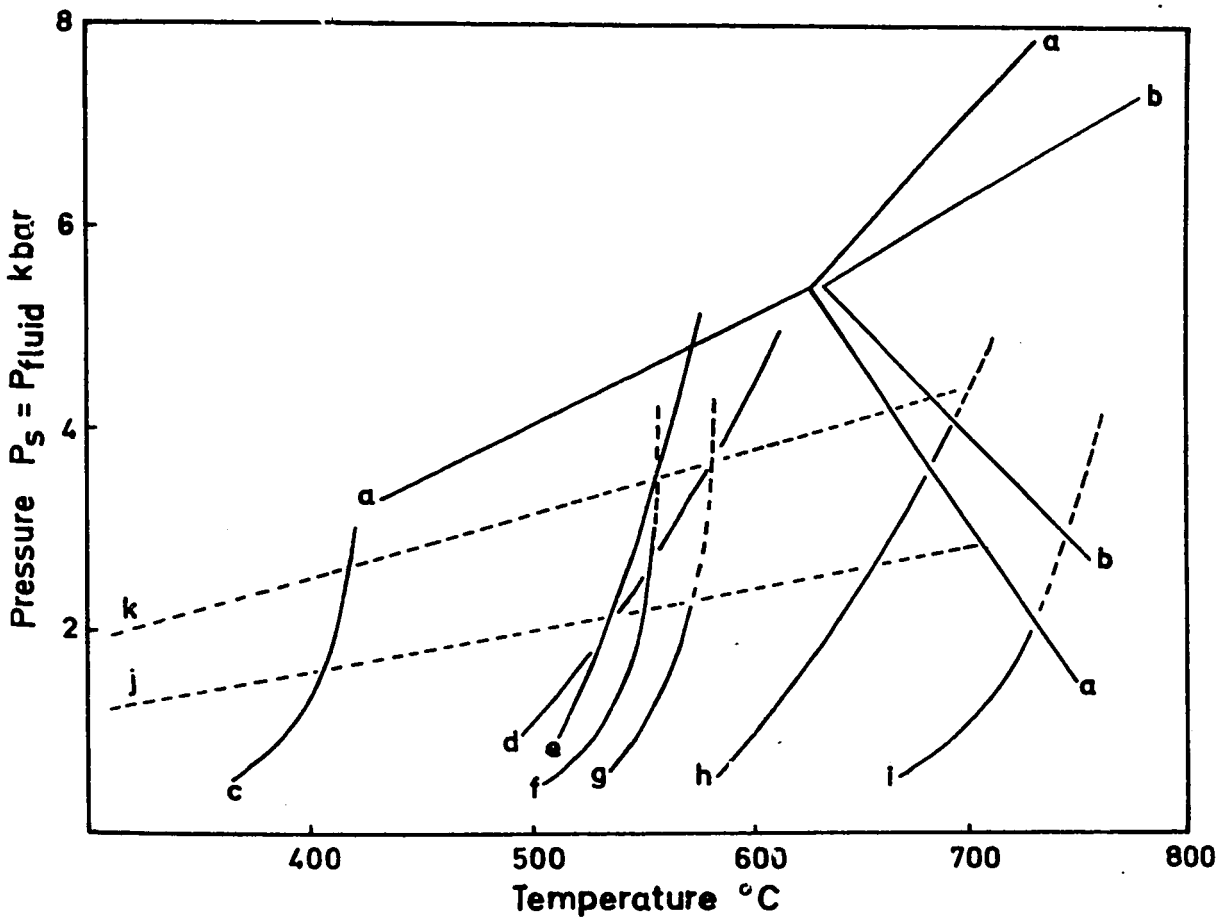

Figure 9. Inferred P-T conditions of metamorphism

gedrite and sillimanite, were formed at higher temperatures. The maximum total pressures probably did not exceed 4.5Kb.

The experimental conditions inferred in this section, indicate that the metamorphic pattern in the present case approximately followed the low pressure metamorphic path of Miyashiro (1961, 1972). The pressures estimated would correspond to a depth of about 14 Km. Of course, this is true only when the pressures operated solely due to load, and the effects of directed and water pressures are negligible. The effect of directed pressure may be important at lower grades (Turner and Verhoogen, 1961) and can be conveniently neglected at higher grades (Thompson, 1955). Water released through dehydration reactions when not removed from the system develop a fluid pressure and thus reduces the value of equilibrium temperature of metamorphic reactions. The normal geothermal gradient which is about $15^{o}C/Km$ (Turner, 1968) would give a temperature of $210^{o}C$ at 14 Km depth. Therefore, it is obvious that higher gradients of the order of $45^{o}C/Km$ must have been operative to reach the estimated temperatures. As no high-pressure metamorphic facies such as glaucophane schist facies rocks are recognized in Archean terranes (de Roever,

1965), it is logical to assume that the gradients during these times were most probably steeper than during later dates. However, steeper thermal gradients are not confined to Archean times, for example in Carpathians, Boldizsar (1963) measured gradients of the order of 70^{o}C/Km. Hence gradients that have been postulated for the present study area are not unreasonable. The inferred P-T conditions for the study area are shown in Figure 9.

CHEMISTRY OF THE ROCKS

Introduction

The mineral assemblages of the Yellownife metasediments differ from layer to layer regardless of the metamorphic zonation, possibly due to differences in bulk chemistry. In order to investigate the effect of bulk chemistry on mineralogy, a series of samples with different mineral assemblages and metamorphic grade was chosen for analysis. The location of the samples is given in Figure 2.

Samples were prepared by pulverizing about half of the hand specimen. Coning and quartering sampling techniques were employed to pick up the small amounts of sample needed for the analysis. Analysis was performed by employing a combination of analytical techniques: atomic absorption, wet chemical, and X-ray fluorescence. The details are given in Appendix II.

Chemical Composition

A glance at the chemical analysis (Tables 4, 5 and 6) shows a notable range of chemical composition. This is very conspicuous, especially with regards to SiO_2, Al_2O_3 and alkalis. Probably these variations are due to the position from which part of the

Table 4: Chemical Composition of Cordierite-Gedrite Bearing Rocks

	14	21	27	32	39A	41	52	74	78	109	142A	K	H	C
SiO_2	67.00	66.60	64.60	54.90	67.00	65.42	65.00	69.90	65.20	65.00	66.70	65.21	66.24	64.43
Al_2O_3	15.30	15.52	15.60	18.70	15.10	16.24	18.22	14.90	17.10	15.70	15.10	14.76	15.28	15.48
TiO_2	0.51	0.90	0.59	0.69	0.48	0.92	0.62	0.49	0.95	0.59	0.57	0.66	0.64	0.62
Fe_2O_3	1.34	n.d.	1.64	1.11	1.06	n.d.	n.d.	1.33	n.d.	1.72	1.34	1.36	0.70	6.54
FeO	4.34	5.85	4.78	8.11	4.34	5.00	4.92	4.02	5.47	4.73	4.57	5.11	4.53	n.d.
MgO	2.79	2.77	3.18	4.50	2.64	2.62	2.59	2.57	2.66	2.90	2.85	2.92	2.74	3.12
MnO	0.14	0.12	0.13	0.18	0.12	0.09	0.08	0.11	0.09	0.11	0.13	0.12	0.06	n.d.
CaO	1.90	1.43	1.85	1.75	1.95	1.70	1.29	1.60	1.33	1.76	2.00	1.69	1.70	2.22
Na_2O	3.61	4.00	3.72	3.90	3.95	3.56	4.48	4.05	3.40	4.18	3.40	3.84	3.12	3.74
K_2O	1.44	1.48	1.68	2.09	1.55	1.29	1.15	1.30	1.08	1.50	1.62	1.47	1.91	2.44
H_2O^+	1.65	1.36	2.10	2.46	1.50	2.00	1.50	1.20	1.62	1.73	2.40	1.77	2.49	n.d.
H_2O^-	0.05	0.06	0.10	0.12	0.06	0.10	0.06	0.02	0.04	0.04	0.10	0.07	0.08	n.d.
Total	100.07	99.76	100.05	98.71	99.73	98.94	99.89	101.50	100.12	100.26	99.46	98.98	99.87	98.64
Oxidation ratio	21.55		23.47	10.90	17.93			20.39		24.54	20.64	19.91		

K Average of 11 cordierite-gedrite bearing rocks

H Average of 3 unmetamorphosed greywackes from Yellowknife (Henderson 1972)

C Average of 25 Wyoming Greywackes (Condie 1967)

Table 5: Chemical Composition of Some Metasedimentary Rocks

	Aluminosilicate bearing rocks				Garnet-Cordierite-Biotite rocks						Low Grade rocks					
	62	3L1	446	450	2	19	43	89	151A	191	215	221A	254	268	283	301
SiO_2	64.00	58.50	62.20	56.80	65.25	65.79	n.d.	n.d.	63.24	67.10	n.d.	n.d.	n.d.	n.d.	59.80	57.60
Al_2O_3	18.95	21.50	18.20	22.40	16.40	16.00	n.d.	n.d.	18.00	15.40	n.d.	n.d.	n.d.	n.d.	19.20	18.20
TiO_2	0.80	0.72	0.69	0.76	0.61	0.74	n.d.	n.d.	0.81	0.55	n.d.	n.d.	n.d.	n.d.	0.69	0.70
Fe_2O_3	1.06	1.22	0.87	0.63	n.d.	n.d.	n.d.	n.d.	n.d.	0.59	n.d.	n.d.	n.d.	n.d.	1.34	2.96
FeO	5.50	6.11	5.49	6.13	5.04	5.21	5.40	5.44	7.25	4.78	6.28	6.69	6.43	6.12	4.71	6.76
MgO	2.69	2.75	2.95	3.01	2.74	2.71	2.80	2.70	3.20	3.10	3.21	2.94	3.06	3.40	3.25	4.00
MnO	0.07	0.08	0.10	0.09	0.13	0.16	0.14	0.11	0.11	0.12	0.10	0.11	0.13	0.12	0.11	0.14
CaO	0.89	1.44	1.70	1.35	2.10	0.85	2.00	2.20	1.50	1.00	1.22	0.86	1.41	1.35	0.72	1.11
Na_2O	2.48	2.55	2.90	2.33	3.70	4.34	3.50	3.50	3.00	1.97	2.71	2.60	2.41	3.00	3.00	2.22
K_2O	2.72	3.00	2.55	2.95	2.60	2.25	1.78	1.87	2.51	2.60	2.51	2.98	2.70	3.02	3.37	3.40
H_2O^+	1.55	1.91	2.20	2.50	n.d.	n.d.	n.d.	n.d.	2.00	2.60	n.d.	n.d.	n.d.	n.d.	2.76	2.52
H_2O^-	0.02	0.05	0.10	0.04	n.d.	n.d.	n.d.	n.d.	0.05	0.12	n.d.	n.d.	n.d.	n.d.	0.10	0.15
Total	100.63	99.83	99.95	98.99	98.57	98.15	15.62	15.82	101.67	99.93	15.03	16.18	16.04	17.01	99.05	99.74
Oxidation ratio	14.71	15.14	12.38	8.37						9.76					20.21	28.24

n.d. not determined, where Fe_2O_3 is not determined total Fe is expressed as FeO.

151A Cordierite-Biotite rock

turbidite horizon the sample was collected. Henderson (1972) has reported the analyses of greywackes and mudstones from a graded sequence near Yellownife town in which an apparent variation in these elements can be seen. In the present study, at higher grades, this can be inferred from the type of a mineral assemblage. For example, the cordierite-gedrite-bearing rocks are confined to coarser and lower horizons of the turbidite, while the cordierite-biotite and alumino-silicate-bearing rocks occur in top portions. The top portion of the graded sequence is more argillitic and tends to be richer in Al_2O_3 and K_2O, and poorer in SiO_2 and Na_2O relative to the lower portions. Thus the alkalis, Na_2O and K_2O, when plotted against each other show an antipathetic relation (Fig. 10). There is no information about the position of the samples with reference to the graded sequence in the data of Kretz (1967), Davidson (1967), and also a few in the present study. However, if the antipathetic relation obtained for Na_2O-K_2O applies in general, the approximate position of these samples can be ascertained.

Figure 11 represents a triangular variation diagram comprising the elements Na_2O, K_2O and CaO.

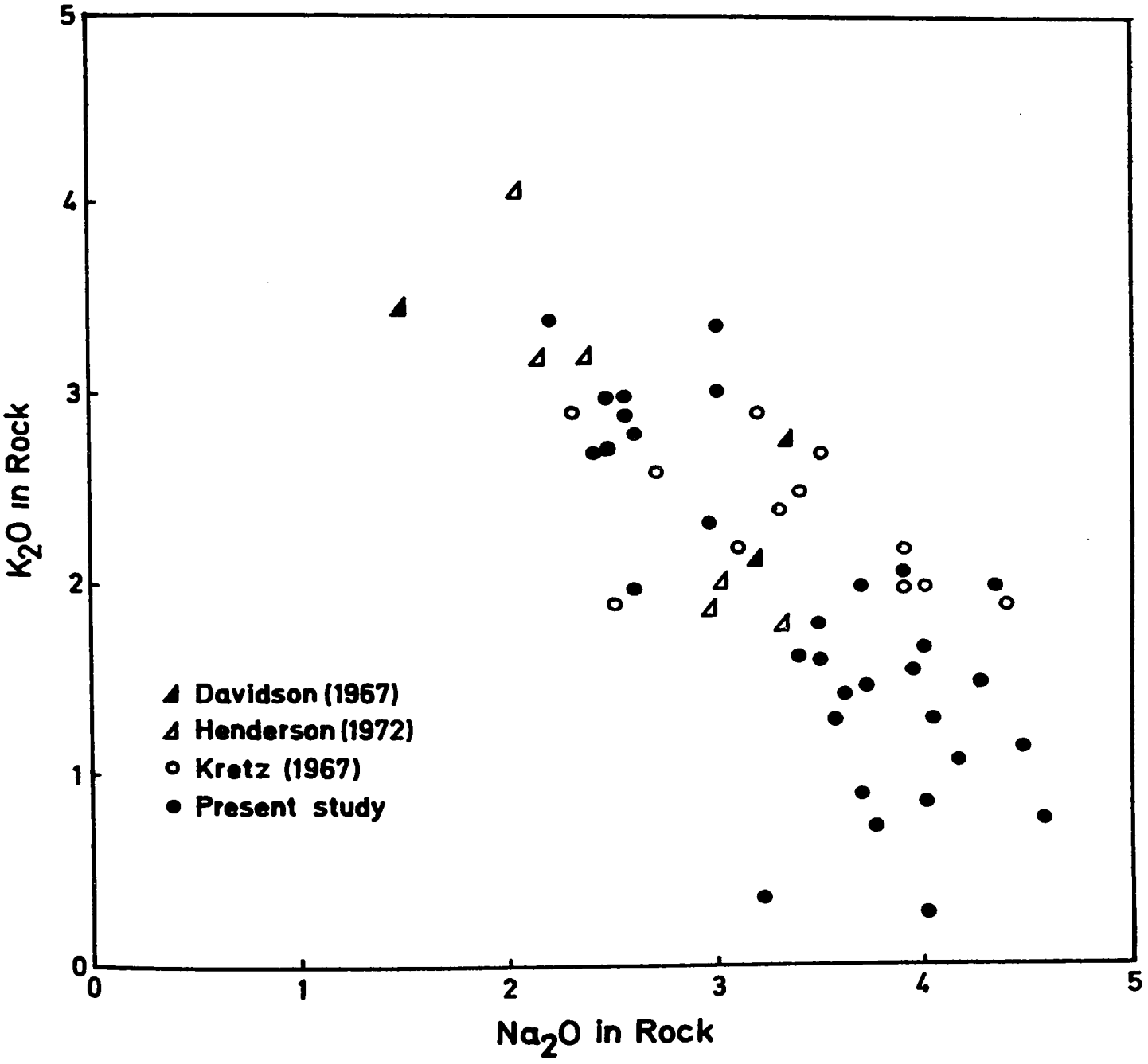

Figure 10. Variation diagram showing the relation between Na_2O and K_2O in the metasedimentary rocks.

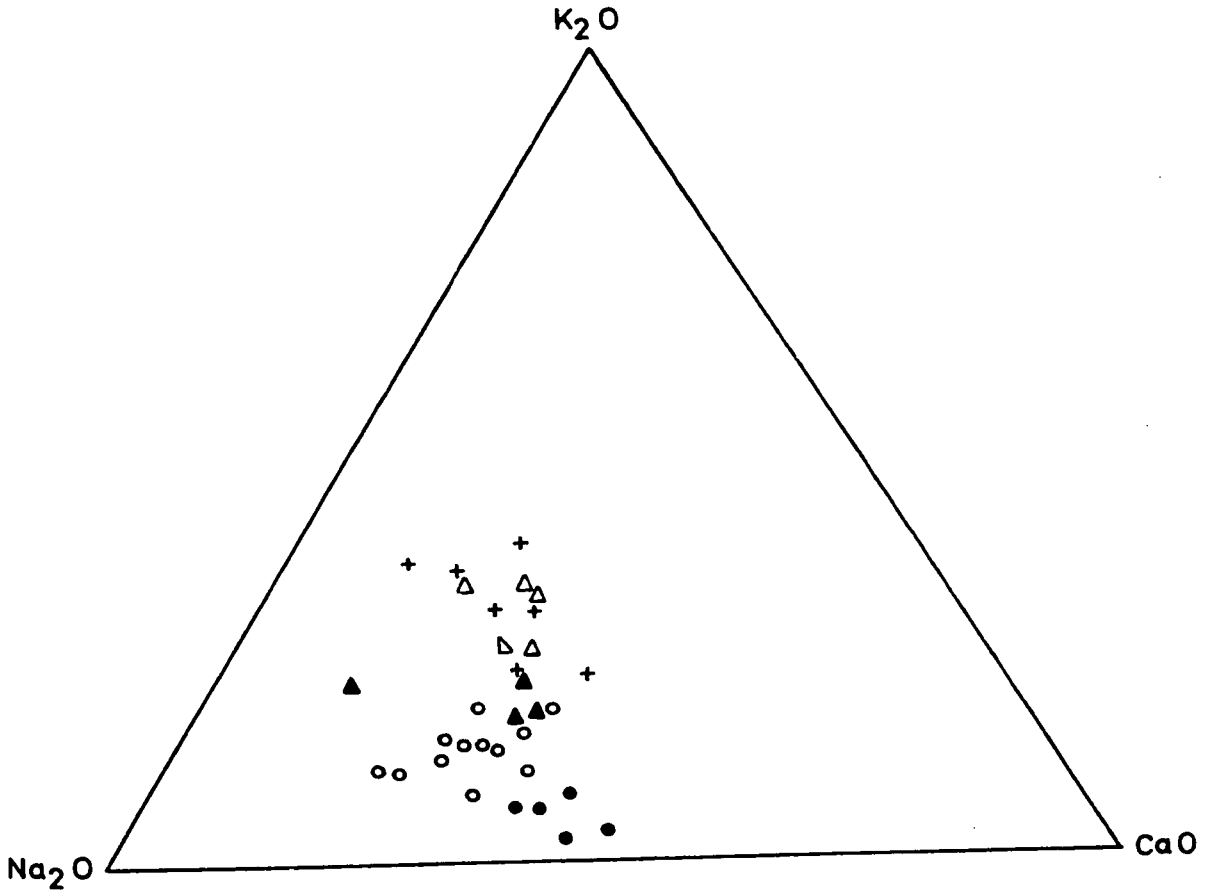

Figure 11. Triangular variation diagram of alkalies and CaO in the metasedimentary rocks.

On this diagram, variations in K_2O and Na_2O are very apparent due to a wider range, while those of CaO are not significant due to its narrow range.

Chemical Controls on the Formation of Minerals

General Statement

It is well known that metamorphic mineral paragenesis is governed by physical conditions as well as bulk composition. This is illustrated in the rocks of the present study, where different mineral assemblages are formed in different beds or different portions of the graded beds, particularly in the gedrite zone. The dependence of mineral content on bulk composition will now be examined in some detail.

Oxidation Ratio

The oxidation ratio of the rock, defined as $2Fe_2O_3 \times 100/(2Fe_2O_3 + FeO)$ in moles (Turner, 1968) may be considered as one of the parameters that can influence mineral composition and paragenesis. Examples of this can be found in the works of Chinner (1960), Mueller (1961), Eugster and Wones (1962) and Reinhardt (1968). Although oxidation may be influenced by the degree of metamorphism, Chinner (1960), Mueller (1960), Zen (1963) and Guidotti (1970) have demonstrated

varying amounts of oxidation in different metasedimentary layers, indicating original differences. Miyashiro (1964) discussed that oxidation is highly influenced by the presence or absence of graphite in the metamorphic rocks.

In the present study, data on the oxidation ratio of unmetamorphosed rocks is not available. However, in the nearby area, Henderson (1972) has analyzed six least metamorphosed greywackes and argillites where the oxidation ranges from 10.77 to 14.09 with an average of 12.81. Pettijohn (1963) showed that low oxidation is characteristic of Archean greywackes.

The oxidation state in three samples in the low grade rocks from the study area varies from 9.76 to 28.24 as shown in Table 5. At higher grades, in the cordierite-gedrite-bearing rocks the oxidation varies from 10.90 to 24.54 with an average of 19.91. These wide ranges of oxidation ratio in samples of the same mineral assemblages may be attributed to different amounts of graphite originally present in these rocks. The occurrence of graphite is observed in the lower grades and was evidently eliminated at higher grades. According to Miyashiro (1964) the Fe_2O_3 content of graphite-bearing rocks tends to decrease with progressive

metamorphism. Miyashiro proposed the following reaction between graphite and gases: $(C) + (O_2) = (CO_2)$.

Neglecting the effect of pressure on solid phases, the oxygen fugacities are controlled by the equation, $\Delta G^o = -RT \ln \frac{f_{CO_2}}{f_{O_2}}$ where ΔG^o is the standard free energy of the reaction, R, the gas constant, T, the equilibrium temperature in degrees Kelvin, f, the fugacity. The ratio f_{CO_2}/f_{O_2} will be constant at a given temperature. If the fugacity of CO_2 tends to be uniform throughout the area, the oxygen pressures in graphite-bearing rocks also would be uniform (Miyashiro, 1964). However, the differences in oxidation ratios observed in the rocks indicate that this is not the case in the area.

The oxidation ratio in aluminosilicate rocks near the contact drops considerably (12.65, average of 4 samples). Reducing conditions near the contacts of plutons have been noted elsewhere by Compton (1961), Chinner (1962), and Best and Weiss (1964). In the Santa Rosa aureole (Compton, 1961) oxidation increased with increasing metamorphism and decreased rapidly at the contact. Miyashiro (1964) indicated that reducing gases such as H_2 and CO may come from the deep

interior of the earth with the ascending magmas, and hence one might expect to find a higher degree of reduction in the vicinity of igneous intrusions.

In view of the wide range of oxidation ratios observed within a single assemblage, such as cordierite-gedrite-garnet-biotite, the oxidation ratio probably did not greatly influence the mineral paragenesis in the rocks of the present study.

Variation in Al, Ca, Mg, Fe and K Content

In 1920 Eskola introduced ACF and AKF diagrams to depict mineral and chemical variations in terms of Al_2O_3, CaO, (Mg,Fe)O and Al_2O_3, K_2O, (Mg,Fe)O. The main drawback of these diagrams is that minerals such as albite, ilmenite, magnetite and titanite cannot be represented. Moreover, the two components MgO and FeO are combined into one.

The AKF values for the compositional data (Tables 4, 5 and 6) are plotted in Figure 12. It is evident from the diagram that these data fall in two fields: one defining the field of aluminosilicate-bearing rocks while the other containing a cluster of the rest of the assemblages. The 'ACF' values for the same data are also plotted on Figure 12 (uncorrected for biotite), which gives a similar trend. Hence it appears that in the present study

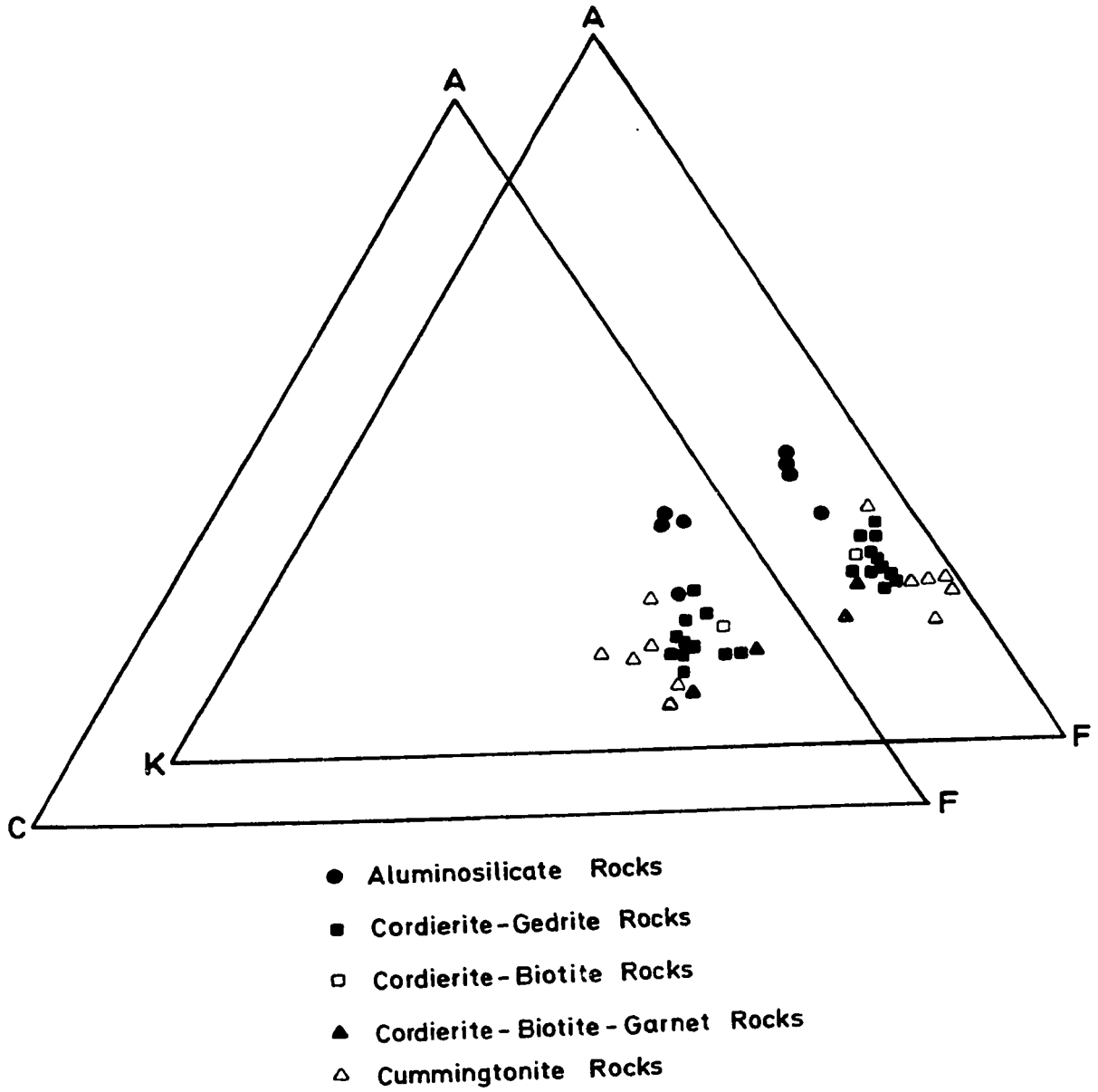

Figure 12. AKF and ACF diagram showing the composition field of the metasedimentary rocks.

these diagrams are useful only to demarcate the aluminosilicate-bearing rocks from the other assemblages.

In view of the inadequacy of the AKF and ACF diagrams, other plots were sought to separate different fields of the various assemblages. Lal and Moorhouse (1969) had indicated that cordierite-gedrite-bearing rocks, in nature, will be formed when the K_2O content of the rock is low and the $(MgO + MnO + FeO)/((Al_2O_3 - (Na_2O + 2CaO))$ ratio is high. We shall explore the possibility by plotting these two variables, one against the other, to see if different fields of various assemblages can be separated. As is evident from Figure 13, the samples containing different mineral assemblages can be separated into different fields. Thus samples with high $(MgO + FeO + MnO)/((Al_2O_3 - (Na_2O + 2CaO))$ and low K_2O contents give rise to cordierite-gedrite and cummingtonite-bearing rocks. When the K_2O values are higher and the values of the other parameter are lower, aluminosilicate-bearing rocks will be formed. Rocks containing assemblages of cordierite-biotite and cordierite-garnet-biotite occupy an intermediate position. The boundary defined in the figure is quite arbitrary. The negative slope of line A of

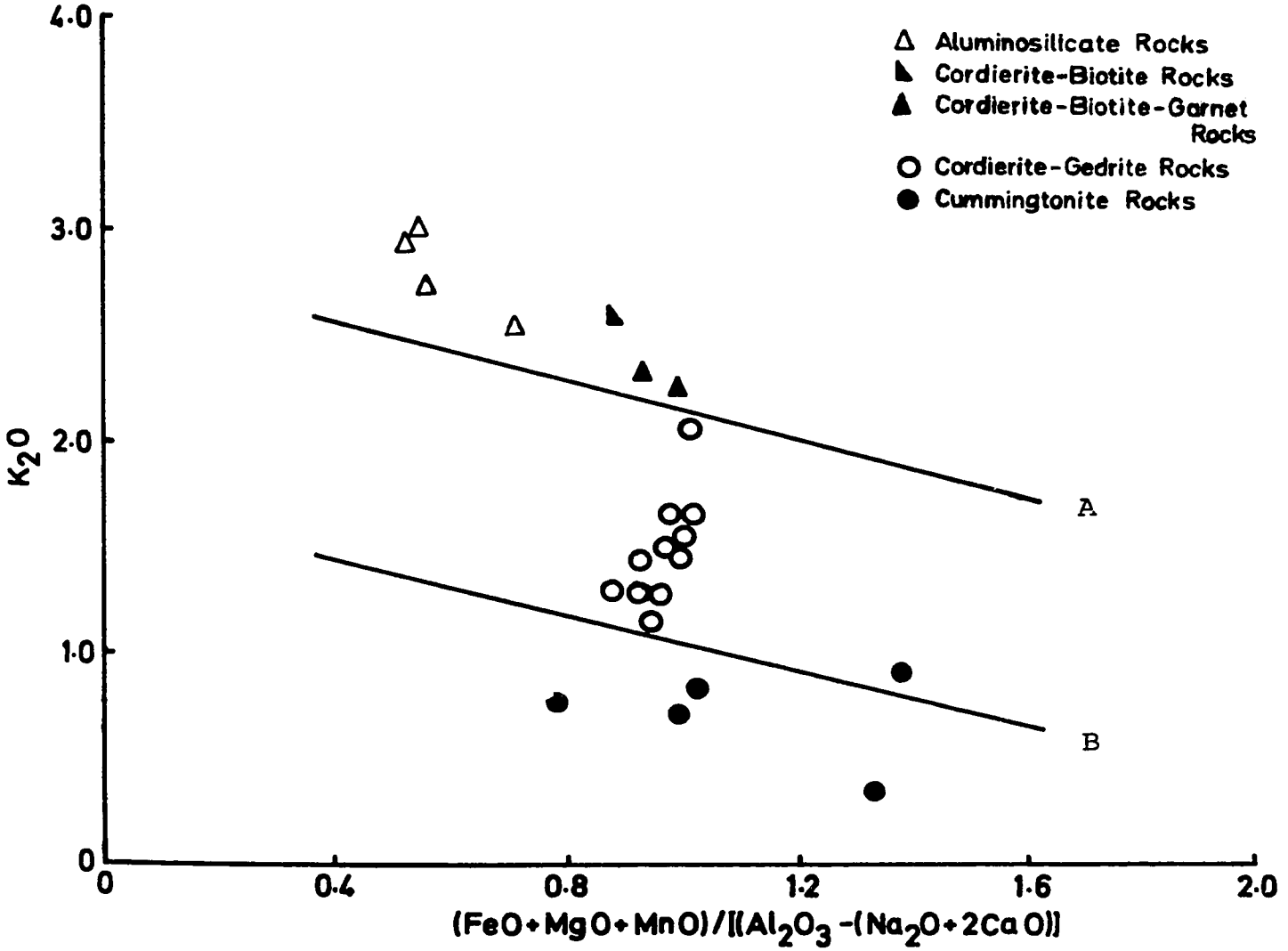

Figure 13. Diagram representing the different compositional fields of various assemblages.

Figure 13 is obtained from Figure 16: reasons for this are given below. Line B was drawn parallel to line A.

Factors Controlling the Appearance of Cordierite

Cordierite-bearing assemblages are commonly found in thermal aureoles, and consequently it has been treated as an antistress mineral by Harker (1939). However, Read (1952), Miyashiro (1961) and Zwart (1963) showed that this mineral can also grow under conditions of regional metamorphism. This is further substantiated by the experimental work of Schreyer and Yoder (1964) where they covered conditions of both contact and regional metamorphism.

Wynne-Edwards and Hay (1963) and Winkler (1965) suggested that cordierite in regional metamorphism forms in lime-poor and Mg-rich rocks, which are somewhat rare in nature. It is noteworthy that in metamorphic aureoles (Chinner, 1959, 1962) and low pressure metamorphism (Hess, 1969), the compositional range of cordierite is much wider, and in these environments, cordierite can form in rocks of normal composition.

Chinner (1959) has defined the field of coexisting cordierite and garnet from different environments, as shown in Figure 14. The data of the present study (analyses given in Tables 8 and 16, pages 91 and 118),

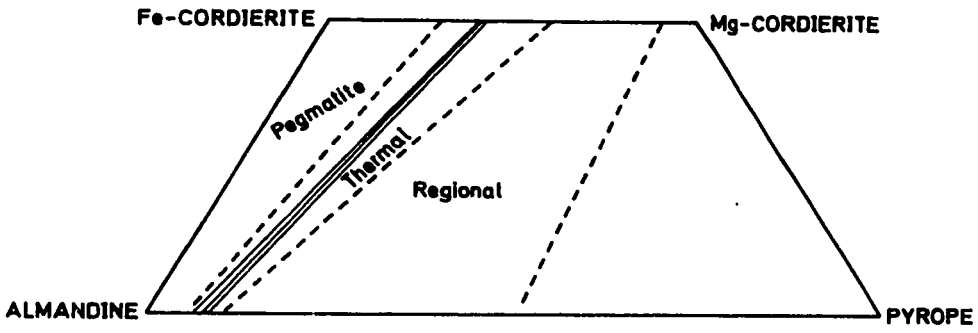

Figure 14. Compositional fields of coexisting garnet and cordierite in different metamorphic environments.

when plotted on this diagram, fall in the thermal metamorphic field; accordingly a wider range bulk composition favorable to the formation of cordierite is expected. The writer has noted earlier (Chapter II) that the coexisting cordierite and garnet of the present study did not crystallize in response to the intrusion of the Sparrow Lake pluton, but that these minerals are for the most part, products of a low pressure regional metamorphism. Therefore, the thermal metamorphic field of Chinner's diagram should possibly cover cordierite-garnet pairs from low pressure regional metamorphism as well.

Factors Controlling the Crystallization of Garnet

Almandine coexisting with cordierite and biotite (with or without gedrite) is stable in both thermal metamorphism (Eskola, 1914; Simonen, 1948; Gelman, 1963) and regional metamorphism (Pye, 1957; Heitanan, 1959; Sims and Gable, 1963).

Two factors have been suggested to explain the occurrence of garnet in different metamorphic environments, namely physical conditions and chemical composition. Harker (1939) and Turner (1948) considered that in the vicinity of high level intrusions, where hydrostatic or near hydrostatic pressures prevail,

garnet will be formed. On the other hand, Eskola (1914, 1915) and Chinner (1959, 1962) showed that a high Fe/Fe + Mg ratio of the rock favors the formation of garnet, because of the limited solubility of FeO in cordierite. Turner and Verhoogen (1961) also suggested that high FeO/MgO ratios of the rock are necessary for the formation of garnet. According to Wynne-Edwards and Hay (1962) and Reinhardt (1968) CaO and oxidation would permit the formation of garnet in the cordierite-biotite rocks.

At Yellowknife, the occurrence of garnet is restricted to certain beds, and bulk compositional differences obviously played a prominent role in its formation. In general, the scarcity of almandine garnet in thermally metamorphosed aureoles is a consequence of the restricted compositional field in which garnet can form under such conditions (Chinner, 1959, 1962).

Considering the compositional parameters that might have stabilized garnet in rocks of the present study, it is found that the differences of these parameters between garnetiferous and non garnetiferous rocks is small. Only the difference in average oxidation ratio between garnetiferous and alumino-

silicate rocks is prominent, but this cannot be considered as a parameter that might have stabilized garnet in view of the wide range of oxidation ratios within the garnetiferous rocks. Other variables such as the MnO content of the rock may also be considered. It is interesting to note that a plot of the weight percents of garnet (enumerated in Table 3) plotted against the MnO content of the rock (Fig. 15) shows a correlation which suggests that the MnO content of the rock did indeed control the formation of garnet to some extent. The analyses of cummingtonite-bearing rocks also shows higher MnO contents. These rocks contain garnet occasionally. The frequent occurrence of garnet in these rocks has been noted about 100 Km to the east of the study area near Benjamin Lake (A. Davidson, personal communication).

The importance of MnO in the stabilization of garnet may be analysed furthermore by considering the assemblage garnet-cordierite-gedrite-biotite. Considering this assemblage in terms of an AFM projection, it contains an excess phase. This additional phase cannot be related to retrograde reactions or a relict phase. Texturally, garnet is observed to be enclosed in cordierite which may be considered as a relict phase. But at the same time

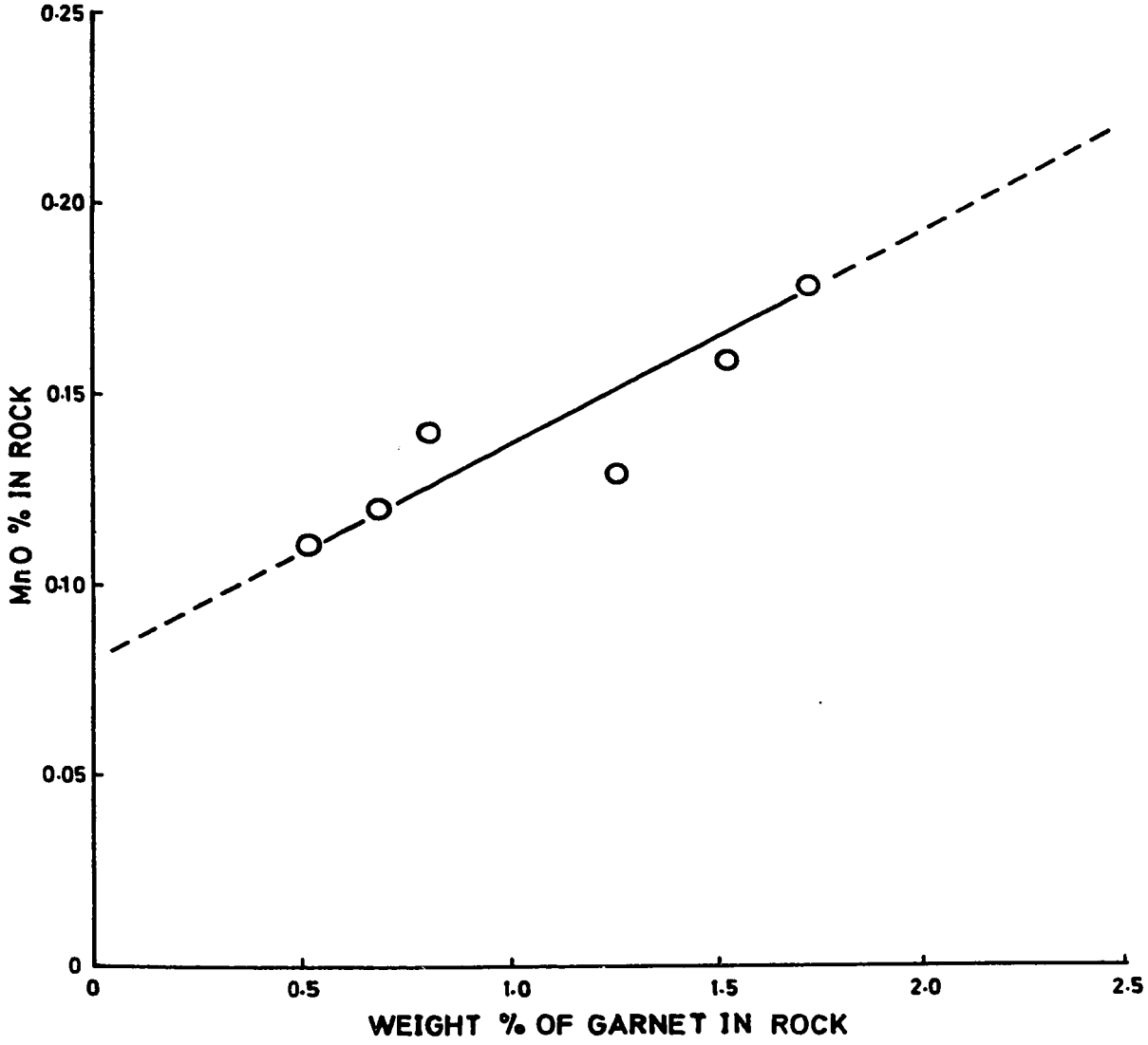

Figure 15. Figure showing the relation between MnO content of the rock and weight percent of garnet

fresh euhedral crystals of this mineral are also observed. On this account other possibilities appear to be more important. The garnet analyses presented below shows that they contain appreciable amounts of MnO and some CaO, thus deviating from the pure Fe-Mg system. As a consequence of this almandine would be stabilized beyond the range of conditions and bulk compositions in which it would occur, if it were a pure Fe-Mg system. Miyashiro (1953) suggested that almandine in the low pressure metamorphic terrains would be richer in Mn. Hsu (1968) had shown that Mn-garnet can occur at high temperatures. Green (1963) also found garnets close to the composition of those of Yellowknife in an assemblage staurolite-garnet-biotite-sillimanite from New Hampshire, and suggested that the presence of garnet is possibly due to high Mn contents. Therefore, it appears, as suggested by Miyashiro (1953), in low pressure metamorphic terrains garnet contains high concentrations of Mn and further may possibly occur as an additional phase.

Compositional Controls on the Cummingtonite-bearing Rocks

Cummingtonite-bearing rocks occur as thin layers and ellipsoidal lenses parallel to bedding and as silicified material along minor slip planes. Originally,

these rocks might have been thin acidic sills and dykes, or siliceous material extracted by concretionary growth during diagenesis, and silicification along slip planes of foliation and/or bedding. The details and mechanism of how this material was formed is not the scope of this study. It is only attempted here to define the compositional characteristics of the material that favour the formation of cummingtonite in the study area.

Chemical analysis was performed on two kinds of rocks that contain cummingtonite; a. thin layers (samples 24 and 286) and b. concretionary like masses (samples 143A and 173A). In the second variety biotite is absent at the core, where K_2O concentrations are low (107 and 173A) and is present at the outer rims when K_2O concentrations are relatively higher (107b and 173A,b). The weight percent of cummingtonite changes from core to the rim of these concretions. At the core, cummingtonite is finer and more abundant while at the border, it is coarser and relatively less abundant (see Appendix V).

A comparison of the analyses of cummingtonite-bearing rocks with those of gedrite-bearing rocks shows strong similarities, except for higher CaO and

Table 6: A Chemical Analysis of Cummingtonite-bearing Rocks

	24	107a	107b	173a	173b	286
SiO_2	67.40	65.23	65.75	65.30	66.00	66.89
Al_2O_3	15.17	16.04	17.12	17.27	17.48	18.05
TiO_2	0.95	1.06	1.01	0.84	0.69	0.68
FeO	5.57	6.79	5.80	5.38	4.00	5.16
MgO	2.75	2.89	2.27	2.38	1.78	2.22
MnO	0.14	0.13	0.11	0.12	0.06	0.09
CaO	2.66	2.89	2.45	2.91	2.68	1.94
Na_2O	3.70	3.24	3.76	4.04	4.58	4.06
K_2O	0.92	0.35	0.73	0.26	0.79	0.86
Total	99.26	98.62	99.00	98.50	98.06	99.89

SiO_2,Al_2O_3 and TiO_2 by R. Patchineelam, Institut für Mineralogie, Darmstadt, West Germany.

Others by: D.C. Kamineni

lower K_2O contents in the former. Perhaps, on account of this similarity, gedrite is found in a few cases in these rocks at higher grades. The higher CaO content of these rocks is accompanied by higher An content (An_{29-36}). The crystallization of more anorthite molecule in plagioclase in these rocks would naturally consume larger amounts of Al_2O_3. Thus the free Al_2O_3 available to go into the structures of gedrite or cordierite will be limited. The most feasible ferromagnesian mineral to form under these conditions would be cummingtonite.

Cordierite-Gedrite-Bearing Rocks

The origin of cordierite-gedrite-bearing rocks has been a subject of interest since Eskola (1914) first described them from the Orijarvi area in Finland. The difficulty in understanding the origin of these rocks arises in accounting for the origin of original material, as there are no chemical equivalents found in the known varieties of igneous and sedimentary rocks. The compositional field of cordierite-gedrite-bearing rocks, described so far, can be defined by a system containing SiO_2-Al_2O_3-FeO-MgO, the main characteristics being the paucity of alkalies. On account of these rare bulk compositions one has to resort to the processes that concentrate

these elements, either prior to or during the formation, in accounting for the origin.

Numerous varieties of rock types have been considered to be the original constituents of the cordierite-gedrite rocks. For example, salic tuff and lava with leptite (Eskola, 1914; Osborne, 1939; Bugge, 1943), intermediate or mafic tuff (Tilley and Flett 1930; Tilley 1935; Wilson 1935; Bugge 1943), calcareous shale or limestone intercalated with spilitic tuff (Reynolds, 1947) salic plutonic rocks (Kuroda, 1954), ultramafic rocks contaminated by aluminous rocks (Prider, 1940) and argillaceous rocks intercalated with leptite and sandy rocks (Tuominen and Mikkola, 1950).

The earliest theories to explain the formation of these rocks dealt with Mg-Fe metasomatism (Sundius, 1935; Bugge, 1943; Geijer, 1963), and leaching of alkalies. Eskola favoured both these theories. Tilley and Flett (1930) proposed weathering prior to metamorphism, whereas Tuominenn and Mikkola (1950) advocated structural movements during early stages of metamorphism. Vallance (1967) convincingly showed that isochemical metamorphism of pillow lavas can give rise to these rocks. Recently some workers took

a different approach, originally proposed by Eskola (1933), Barth (1933) and Sorby (1964) by considering the phenomena of partial melting as a possible mechanism in concentrating the suitable bulk compositions. This hypothesis applies to migmatitic and high grade metamorphic terrains. Grant (1967) from a theoretical and experimental point of view, and Lal and Moorhouse (1969) with a field example, elegantly demonstrated how this process accomplishes the formation of cordierite-gedrite-bearing rocks. Consequently, cordierite-gedrite-bearing rocks can be produced from almost any kind of rock, of course by number of different ways.

Cordierite-gedrite-bearing rocks of the present study are restricted to certain beds in the metasediments. The transition from these rocks to those that do not contain gedrite is very sharp and at times can be noted in the size of a hand specimen. The restricted occurrence of these rocks suggests that bulk compositional differences have strongly influenced the paragenesis.

Whether the rocks containing cordierite and gedrite attained suitable bulk compositions before or during metamorphism will now be considered. Chemically, the cordierite-gedrite-bearing rocks from the study

area are somewhat different from the rocks that have been described earlier by most of the other workers; they differ especially in containing a large amount of Na_2O, and a relatively higher amount of CaO and K_2O. This is reflected by the presence of minerals such as sodic oligoclase and biotite. The common opaque mineral is ilmenite, with local pyrrhotite and magnetite.

Theories proposed by other workers do not appear to apply to the Yellowknife rocks. Since there is no regional migmatization in the area, the Fe-Mg metasomatism can be ruled out. As these rocks contain low ratios of Al_2O_3 / Na_2O (≈ 5) and some Ca and K, the original material was immature with reference to weathering. Hence weathering prior to sediment transport and deposition was not an effective process. Nowhere are these rocks observed to possess a phacolithic shape in the crests of the folds, and therefore, the process of concentration of elements by deformation is not in evidence. Finally, the separation of alkalies by anatectic melting is precluded as these rocks are not poor in Na_2O and also not completely free from K_2O. Further, no evidences of partial melting are found.

The bulk chemical analyses (Table 4) of the rocks shows that they are relatively impoverished in potash and somewhat enriched in soda. When this analysis is compared with the least metamorphosed greywackes and also lower grade equivalents, it appears that the compositional characteristics were evolved during the process of sedimentation and diagenesis. These rocks are confined to the lower and hence the coarser horizon of the turbidite sequence, and as has been mentioned earlier there is a remarkable compositional difference between the lower and upper horizons, except for the CaO contents. Henderson (1972) and this study found that the upper fine argillitic horizons of the turbidite sequence are richer in K_2O and Al_2O_3 while the lower and coarser horizons are poorer in these constituents. As the analysis of cordierite-gedrite-bearing rocks compare well with those of the unmetamorphosed greywackes (see Table 4), the low potash contents in the greywackes was accomplished during sedimentation itself. In addition to the chemical sorting during sedimentation, changes in provenance also must have influenced the compositional differences. The source material varies over a wide range, varying from

basic to acidic volcanics and also granodioritic material in the area (Henderson, 1972). Naturally, material derived from a granodioritic or acidic (dacitic) volcanic source would be impoverished in K_2O.

The relatively high amounts of Na_2O and low CaO contents seem to be characteristic of Archean greywackes. In case of the Early Precambrian greywackes of Wyoming, Condie (1967) proposed the following reaction between clastic plagioclase and Na ions in sea water (or interstitial water) to account for the observed compositions:
$2Na + 4SiO_2 + CaAl_2Si_2O_8 \rightleftharpoons 2NaAlSi_3O_8 + Ca^{2+}$ (in aqueous solution).

A reaction of this type would satisfactorily explain the loss of Ca and enrichment of Na in the greywackes. Therefore, the writer concludes that the observed bulk compositions of the cordierite-gedrite-bearing rocks were achieved during the process of sedimentation and diagenesis.

Compositional Field of Cordierite-Gedrite-bearing Rocks in Nature

The cordierite-gedrite-bearing rocks are known to occur, irrespective of the original material and mode of formation, in rocks that are poor in potash

and are characterized by high values of the ratio $(MgO + MnO + FeO) / ((Al_2O_3 - (Na_2O + 2CaO))$ (Lal and Moorhouse 1969). An attempt is made here to decipher the compositional field of these rocks, in relation to these two variables. For this purpose the analytical data of Tilley (1935, 1937), Prider (1940), Seki (1957), Froese (1963), Vallance (1967) and Lal and Moorhouse (1969) were collected and plotted in Figure 16. It is obvious from Figure 16 that these rocks do define a compositional field. Although all the analyses falls below a straight line of negative slope, some irregularities should be pointed out on this diagram. In the region A, andalusite-biotite and plagioclase rocks would form while in region B plagioclase-biotite rocks would form.

The two variables, K_2O and $(FeO + MgO + MnO) / ((Al_2O_3 - (Na_2O + 2CaO))$ may be related by an equation that defines the range of values K_2O can take. Let $Y = K_2O$ and $X = (FeO+MgO+MnO) / ((Al_2O_3 - (Na_2O + 2CaO))$. For $X \geq 0.7$, Y may take a range of values defined by $0 \leq Y \leq -0.77X + 3.02$.

From this relation, it may be concluded that when the bulk compositions satisfy the above equation, cordierite-gedrite-bearing rocks would form in nature,

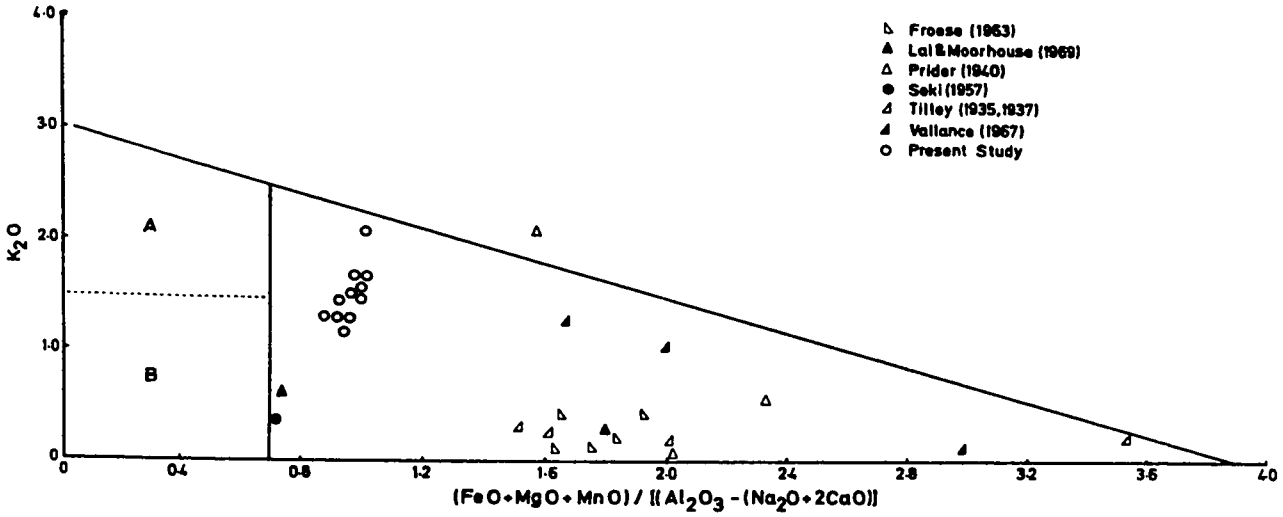

Figure 16. Diagram showing the compositional field of cordierite-gedrite bearing rocks in nature.

provided that approximate P-T conditions exist.

Conclusions

Original bulk compositional differences played a dominant role in the development of various mineral assemblages. Nevertheless, the zonal arrangement of these minerals around the Sparrow Lake pluton indicates that physical conditions also certainly played a major role in the development of these minerals. For example, east of the Sparrow Lake, gedrite is restricted to a zone. The absence of cordierite-gedrite-bearing rocks beyond the gedrite zone and above the cordierite isograd is not due to the lack of rocks of suitable bulk composition, but due to differences in physical conditions. It has been shown in the previous sections that gedrite grew under static conditions, mainly under the influence of the Sparrow Lake pluton, while the cordierite near the cordierite isograd grew during the late synkinematic (D_2) stage of deformation under dynamic conditions. The temperatures associated with the formation of cordierite-gedrite-bearing rocks were probably also higher as may be expected from the progressive nature of the metamorphism.

From the above discussion, it may be concluded

that there are certain limits of physical conditions beyond which minerals like gedrite and sillimanite will not form, no matter how favourable the composition of the rock might be.

MINERALOGY

Introduction

A detailed study of some of the minerals has been carried out in the study area. The main aspects that are discussed here are the chemistry of biotite, cordierite, gedrite, cummingtonite, garnet, plagioclase and andalusite, and the structural state of cordierite.

The structural state of cordierite and hence the ordering of Al and Si in this mineral was determined by using X-ray diffraction techniques. The ordering of Fe^{2+} in gedrite and cummingtonite was examined in terms of site populations, employing the Mössbauer techniques. The oxidation state of iron in these minerals was also confirmed by this method. In addition, X-ray diffraction work on the amphiboles was performed mainly to establish the presence of gedrite and other species. Information on the X-ray and Mössbauer methods are given in Appendices III and IV.

Biotite

Biotite occurs over a wide range of metamorphic environments. It has a general formula $X_2Y_6Z_8O_{20}W_4$, where the principal substitutions are X = K, Na, Ca; Y = Fe^{+2}, Mg, Al, Mn^{+2}, Ti^{+4}, Fe^{+3}; Z = Al, Si and W = $(OH)^{-1}$, O^{-2}, F^{-1}. Atoms in the X-site are coordinated by 12

oxygens, Y by 6 oxygens and Z by 4 oxygens. Structural investigations on biotite crystals intermediate between Fe and Mg end-members, that approximate to the biotite compositions of metamorphic pelites is lacking, and hence the information on the ordering of elements within the octahedral sites is not known.

The composition of metamorphic biotite can be approximated in terms of four end-members: phlogopite $K_2Mg_6Al_2Si_6O_{20}(OH)_4$, annite $K_2Fe_6Al_2Si_6O_{20}(OH)_4$, eastonite $K_2Mg_5AlAl_3Si_5O_{20}(OH)_4$ and siderophyllite $K_2Fe_5AlSi_5Al_3O_{20}(OH)_4$ (Winchell, 1951; Deer, Howie and Zussman, 1962). In this series Fe^{+3} is included in Al^{+3} and the Ti is disregarded.

Analysis of biotite from the study area was carried out on a Techtron AA4 model atomic absorption spectrophotometer. The elements analysed by this technique are Fe, Mg, Mn, Li, K and Zn. Si, Al and Ti were determined on an ARL electron microprobe. In addition a few Fe_2O_3 determinations were performed by titrimetric methods. Mineral separation, sample purity, analytical procedure and accuracy are discussed in Appendices I and II.

An inspection of the analysis given in Table 7 shows that the sums of weight percentages of oxides

Table 7: Chemical Composition of Biotites

	3	12	14	21	27	32	39	41	52	62	69	74	78	109	120	151A	171	197	2	24	107b	139b	143A,b	173A,b	286	84
SiO_2	36.50	36.92	36.90	37.20	36.33	36.80	36.50	37.80	36.80	35.50	37.52	36.51	37.50	37.50	35.31	36.00	36.40	37.89	n.d.	n.d.	n.d.	n.d.	n.d.	n.d.	n.d.	n.d.
TiO_2	1.95	1.73	1.73	1.81	1.67	1.68	1.77	1.45	1.60	2.21	1.85	1.62	1.65	1.67	1.81	1.88	1.58	1.61	n.d.	n.d.	n.d.	n.d.	n.d.	n.d.	n.d.	n.d.
Al_2O_3	20.73	18.06	17.29	17.13	17.69	17.28	17.99	16.77	17.31	18.93	18.62	16.67	16.82	15.60	18.36	18.57	17.68	16.94	n.d.	n.d.	n.d.	n.d.	n.d.	n.d.	n.d.	n.d.
Fe_2O_3	n.d.	n.d.	4.18	n.d.	n.d.	n.d.	3.14	n.d.	n.d.	3.10	n.d.	n.d.	n.d.	n.d.	n.d.	n.d.	4.45	n.d.	n.d.	n.d.	n.d.	n.d.	n.d.	n.d.	n.d.	n.d.
FeO	18.04	19.58	15.23	19.91	18.17	19.45	18.56	18.01	19.30	18.01	18.65	19.93	18.62	18.93	21.68	20.80	17.67	18.01	17.42	18.66	17.77	18.95	18.05	17.37	17.50	18.60
MnO	0.14	0.14	0.12	0.09	0.10	0.08	0.13	0.15	0.09	0.12	0.16	0.11	0.10	0.11	0.11	0.17	0.12	0.14	0.13	0.10	0.12	0.09	0.10	0.09	0.12	0.14
MgO	9.82	11.42	10.82	9.95	12.02	10.69	9.62	11.73	11.40	9.28	9.06	11.60	11.60	11.07	9.03	10.36	9.70	9.86	10.28	10.60	9.50	9.91	9.05	9.27	9.20	11.40
CaO	0.27	0.16	0.23	0.18	0.16	0.27	0.22	0.19	0.20	0.18	0.28	0.15	0.23	0.18	0.22	0.21	0.21	0.21	0.28	0.19	0.40	0.45	0.24	0.31	0.35	0.20
Li_2O	0.04	0.04	0.03	0.05	0.04	0.04	0.03	0.18	0.04	0.01	0.07	0.03	0.03	0.04	0.03	0.03	0.04	0.04	0.06	0.05	0.03	0.03	0.04	0.03	0.02	0.04
Na_2O	0.35	0.34	0.44	0.27	0.44	0.55	0.30	0.43	0.30	0.24	0.30	0.35	0.58	0.88	0.28	0.24	0.34	0.41	0.66	0.47	0.55	0.62	0.71	0.96	0.76	0.40
K_2O	8.65	8.81	8.72	8.69	8.28	8.20	8.63	8.43	8.35	10.02	8.45	8.78	8.17	8.49	9.03	9.02	8.71	8.88	8.00	8.15	7.91	7.77	7.51	7.65	7.69	7.89
Total	95.49	97.20	95.69	95.28	94.90	95.04	96.89	95.14	95.39	97.65	94.96	95.70	95.30	94.52	95.86	97.33	96.90	93.77	36.83	38.22	36.28	37.72	35.90	35.68	35.64	38.57
Zr in ppm	380	320	350	330	370	350	420	390	400	410	420	400	400	380	425	420	440	430	310	350	320	300	300	300	310	350

Table 8: Chemical Composition of Cordierites

	3	12	14	21	32	39	41	52	62	69	74	78	120	151A	171	197
SiO_2	48.15	48.91	49.10	47.50	48.94	47.60	49.97	48.00	49.60	47.50	48.00	47.91	48.93	49.05	47.68	46.95
Al_2O_3	31.67	31.25	29.95	33.05	32.00	31.55	30.68	32.50	31.01	31.68	32.02	32.11	29.66	31.83	33.00	31.80
FeO	8.04	8.27	7.35	8.09	7.69	8.97	7.03	7.20	7.57	8.61	7.71	7.79	9.68	8.40	8.92	9.15
MnO	0.33	0.32	0.22	0.28	0.10	0.30	0.40	0.26	0.48	0.35	0.20	0.19	0.49	0.05	0.15	0.38
MgO	8.39	8.26	8.32	8.54	8.46	8.26	7.96	8.78	7.50	8.21	8.78	9.23	7.70	7.01	6.95	7.73
CaO	0.30	0.38	0.35	0.22	0.16	0.32	0.20	0.33	0.24	0.32	0.17	0.16	0.31	0.40	0.28	0.31
Na_2O	0.30	0.41	0.57	0.46	0.68	0.47	0.59	0.61	0.35	0.51	0.62	0.51	0.30	0.32	0.40	0.44
K_2O	0.52	0.31	0.71	0.45	0.60	0.31	0.40	0.46	0.69	0.81	0.60	0.33	0.66	0.74	0.68	0.70
Total	97.70	98.81	96.57	98.47	98.50	97.67	97.23	98.04	97.44	97.99	98.06	98.23	97.73	97.80	98.06	97.46

n.d. not determined, where Fe_2O_3 not determined total Fe expressed as FeO.

FeO in Biotites 14, 39, 62, and 171 by Dr. N. Suhr, Pennsylvania State University

Others by D.C. Kaminsni.

Table 9: Chemical Composition of Gedrites

	21	32	14	27	41	52	74	78	109
SiO_2	43.64	43.50	43.20	44.12	42.62	44.00	43.80	44.50	42.10
TiO_2	0.31	0.25	0.28	0.29	0.34	0.20	0.11	0.23	0.20
Al_2O_3	16.42	18.50	15.20	13.61	15.57	14.62	17.60	12.27	16.70
Fe_2O_3	1.26	n.d.	n.d.	n.d.	n.d.	n.d.	n.d.	n.d.	n.d.
FeO	24.52	23.54	25.41	26.05	25.81	25.73	23.00	27.88	26.81
MnO	0.77	0.44	1.06	0.88	1.20	0.76	0.84	0.81	1.03
MgO	8.95	7.89	10.18	12.35	11.52	11.72	9.53	11.94	9.45
CaO	0.42	0.59	0.31	0.38	0.38	0.24	0.36	0.34	0.50
Na_2O	1.23	1.64	0.99	0.71	0.92	0.90	0.85	0.84	1.67
K_2O	0.20	0.28	0.12	0.09	0.11	0.08	0.14	0.09	0.15
H_2O	2.36	2.59	2.67	2.50	2.11	2.65	2.80	2.30	2.19
Total	100.08	99.22	99.42	100.98	100.58	100.90	99.03	101.20	100.80
Zn in ppm	310	330	350	400	400	420	370	420	380

Table 10: Number of Cations in Biotite on the basis of 22 Oxygen Ions

	3	12	14	21	27	32	39	41	52	62	69	74	78	109	120	151A	171	197
Si	5.402	5.490	5.525	5.851	5.780	5.581	5.595	5.678	5.556	5.306	5.651	5.535	5.642	5.726	5.402	5.390	5.450	5.490
Al	2.598	2.510	2.475	2.149	2.220	2.419	2.405	2.322	2.444	2.694	2.349	2.465	2.358	2.274	2.598	2.610	2.550	2.510
Σ	8.000	8.000	8.000	8.000	8.000	8.000	8.000	8.000	8.000	8.000	8.000	8.000	8.000	8.000	8.000	8.000	8.000	8.000
Al	1.018	0.655	0.575	0.914	0.825	0.670	0.845	0.647	0.637	0.649	0.956	0.515	0.624	0.533	0.713	0.666	0.570	0.641
Ti	0.217	0.193	0.193	0.206	0.184	0.191	0.203	0.163	0.181	0.248	0.209	0.184	0.186	0.192	0.208	0.211	0.211	0.190
Fe^3			0.472				0.361			0.348							0.500	
Fe^2	2.232	2.435	1.907	2.526	2.298	2.467	2.379	2.262	2.437	2.251	2.349	2.521	2.343	2.423	2.770	2.604	2.212	2.296
Mn	0.017	0.017	0.014	0.011	0.013	0.012	0.016	0.020	0.011	0.014	0.020	0.016	0.013	0.014	0.014	0.021	0.014	0.017
Mg	2.166	2.531	2.249	2.249	2.707	2.416	2.197	2.626	2.565	2.067	2.034	2.622	2.600	2.519	2.058	2.311	2.164	2.242
Li	0.022	0.024	0.018	0.028	0.051	0.024	0.018	0.108	0.023	0.005	0.021	0.018	0.018	0.012	0.018	0.018	0.024	0.024
Y	5.673	5.857	5.594	6.060	5.590	5.780	6.019	5.826	5.854	5.582	5.589	5.874	5.784	5.673	5.785	5.831	5.661	5.898
Ca	0.043	0.037	0.037	0.029	0.012	0.044	0.036	0.030	0.032	0.029	0.044	0.024	0.037	0.029	0.036	0.041	0.033	0.034
Na	0.100	0.078	0.126	0.078	0.127	0.160	0.088	0.124	0.087	0.068	0.087	0.102	0.168	0.259	0.083	0.068	0.097	0.121
K	1.633	1.671	1.665	1.681	1.595	1.586	1.688	1.614	1.608	1.910	1.624	1.699	1.578	1.653	1.761	1.722	1.663	1.727
X	1.773	1.792	1.828	1.788	1.734	1.790	1.812	1.768	1.727	2.007	1.755	1.825	1.773	1.941	1.880	1.831	1.793	1.882

Table 11: Number of Cations in Cordierite on the basis of 18 Oxygens

	3	12	14	21	32	39	41	52	62	69	74	78	120	151A	171	197
Si	5.065	5.075	5.162	4.916	5.043	4.985	5.191	4.966	4.952	4.968	4.784	4.959	5.141	5.100	4.953	4.947
Al	0.935	0.925	0.838	1.084	0.957	1.015	0.809	1.033	1.048	1.032	1.216	1.041	0.859	0.900	1.047	1.053
Σ	6.000	6.000	6.000	6.000	6.000	6.000	6.000	6.000	6.000	6.000	6.000	6.000	6.000	6.000	6.000	6.000
Al(Y)	2.945	2.893	2.568	2.949	2.930	2.878	2.946	2.930	2.668	2.873	2.545	2.877	2.814	3.001	3.000	2.897
Fe^2	0.738	0.717	0.646	0.700	0.663	0.785	0.613	0.623	0.632	0.753	0.642	0.674	0.850	0.730	0.777	0.806
Mn	0.002	0.028	0.016	0.016	0.009	0.026	0.035	0.024	0.040	0.030	0.017	0.016	0.004	0.004	0.013	0.034
Mg	1.251	1.276	1.303	1.317	1.297	1.273	1.232	1.353	1.116	1.280	1.298	1.424	1.205	1.086	1.179	1.214
Ca	0.033	0.042	0.039	0.024	0.015	0.035	0.022	0.036	0.029	0.036	0.018	0.017	0.035	0.044	0.031	0.035
Na	0.060	0.047	0.115	0.092	0.135	0.094	0.118	0.122	0.068	0.103	0.112	0.102	0.060	0.064	0.080	0.088
K	0.069	0.020	0.095	0.057	0.066	0.040	0.052	0.062	0.082	0.101	0.075	0.044	0.088	0.097	0.090	0.094
X	2.100	2.185	2.214	2.181	2.185	2.253	2.072	2.212	2.030	2.304	2.162	2.277	2.282	2.025	2.116	2.267

Table 12: Number of Cations in Cedrite on the basis of 24 Oxygens

	14	21	27	32	41	52	74	78	109
Si	6.429	6.457	6.490	6.405	6.718	6.350	6.427	6.604	6.278
Al	1.571	1.543	1.510	1.595	1.282	1.650	1.573	1.396	1.722
Σ	8.000	8.000	8.000	8.000	8.000	8.000	8.000	8.000	8.000
Al	1.095	1.320	0.847	1.621	0.646	0.828	1.457	0.750	1.213
Ti	0.031	0.027	0.032	0.030	0.040	0.022	0.024	0.025	0.022
Fe^3		0.130							
Fe^2	3.162	3.034	3.204	2.899	3.402	3.099	2.823	3.469	3.343
Mn	0.133	0.096	0.110	0.049	0.160	0.093	0.110	0.102	0.130
Mg	2.257	1.973	2.707	1.732	2.706	2.515	2.082	2.641	2.099
Ca	0.049	0.066	0.099	0.092	0.066	0.036	0.099	0.053	0.080
XY	6.727	6.655	6.957	6.423	7.018	6.593	6.555	7.031	6.887
Na	0.284	0.352	0.202	0.462	0.280	0.251	0.241	0.241	0.482
K	0.021	0.037	0.016	0.030	0.023	0.014	0.020	0.016	0.027
A	0.305	0.389	0.218	0.492	0.303	0.265	0.261	0.257	0.509
OH	2.651	2.328	2.452	2.541	2.218	2.544	2.740	2.276	2.177

Table 13: Analysis of Plagioclases

Sample No.	Na_2O	CaO
2	6.97	5.81
12	6.93	5.63
14	7.97	5.63
21	8.47	4.65
27	7.87	5.63
32	8.21	5.05
41	7.74	5.57
43	7.06	5.28
52	8.79	3.66
74	8.04	5.45
78	8.24	5.40
109	8.47	4.92
209	9.52	3.61
303	9.95	2.77

fall between 95.04 to 97.67%. This compares well with the weight percentages of oxides without water, given by Deer, Howie and Zussman (1962), for metamorphic biotite crystals. As water is not determined, the analysis for the biotites is recalculated on an anhydrous basis of 22 oxygen atoms. Some of the Al atoms are allocated to tetrahedral sites along with Si so that this site is filled. The number of tetrahedral Al atoms exceeds 2 as may be expected from metamorphic biotites, while the ions occupying the Y site total less than 6 (5.582-6.019). This is reasonable in view of the high Al in the Z position. The inter-layer binding cations in the X site number less than 2 as is frequently the case for metamorphic biotites (Lambert, 1959; Butler, 1967; and Kwak, 1970).

The analyses of biotite (Table 7) show certain compositional variations, especially with regards to Al, Mg and Fe^{+2}. Compositional variations in biotite crystals could be attributed to (1) metamorphic grade (2) mineral paragenesis and (3) differences in original composition of rock. Variation of biotite composition with metamorphic grade has been discussed by numerous workers (see Deer, Howie and Zussman, 1962). Several conflicting trends were found. For example increase

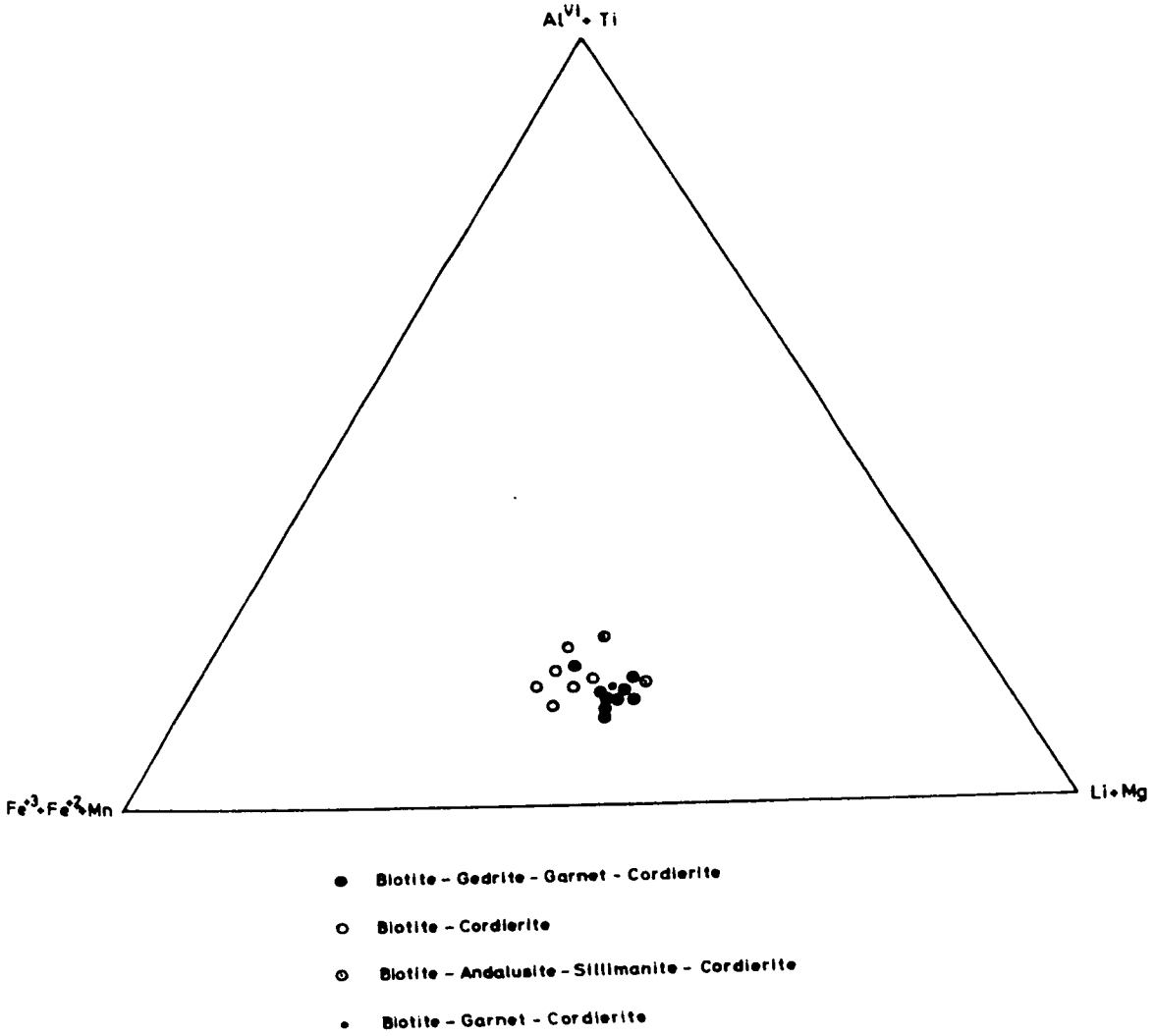

Figure 17. Triangular plot in terms of Fe^{+3}+ Fe^{+2}+ Mn, Li+Mg, and Al^{VI}+Ti representing the compositional field of biotite.

in Mg and decrease in Fe^{+2} and vice versa, increase in Ti and decrease in Al and vice versa with prograde metamorphism. These differences are essentially due to the influence of paragenesis on biotite composition. Bulk compositional differences such as original oxidation state and titanium content could also influence biotite compositions. In this case, however, the several rock specimens analysed show some variation in oxidation and little variation in titanium content. No meaningful correlation was observed when rock oxidation ratio was plotted against M/FM ratio in biotites. It therefore appears that paragenesis has influenced the biotite composition. In order to visualise the compositional variations on the basis of paragenesis, the atomic percentages of Fe^{+2}+ Fe^{+3}+Mn, Al^{vi}+ Ti^{+4} and Mg+Li of biotite are plotted on a triangular diagram. Li was combined with Mg as according to Goldschmidt's rules, it is known to camouflage Mg. The plot (Fig. 17) shows clustering of some samples. The biotite coexisting with gedrite tend to fall towards the Mg+Li corner, whilst the other biotites group towards the Fe+Mn corner of the triangle. On the basis of this plot it may be stated that the influence of paragenesis must be regarded

and taken into account before biotite compositions can be used as an indicator of metamorphic grade.

Cordierite

The mineral cordierite has an ideal formula $X_2^{VI}Al_4^{IV}Si_5^{IV}O_{18}.nH_2O$ and is restricted to certain metamorphic environments. The X-positions in this mineral are occupied by Mg, Fe^{+2}, Mn, Na, Ca and K. Al may be replaced by minor amounts of Fe^{+3}. Some Na and K together with water may go to channels along c-axis. This is particularly true with K which is too big to fit in 6-fold coordination as shown by Folinsbee (1942). Detailed single crystal work (Gibbs, 1966) on low cordierites such as that commonly present in metamorphic rocks, indicates that there is only one octahedral site and hence no ordering of elements is expected in this position. However, Al and Si ordering is recognized in tetrahedral positions. (Gibbs, 1966).

Chemical analysis on the cordierites from the study area was carried out solely on the electron microprobe. Other methods were impossible due to the intense intergrowth with quartz, plagioclase, biotite and opaques. Analysis was carried out for Si, Al, Fe (total), Mg, Ca, Mn, Na and K. The experimental conditions and other details are given in Appendix II.

The analyses (Table 8) are recalculated (Table 11) on the basis of 18 oxygen ions. All the Si is allotted to Z-sites, the remainder (to total 6) being filled with Al. The remaining Al accounts for cations in the Y-site, usually approximate to 3 in number. All the rest of the ions Fe^{+2}, Mg, Mn, Ca, Na and K are allotted to X-sites. The total of these ions in the X-sites (see Table 11) consistently summed up to more than two. This indicates that the allotment of alkali ions such as K and Na to X-sites is not justified. As has been stated by Folinsbee (1942) all the alkali ions must be entering the channels along the Z-direction.

The analyses of cordierites presented in Table 8 show a considerable variation, especially of Fe and Mg. Chemical variation in cordierite with metamorphic grade has so far not been tested. However, compositional differences in various metamorphic environments have been found. Chinner (1962) has shown that Fe/Mg ratios of coexisting garnet-biotite-cordierite in regional metamorphic rocks is fairly low. This has been proved in the works of Heald (1950), Barker (1962), Reinhardt (1968), Lal and Moorhouse (1968), Saxena and Hollander (1969) and Gorbatschev (1968). An opposite trend has been observed in contact

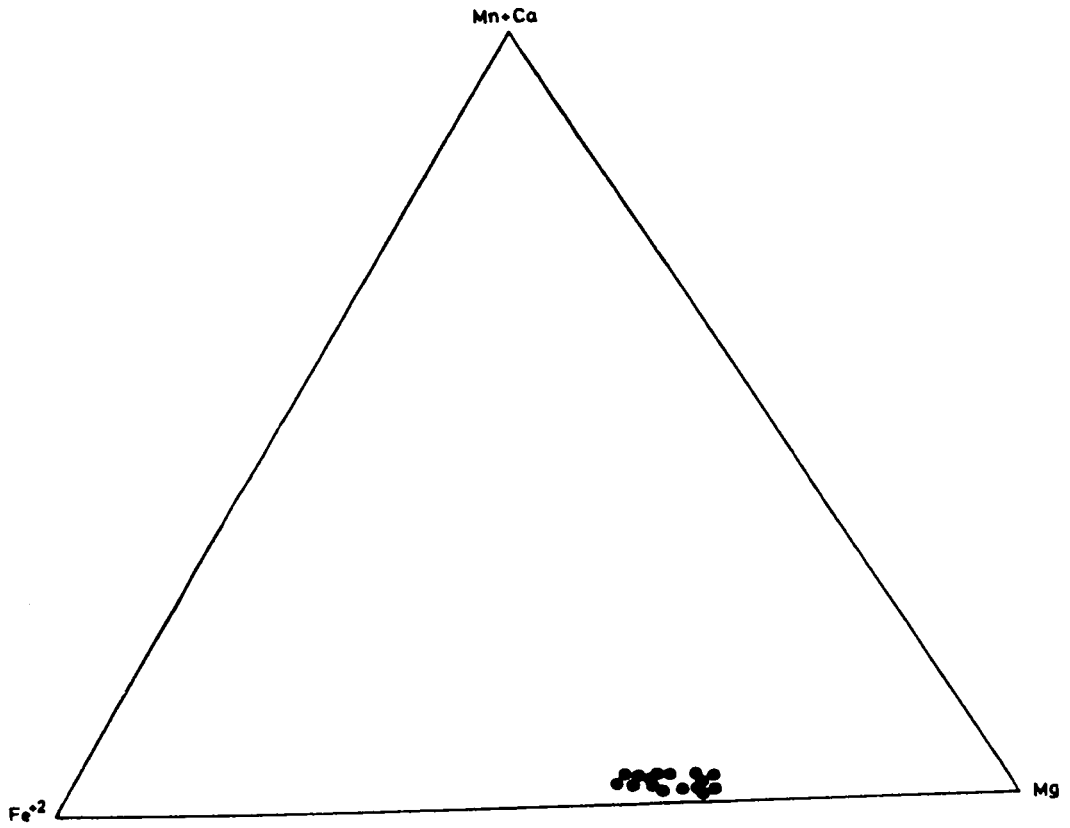

Figure 18. Triangular diagram in terms of Fe^{+2}, Mg and Mn+Ca representing the compositional field of cordierite.

metamorphic rocks as is indicated in the studies of Stewart (1942), Chinner (1962), Best and Weiss (1964) and Okrusch (1971).

The composition of the cordierites is represented on a triangular diagram (Fig. 19) in which the octahedral elements Mg, Fe, Mn and Ca are represented on each of the corners. In this, Ca is included in Mn primarily because of the latter's lower concentrations. By doing this a better plot could be obtained. The plot (Fig. 18) depicts an appreciable variation in Fe and Mg and a little variation in Mn+Ca contents. The cordierites below the gedrite zone are rich in iron and hence they plot towards Fe corner of the diagram.

The Mg/Fe ratios of cordierites are plotted on the geological map (Fig. 19) to determine whether these values correspond to differences in physical conditions. As is evident from the triangular plot (Fig. 18) the Mg/Fe ratios of cordierites (Fig. 19) below the gedrite zone are much lower than the rest, which are richer in iron. The differences in Mg/Fe may be related to the differences in paragenesis. According to Hess (1969), in the simple Fe-Mg system, garnet and alumino-silicate will react under lower pressures to yield cordierite, and in the absence of garnet, cordierite

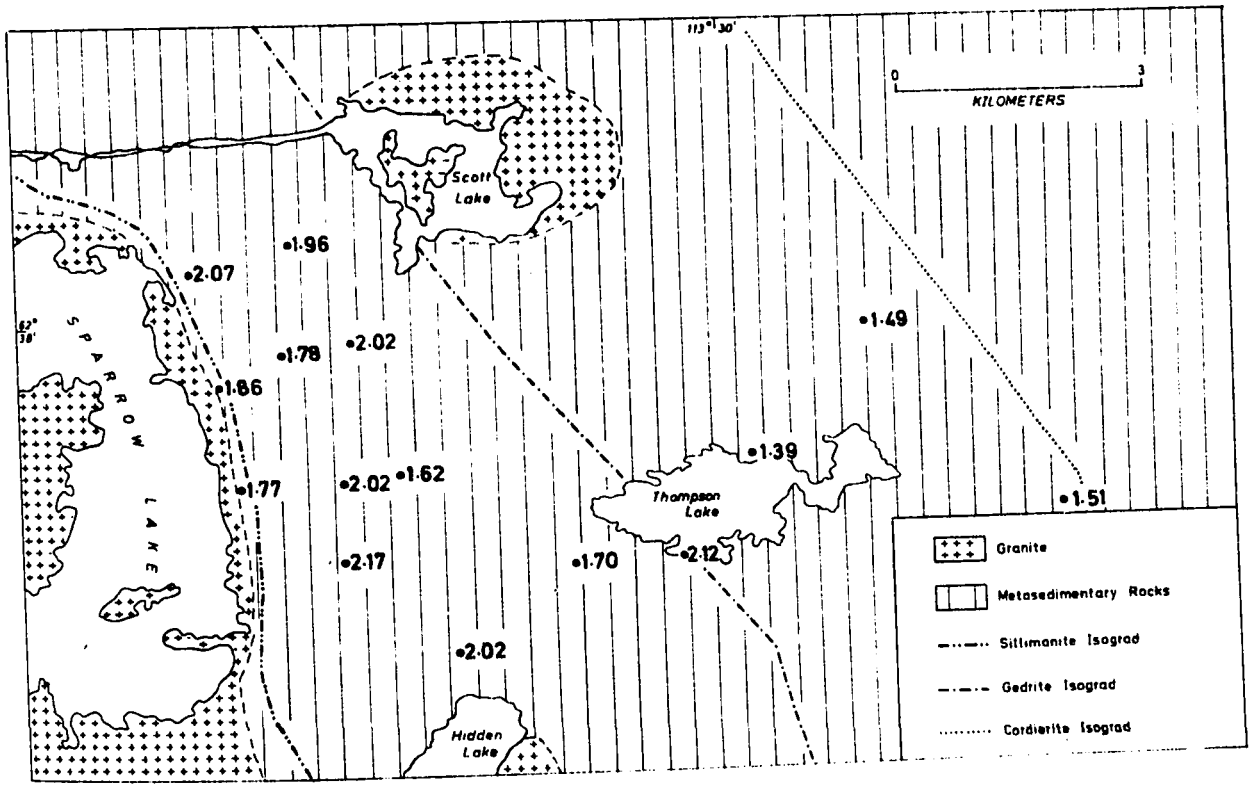

Figure 19. Areal distribution of Mg/Fe ratio in cordierite.

would be Fe rich. On the other hand, when the system contains Mn and Ca, garnet will be stabilized at the expense of Fe cordierite. Most of the cordierites examined above the gedrite zone coexist with garnet while below the gedrite zone garnet is absent. The dependence of Mg/Fe ratios of cordierites on paragenesis may be further evident when we consider sample 39 which falls in the gedrite zone but possesses an Mg/Fe ratio comparable with the cordierites below the gedrite isograd. Sample 39 does not contain any garnet.

Structural State of Cordierite

Miyashiro (1957) found that cordierite forms hexagonal polymorphs and also a continuous series exist from orthorhombic pseudohexagonal to a slightly distorted hexagonal structure. The structural state was defined by Miyashiro in terms of a distortion index, as follows:

$$\Delta = 2\theta_{131} - (2\theta_{511} + 2\theta_{421})/2$$

The distortion index relates the separation of these peaks on a CuKα diffractogram to the deviation from hexagonal geometry of the disordered cordierite (Iiyama, 1956). On the basis of distortion index values Schreyer and Schairer (1961) subdivided Mg-cordierite into high cordierite ($\Delta = 0.0$), intermediate

($0.0<\Delta<0.20$) and low cordierite ($0.20<\Delta<0.30$).

The different states of cordierite were generally believed to be due to the Al and five Si atoms in the Z position, the degree of ordering determining the structural state of cordierite. These cations are ordered in low cordierite, disordered in high cordierites and of intermediate order in intermediate cordierites. Detailed crystallographic work on low cordierite by Gibbs (1965) and Meagher (1967) confirmed the Al-Si cation ordering and a possible Mg and tetrahedral Al ordering at high temperatures.

It has been shown that the distortion index of cordierite is dependent on BeO content (Newton, 1966), water content (Schreyer and Yoder, 1964), and thermal history (Harwood and Larson, 1969).
Despite the fact that the distortion index is affected by water and BeO contents, it can be shown theoretically that the Al-Si order-disorder is directly related to temperature. That is, according to the second law of thermodynamics, entropy will be larger at higher temperatures and hence disorder greater. Thus, it may be stated that under uniform bulk chemistry the structural state of cordierite should yield information on the thermal history of the rocks.

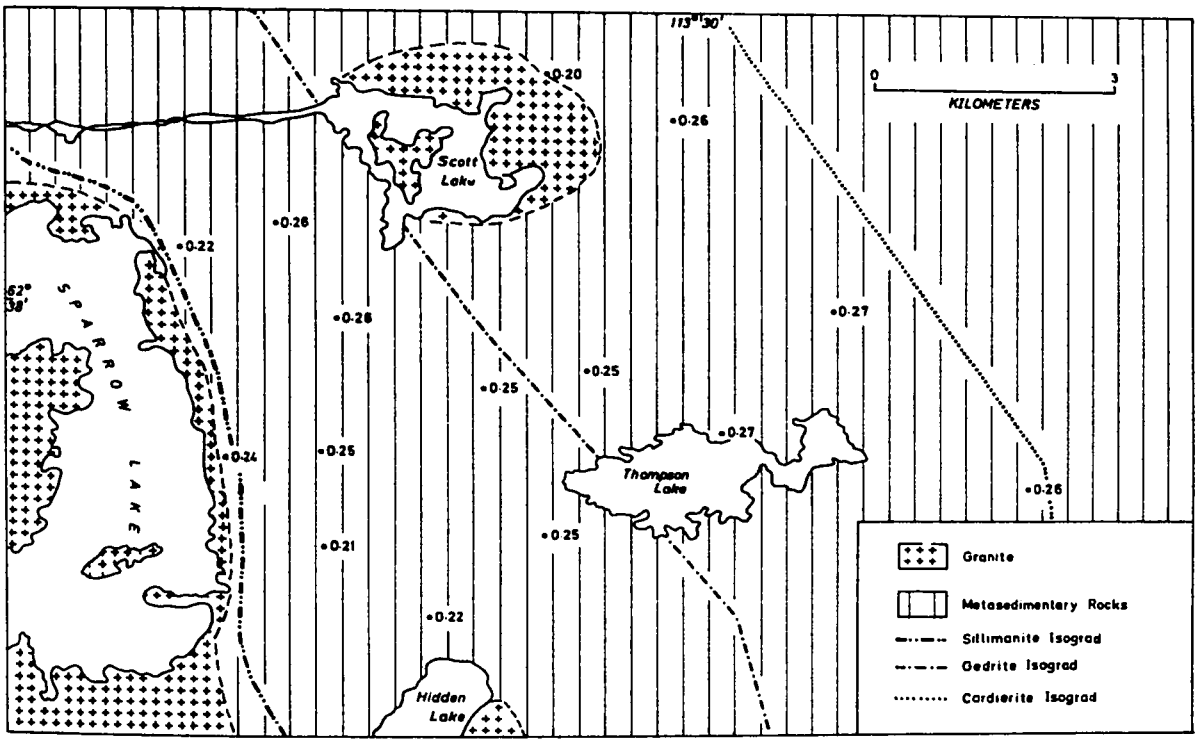

Figure 20. Areal distribution of delta-index in cordierite in the study area.

Fifteen cordierite-bearing samples were chosen at different distances from the granitic pluton. The cordierite was concentrated by the standard procedures of magnetic separation and using heavy liquids (see Appendix I). After concentration it was pulverized to a fine powder. The delta index was determined from X-ray powder diffractograms, obtained on a Norelco diffractometer with Ni filtered CuKα radiation. Other conditions were: ratemeter settings $1x8.0x10^2$ (scale-factor, multiplier and time constant respectively), a scanning speed of 4^{o} per minute. The region between 28.5 2θ and 30.5 2θ was scanned back and forth at least six times for each sample and an average distortion index was calculated.

The distortion index values determined were plotted on the map (Fig. 20) to examine the distribution and variation with reference to the pluton. Figure 20 shows that the variation of distortion index values around the pluton is unsystematic. However, those cordierites with the highest distortion index lie farther away from the Sparrow Lake pluton. Sample 130 has the lowest distortion index value and it is situated on the contact of the Scott Lake pluton. Irregular variation of distortion index of this sort

could be attributed to local heating of cordierites by small granitic plugs, pegmatites or other dykes. Pegmatites in the study area are very common (see Kretz, 1967) and extend as far as the gedrite zone.

Plagioclase Feldspar

Plagioclase feldspar is a common mineral in metamorphic rocks over a wide range of bulk compositions. Plagioclase has a frame work structure of linked (Si, Al)-O tetrahedra, and contains Ca and Na ions in large interstices in 8-fold coordination.

The plagioclase feldspar in the rocks of the study area is generally untwinned. In a few instances where it is twinned, an estimation of the extinction angle revealed them to be of oligoclase composition. In a few instances at higher grades (samples 27 and 14) an antiperthitic texture was observed.

Sodium and calcium contents of plagioclase feldspar in 14 samples were determined on an ARL electron microprobe. Several untwinned plagioclase grains were picked up during this analysis. The analytical condition and other details are given in Appendix II. No evidence for chemical zoning is observed in these plagioclase crystals; however some irregular variations from grain to grain were observed,

indicating local inhomogeneities. Inspite of these compositional variations from grain to grain, no indication of coexisting albite and oligoclase is observed. This is in contrast to the report of Evans (1964) of plagioclases from low grade schists in New Zealand. In view of these inhomogeneities U-stage work was regarded as being unsuitable as determinations of anorthite content will involve an inevitable bias towards well twinned and perhaps the most convenient grains (Evans, 1964). The analyses are presented in Table 13.

An increase of anorthite content in plagioclase feldspars with metamorphic grade has been recorded by several workers (see Deer, Howie and Zussman 1962). In the present study no systematic correlation with prograde metamorphism is observed. However, two determinations on plagioclases of the greenschist facies showed a lower CaO and higher Na_2O contents compared to cordierite-biotite and cordierite-gedrite zone plagioclase feldspar.

Gedrite

Of the three types of amphiboles found in the Yellowknife-Beaulieu region, gedrite and cummingtonite are more common than actinolite. Gedrite from this

region was reported by Kamineni and Wong (1973).

Gedrite, an orthoamphibole with complex crystal-chemical characterizations, has been studied in detail only recently (Robinson and Jaffe, 1969; Papike and Ross, 1970; Robinson, Ross and Jaffe, 1971). Robinson, Ross and Jaffe (1971) proposed a general formula $A_xR^{+2}_2(R^{+2}_{5-y}R^{+3}_y)(Si_{8-x-y}Al_{x\ y})$ where R^{+2}= Fe^{+2} Mg Mn Ca, R^{+3}=Al+Fe^{+3}, and A= Na+K. Two coupled substitutions are important in this formula; the first concerns the introduction of Na into A sites, which are normally vacant in orthoamphiboles, with the replacement of Al for Si in tetrahedral sites; the second, a substitution of R^{+3} for R^{+2} ions in the octahedral sites coupled with substitution of Al for Si in T-sites.

Gedrite was analysed by using a combination of atomic absorption and electron microprobe techniques. Water was determined in this mineral to obtain a complete analysis. The analytical details are given in Appendices I and II.

The analyses presented in Table 9 are recalculated on the basis of 24 oxygen ions in (Table 12). Si is allotted to tetrahedral sites and the rest of this position was filled with Al. The ions in the X and Y sites approximate to 7, but the ions in the A site

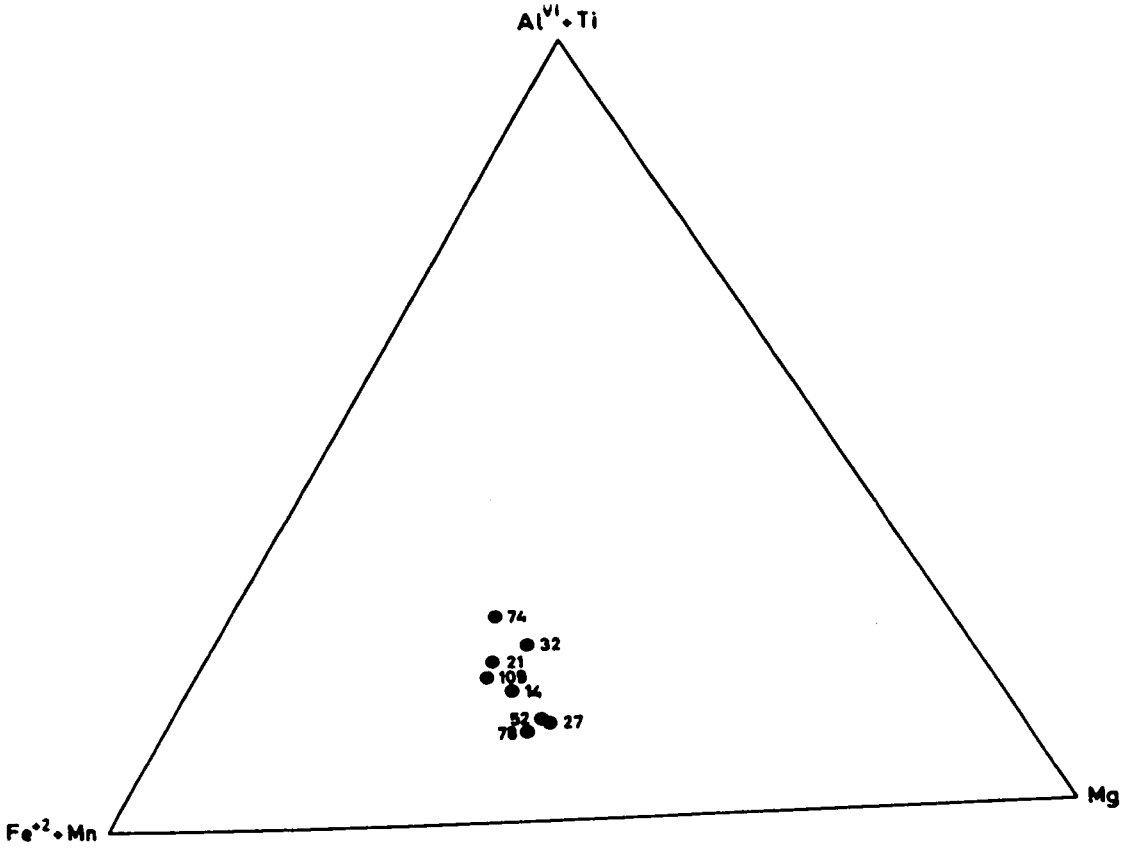

Figure 21. Triangular diagram in terms of $Fe^{2+}+Mn$, $Al^{VI}+Ti$, and Mg representing the compositional field of the gedrites.

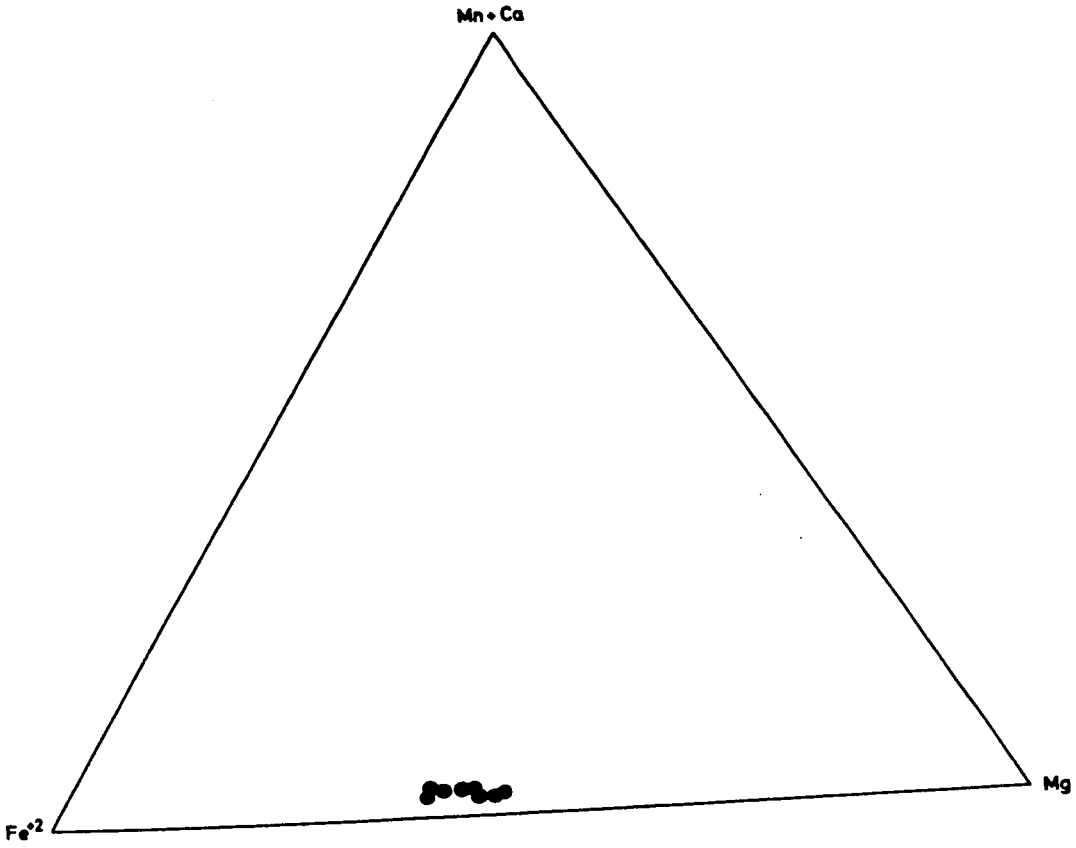

Figure 22. Triangular diagram in terms of Fe^{2+}, Mg, and Mn+Ca representing the compositional field of gedrites.

show considerable deficiency. There are consistently more than 2 OH ions. This may perhaps be due to the presence of F which has been driven off along with water during the determination.

An examination of formula and the analyses of gedrite presented in Tables 9 and 12 reveal that Al, Fe^{+2} and Mg are present in large amounts compared to Ca, Mn, Na and K. From this it can be inferred that the M positions are essentially occupied by Al, Fe^{+2} and Mg. In addition, some Al goes to tetrahedral or T sites.

Because Al_2O_3,MgO and FeO are present in large variable amounts and the other oxide components are present in small amounts only, the chemical analyses can be represented graphically with Al^{vi}, Mg and Fe on each corner of a triangular diagram. In this plot, Ti is combined with Al^{vi} while Mn is included with Fe^{+2}. Figure 21 shows the field of gedrite compositions. Another plot illustrating the compositional field of gedrite in terms of Mg, Fe^{+2} and Mn+Ca is given in Figure 23.

Cummingtonite

The structure of cummingtonite has been investigated by Ghose (1961). Substitutions in this mineral are relatively simple as the A sites are

Table 14: Chemical Composition of Cummingtonites

	24	286	84	107	107b	139	139b	143A	143A,b	173A	173A,b
SiO_2	55.20	54.10									
TiO_2	0.10	0.04									
Al_2O_3	0.35	0.30									
FeO	25.73	26.52	28.20	25.08	26.20	23.38	25.15	24.76	25.66	25.08	25.65
MnO	0.71	0.78	0.90	0.63	0.66	0.61	0.48	0.77	0.72	0.52	0.44
MgO	14.62	14.71	12.35	15.79	14.29	17.08	16.06	14.50	13.75	14.45	13.29
CaO	0.46	0.58	0.38	1.28	0.63	0.82	0.71	0.52	0.30	0.63	0.32
Na_2O	0.23	0.11	0.53	0.28	0.36	0.26	0.47	0.19	0.27	0.25	0.38
K_2O	0.06	0.06	0.04	0.06	0.05	0.05	0.07	0.06	0.04	0.05	0.07
H_2O	2.10	1.87									

Analyses by D.C. Kamineni

normally vacant and hence the octahedral sites do not contain any substantial Al. As with gedrite, considerable non-equivalency is recognized in octahedral sites (Ghose 1961) and they are termed M_1, M_2, M_3 and M_4 sites.

Cummingtonite in the present case was analysed for Fe, Mg, Mn, Na, K, Ca and Zn on the atomic absorption spectrometer. A few samples were analysed for SiO_2, Al_2O_3, and TiO_2 on the electron microprobe. Details of mineral separations and analytical techniques are given in Appendices I and II.

Inspection of the cummingtonite analyses in Table 14 reveals that this mineral is rich in FeO, and MgO with minor amounts of Al_2O_3, Na_2O, K_2O, CaO and MnO. An obvious difference between gedrite and cummingtonite compositions is that the latter is poorer in Al_2O_3 and Na_2O and slightly richer in CaO. Also the Mg/Fe ratio is higher in cummingtonite compared to gedrite.

The CaO content of cummingtonites has attracted the attention of several workers (Layton and Phillips, 1960; Mueller, 1962; and Klein, 1964). The CaO content in Yellowknife cummingtonites varies from 0.30 to 1.28 by weight percent. This is within the limit (1.5%) set by Klein (1964).

Layton and Phillips (1960) suggested that Ca is essential to stabilize the lattice of cummingtonite. Schürmann (1966) on the basis of his experimental work confirmed this, as he could synthesize cummingtonite only when 2.7% of caO was added. On the other hand Mueller (1962) described a number of cummingtonite analyses in which the CaO content is only about 0.5%. From this Mueller concluded that CaO content is not essential to stabilize the cummingtonites and that the presence of such components like CaO and MnO only enlarge the stability field of this mineral. Klein (1964) also showed CaO contents as low as 0.10 in cummingtonites from Quebec. From this view point, it is reasonable to assume the CaO content is not a critical factor for the formation of cummingtonite.

Andalusite

Andalusite is a common metamorphic mineral in aluminous schists of low pressure metamorphism. In the study area this mineral has different modes of occurrence. Three andalusite crystals that occur near the Sparrow Lake pluton, coexisting with fibrolite, cordierite, biotite etc. were analysed, details of which are given in the Appendix II, and the results

Table 18: Chemcial Composition of Andalusites

	62	445	450
SiO_2	37.00	36.15	36.30
Al_2O_3	62.20	63.00	62.50
TiO_2	0.03	0.02	0.02
MgO	0.01	<0.01	0.02
Fe_2O_3	1.32	1.15	1.59
MnO	<0.01	---	<0.01
Total	100.57	100.33	100.44

Analyses by D.C. Kamineni

are presented in Table 18. The analysis was essentially conducted to measure the Fe contents of this mineral, as this component is considered to enlarge the andalusite stability beyond the normal limits (Strens, 1968). However, during the course of this study Okrusch and Evans (1970) and Holdaway (1971) have shown that the enlargement of andalusite stability relative to sillimanite is not geologically significant. In this connection it may be stated that the effect of impurities like Fe^{3+} and Mn in andalusite or sillimanite only effect the kinetics of transition or crystallization rather than having a direct influence on the stability fields. Sluggishness of phase transition reactions is very commonly noted in reaction kinetics in the presence of impurities (see for example, Kracek, 1951).

Garnet

Garnet is a common metamorphic mineral, with a general formula $R_3^{2+}R_2^{3+}Si_3O_{12}$. In garnets of argillaceous rocks, the R^{2+} ions comprise Mg, Fe^{2+}, Mn and Ca, and R^{3+} ions principally by Al^{3+} and Fe^{3+}. The garnets in pelitic schists and phyllites can be approximated by a mixture of four end-members; almandine-$Fe_3Al_2Si_3O_{12}$, pyrope-$Mg_3Al_2Si_3O_{12}$, spessartine-$Mn_3Al_2Si_3O_{12}$ and

grossularite-$Ca_3Al_2Si_3O_{12}$.

The crystal structure of garnet was determined by Menzer (1928) and later refined by Gibbs and Smith (1965). In these investigations, it is observed that in the garnet structure there is only one site each for divalent and trivalent elements. On this basis it is reasonable to approximate garnet as an ideal mixture within a certain compositional range.

In view of the chemical zoning observed in garnets, the analysis was carried out on the electron microprobe. The samples were analysed for Ca, Mn, Mg and Fe for several garnets at the core and rim. Si and Al were also determined in a few cases. In addition to the microprobe analysis, partial bulk analyses of some garnets was obtained on the atomic absorption techniques. The analytical procedure and other details are given in Appendix II.

The core and rim compositions of garnets are presented in Table 15. The degree of zonations in garnets with reference to Fe and Mn is calculated from the relation: (FeO/FeO+MgO+MnO+CaO rim-FeO/FeO+MgO+MnO+CaO core)x 100. This is somewhat similar to the relation used by Drake (1968). Mn zonation is also calculated from a similar relationship as follows:

Table 15: Chemical Composition of Garnets

	2(big crystal) core	2(big crystal) rim	2 (small crystal) core	2 (small crystal) rim	4 core	4 rim	12 core	12 rim	14 core	14 rim
FeO	34.29	36.88	33.49	34.12	27.41	27.66	29.51	31.32	32.57	34.66
MgO	2.46	2.66	1.80	1.91	2.71	2.99	1.74	2.00	2.84	3.22
MnO	8.70	6.13	5.76	5.63	7.91	7.53	6.53	6.21	3.46	2.27
CaO	2.03	1.75	1.74	1.50	2.31	2.25	1.66	1.61	1.79	1.61

	19 core	19 rim	21(big crystal) core	21(big crystal) rim	21(small crystal) core	21(small crystal) rim	32 core	32 rim	39A(big crystal) core	39A(big crystal) rim
FeO	35.22	36.86	33.59	34.89	34.52	35.22	32.33	35.15	31.65	34.40
MgO	2.20	2.34	3.40	3.52	3.55	3.76	2.84	3.22	2.41	2.67
MnO	5.40	4.97	4.84	3.72	4.02	3.70	3.10	1.76	7.45	4.32
CaO	2.10	1.70	1.87	1.40	1.56	1.34	2.89	1.39	1.93	1.48

	39A(small crystal) core	39A(small crystal) rim	40 core	40 rim	41 core	41 rim	43 core	43 rim	59 core	59 rim
FeO	33.95	34.50	32.83	33.33	33.11	34.23	31.83	33.00	32.92	34.94
MgO	2.62	2.94	2.29	2.50	2.57	3.00	2.28	2.47	2.50	2.65
MnO	5.00	4.20	5.63	5.22	3.66	2.99	8.46	7.16	4.95	3.66
CaO	1.68	1.55	1.97	1.72	2.44	1.89	1.84	1.54	1.83	1.50

	core 92	rim	core 115	rim	core 142A	rim	core 143A	rim
FeO	32.99	33.42	32.09	32.33	33.12	34.23	34.31	34.70
MgO	2.25	2.38	2.45	2.40	2.55	3.02	1.85	1.95
MnO	5.72	5.64	5.12	5.01	7.06	5.80	6.13	5.53
CaO	1.92	1.51	1.64	1.56	1.66	1.57	1.52	1.28

Total Fe expressed as FeO

Analyses by D.C. Kamineni

Table 16: Bulk Analyses of Garnets

	12	14	21	32	41
SiO_2	37.50	37.00	36.80	37.41	37.20
Al_2O_3	21.95	21.10	22.00	22.30	21.50
FeO'	28.51	32.22	32.00	31.89	32.67
MgO	1.92	3.15	3.32	2.98	2.59
MnO	7.11	3.05	3.62	3.36	3.29
CaO	1.50	1.54	1.65	1.68	2.00

Total Fe expressed as FeO

Analyses by D.C. Kamineni

Table 17: Number of Ions on the Basis of 24 Oxygens

	12	14	21	32	41
Si (Z)	6.080	6.034	5.914	5.985	6.012
Al (Y)	4.188	4.055	4.167	4.205	4.094
Fe	3.859	4.394	4.300	4.267	4.415
Mg	0.463	0.765	0.795	0.711	0.623
Mn	0.975	0.420	0.493	0.455	0.450
Ca	0.260	0.268	0.284	0.287	0.346
(X)	5.560	5.847	5.872	5.720	5.834

(MnO/MnO+MgO+FeO+CaO core-MnO/MnO+MgO+Feo+CaO rim)x 100. The two elements Mn and Fe are chosen for this purpose as they display more zoning than Ca and Mg.

The degree of zonation values for Fe and Mn termed as Δ Fe and Δ Mn respectively are given in Table 19. As is shown in Table 19 these values change from sample to sample and also crystal to crystal within any one sample. These variations could be attributed to the following causes some of which have been mentioned by Drake (1968) also.

1. The geometric and growth center of the garnet do not coincide and hence the section passing through the geometrical center may not contain the growth center. This would particularly apply to garnets that are irregularly distorted.

This possibility is ruled out in the present investigation as the zoning profile for sample 39A given in Figure 23 shows that the growth center coincides with geometrical center. This is also observed by Kretz (personal communication) in a nearby area.

2. The growth center and geometric center coincide but the analytical cross-section did not pass through the center of the garnet. This likelihood is avoided

Table 19: Size and Degree of Zonation in Garnets

Sample No.	Size of Garnet Millimeters	ΔFe	ΔMn
2	1.50	5.49	5.40
2	0.30	0.82	0.49
4	0.50	0.47	0.98
12	1.00	1.50	2.03
14	1.10	2.89	3.07
19	0.80	1.95	1.26
21	0.35	0.98	0.80
21	1.25	3.27	2.52
32	1.40	6.04	3.30
39A	1.70	6.62	6.65
39A	0.90	1.41	2.33
40	0.70	1.08	0.97
41	1.20	2.04	1.66
43	1.10	3.04	2.83
59	1.00	3.73	3.16
92	0.50	1.19	0.41
115	0.30	0.59	0.26
142A	1.25	2.00	2.65
143	0.65	2.36	1.21

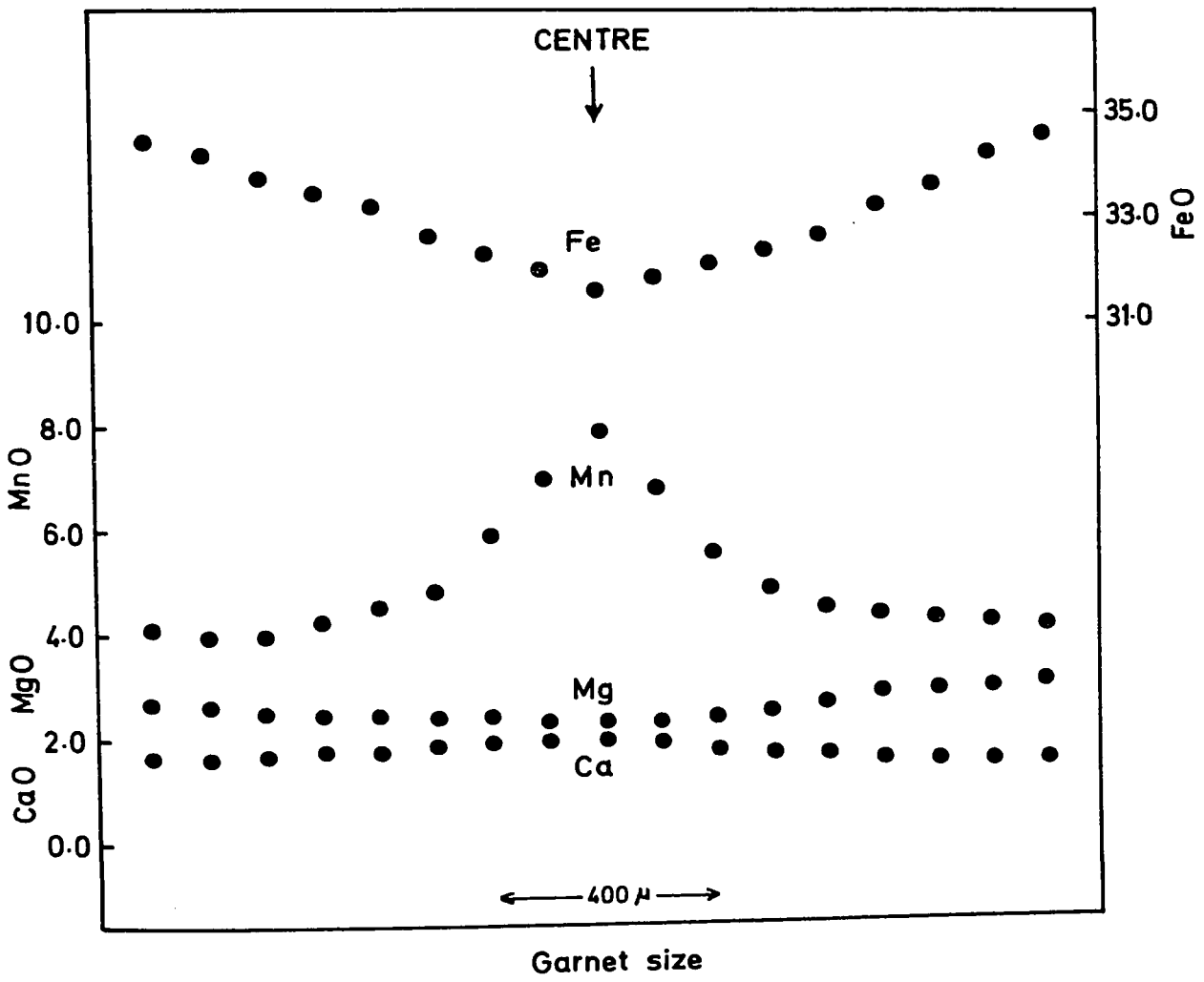

Figure 23. Compositional profiles across a garnet crystal.

by choosing the biggest garnet grains. For example, the sizes of garnets in samples 2, 14, 19, 21, 32 and 89 are known and on this basis the largest grains can be located in the sections.

3. The geometrical and growth center coincide and analytical cross-section also passes through the center, but the different core-rim compositions reflect local differences in bulk composition within the hand specimen. These local differences could be original due to lack of chemical communication over distances in the order of few centimeters. A process of this sort would certainly influence the degree of zonation in garnets. However, in view of the correlation obtained for the size of the garnet and the degree of zonation (Figs 24 and 25) other factors appear to be more important in accounting for the variations.

4. Differences in ΔFe and ΔMn could be attributed to different times of nucleation of garnets and thus the core and rim inherit different compositions, depending on the environmental conditions prevailing during their nucleation. This particularly applies to the observed differences within a sample.

In this process, nucleation of garnets takes place over a period of time and the garnets nucleated in the first instant will attain a bigger size. As a consequence

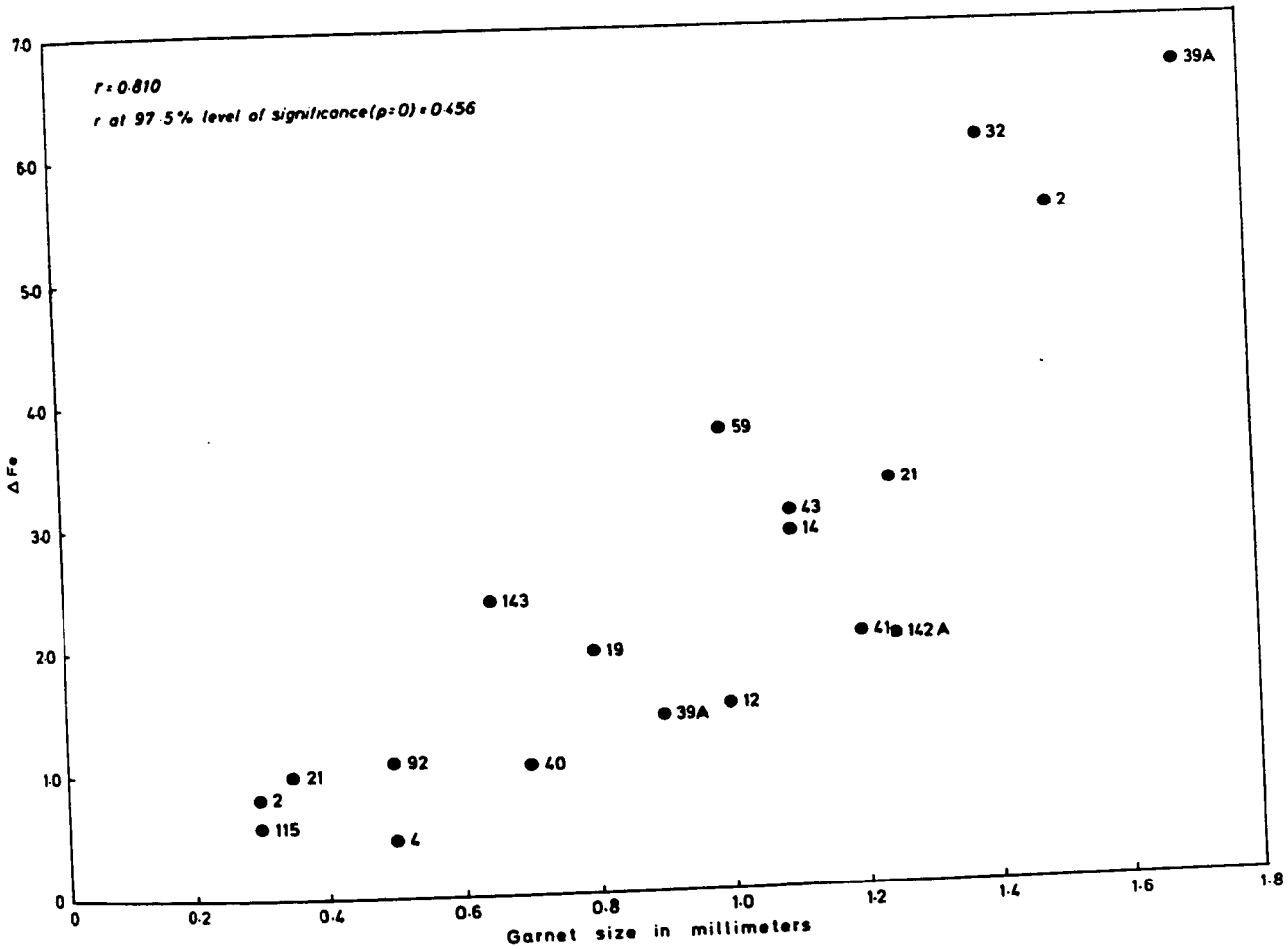

Figure 24. Plot showing the relation between Δ Fe and the size of garnet crystal.

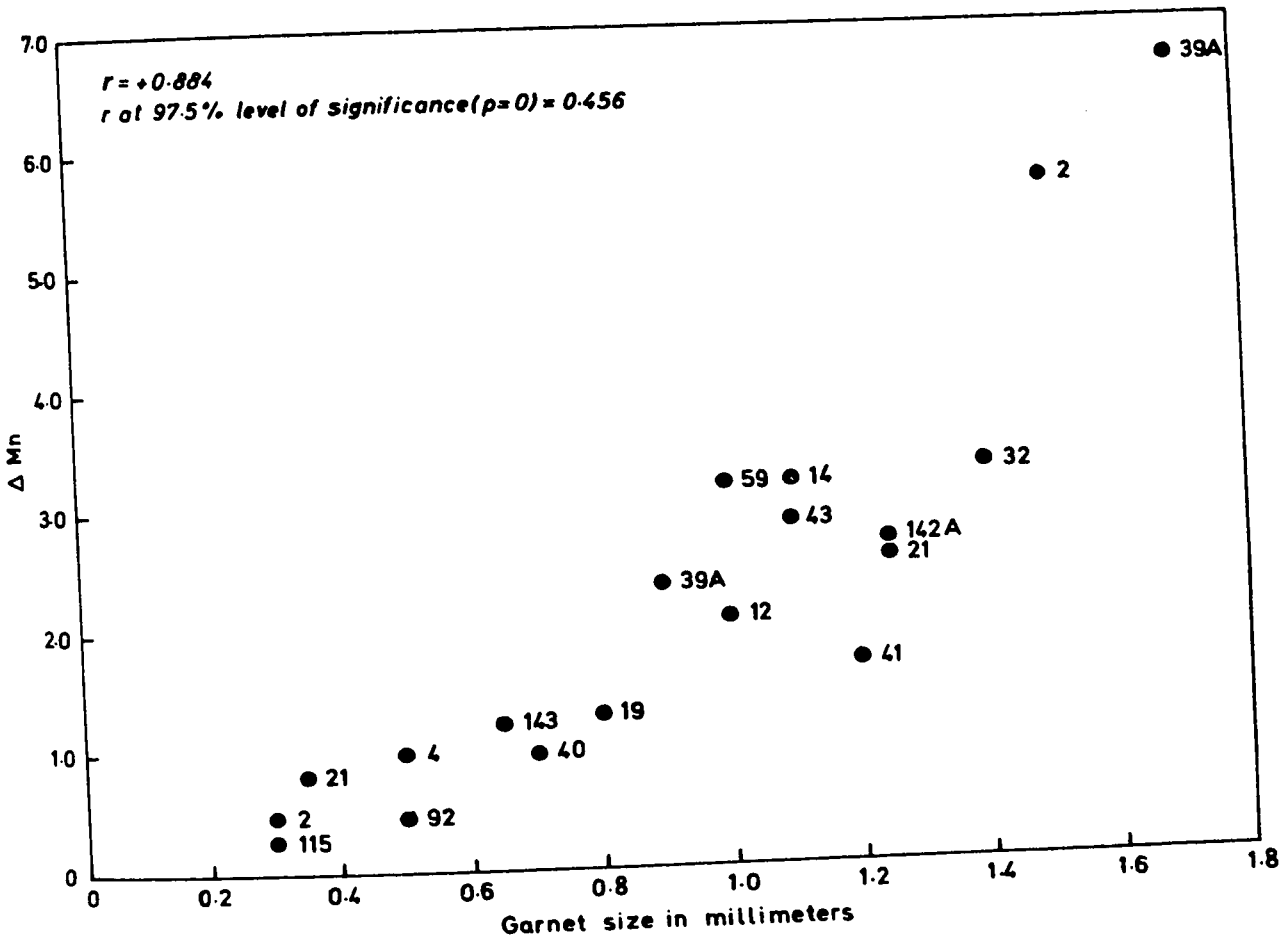

Figure 25. Plot showing the relation between Δ Mn and the size of the garnet crystal.

of this, the chemical environment changes with passage of time due to depletion processes. Hence the garnets nucleated at a later date will have a different core composition from that of the early nucleated ones. Due to the different nucleation times and growth periods, the core compositions of the smaller garnets may compare with the compositions of the bigger garnets near the corresponding size. This model explains, fairly well, the differences in the degree of zonation among garnet crystals within a sample as well as from sample to sample.

The ΔFe and ΔMn values are plotted against the size of the garnet crystals in Figures 25 and 26. In both cases there is a positive correlation between larger ΔFe and ΔMn values and with bigger garnet crystals and vice versa.

5. Exchange reactions with other ferromagnesian silicates would effect the rim compositions to some extent and hence the degree of zonation.

Garnets coexisting with different ferromagnesian minerals will establish exchange relationships with reference to Mg, Fe and Mn with these phases. As a consequence of this, the rims of garnets close to gedrite crystals will have a certain composition whilst the rims of those near a cordierite or biotite

will have another composition. This possibility is tested in sample 32. As the abundance of garnet crystals as well as other coexisting minerals is quite high in this sample (Plate 9), this is considered to be more suitable for this purpose. Three garnet crystals, all belonging to the largest size category of the section and also approximately of the same size, that occur in the vicinity of or in contact with gedrite, biotite and cordierite separately were analysed to obtain the rim compositions for Fe, Mg and Mn. The results tabulated in Table 20 indeed show different rim compositions.

Table 20

Garnet Rim Compositions in the Vicinity of Gedrite, Cordierite and Biotite

Garnet Rim Compositions	FeO	MgO	MnO
Near gedrite	34.90	3.20	1.76
Near cordierite	34.00	3.50	1.62
Near biotite	34.50	3.25	1.50

6. Garnets involved in several phases of metamorphism may become unstable and partially breakdown, but still be present as relicts. As a result of this the rim

compositions of zoned crystals change.

In the present study there is some evidence of breakdown of the garnets and at the same time some idiomorphic forms also are observed. The corroded outlines of garnets must have contributed to the variations in the degree of zonation; the extent of which is not known, however, it may not be significant other than that caused by exchange reactions.

7. The relative rates of breakdown of reactants that participate in the garnet-forming reaction may give rise to different ΔFe and ΔMn values.

The garnet-forming reaction may be considered to involve the breakdown of chlorite and plagioclase, which with quartz results in the formation of garnet, albite and water. Chlorite acts as a main reservoir for Mn, Mg and Fe whilst the anorthite component of plagioclase supplies the calcium component for the garnet. In this reaction, only the anorthite component of plagioclase breaks down leaving the rest of the mineral richer in albite. The relative rates of breakdown of these minerals would be influenced by temperature, water pressure and probably interaction with other phases. Among these parameters water pressure is more important as under high water pressures, the calcic plagioclase is unstable whereas

the stability field of chlorite may be expanded. In instances where there are garnet cores richer in Ca this phenomena may be inferred to have happened, and thus the Mn zonation will be affected. As Ca also like Mn is concentrated at the core, this element will have an influence on the ΔMn values. However, in the present case, as the Ca concentration of garnets is not significantly high, a considerable influence of this possibility is disregarded.

Another possible parameter that might influence the garnet zonation and that may be mentioned in this connection is the rates of diffusion of Mn and Ca. Garnets may be formed right at the grain contacts of plagioclase and chlorite or plagioclase and chlorite could react even if they are not in contact with garnet nucleating in some other convenient place. In situations of the later type presumably the distances from reacting phase to the nucleating garnet would be important. In other words, the closer the reacting phase the more of its components would be concentrated at the garnet core and vice versa.

Apart from the relative rates of breakdown of plagioclase and chlorite, the relative concentrations of the ions also change with time. For example, of the three components Fe, Mg and Mn in chlorite the Mn

chlorite breaks down first as its stability is exceeded much earlier than other components of chlorite (Turnock, 1964; Fawcett and Yoder, 1966; and Hsu, 1968). A process of this depletion type explains the causes of zonation in general, but may not influence the degree of zonation to a greater extent.

8. Apart from garnet, other ferromagnesian minerals like gedrite and/or cummingtonite may also be produced from the breakdown of chlorite, the other phases produced being dependent on the Mg/Fe and Al/Si ratios of chlorite. If this occurs the Mn/Fe ratio of the garnet may be greatly influenced as these minerals also act as a sink for Mn. In the same manner, if cordierite is formed along with garnet the Mg/Fe ratios will be affected. The analyses presented show that this, in fact occurs to some extent.

As is evident from the above discussion, several factors are important in evaluating the differences in the degree of zonation in garnets. Out of the various possibilities that have been listed, two factors seem to be more important than others, in the present case. They are: i. nucleation of garnet over a period of time and ii. exchange reactions of garnet rims with other ferromagnesian minerals. In view of the strong correlation (see Figures 24 and 25)

obtained between the size of the garnets and the degree of zonation, it is quite reasonable to propose that the time at which the garnets started to nucleate is important in controlling the degree of zonation. In other words, as has been mentioned earlier, in a system where the nucleation and growth is continuous, the garnets that started to nucleate earlier will grow larger and hence produce a larger degree of zonation and vice versa. Finally, when the growth of garnets has ceased, the rims of these garnets may equilibrate with coexisting phases and thus the compositions of the rims will be dependent to some extent on the nature of the phase in contact as the exchange coefficient would be different between garnet and other ferromagnesian minerals in each case.

DISTRIBUTION OF ELEMENTS AMONG COEXISTING MINERALS

Introduction

The theory of chemical thermodynamics has proved to be very useful in interrelating certain variables of rock systems (Ramberg and DeVore, 1952; Kretz, 1959, 1960, 1961; Mueller, 1960, 1961). By plotting the concentration of an element in two coexisting phases on a 'distribution diagram' (Kretz, 1959), one can show the nature of the distribution of the element between the phases. A regular array of points, defining a distribution curve, indicates that there was a chemical communication between the mineral phases and that exchange equilibrium was attained. If the distribution of the points is scattered and does not define a smooth curve, several possibilities may be considered: 1) differences in external variables such as temperature and pressure; 2) influence on the distribution of variation in the concentration of another element in one of the phases, and 3) disequilibrium, possibly due to polymetamorphic or post-metamorphic events such as partial retrogression. With these variables in mind a study of exchange equilibrium in rocks can be contemplated.

In the present study, the minerals that have been analysed are common minerals found in the garnet-gedrite

and the cordierite zone. We have seen in Chapter IV that garnet, biotite, cordierite and gedrite show some compositional variations in their content of FeO, MgO and MnO. For this reason it was considered worthwhile to study the variation of these components in these phases on the basis of exchange relationships.

Theory of Exchange Equilibrium

The theory of exchange equilibrium has been discussed by Ramberg and DeVore (1952) and Kretz (1959, 1961). The theories are based on the concept of exchange equilibrium, and often utilize as a first approximation, the ideal solution model.

Let us consider an ion-exchange reaction (for one kind of exchangeable site) in which there is an exchange of Fe and Mg between biotite and cordierite.

$$\underset{\text{Mg-biotite}}{K_{1/3}MgAl_{1/3}SiO_{10/3}(OH)_{2/3}} + \underset{\text{Fe-cordierite}}{FeAl_{3/2}Si_{5/2}Al_{\frac{1}{2}}O_9} \rightleftharpoons$$

$$\underset{\text{Fe-biotite}}{K_{1/3}FeAl_{1/3}SiO_{10/3}(OH)_{2/3}} + \underset{\text{Mg-cordierite}}{MgAl_{3/2}Si_{5/2}Al_{\frac{1}{2}}O_9}$$

At equilibrium and constant P and T, $dG^{biotite} = -dG^{cordierite}$.

Applying the law of mass-action to the above reaction, the equilibrium constant, K, is obtained as follows:

$$K = \frac{(a_{Fe}^{biot})(a_{Mg}^{cord})}{(a_{Mg}^{biot})(a_{Fe}^{cord})} \cdot \exp(-\Delta G^{o}/RT)$$

where a denotes the activity of $K_{1/3}MgAl_{1/3}SiO_{10/3}(OH)_2$ etc., ΔG^{o} is the free-energy of this reaction with components in pure form, R is the gas constant and T is absolute temperature. Since $a_i^{\alpha} = \gamma_i^{\alpha} X_i^{\alpha}$ where X_i^{α} is the mole fraction of species i in phase X and γ_i^{α} is the activity coefficient of the same species in the same phase:

$$\frac{(a_{Fe}^{biot})(a_{Mg}^{cord})}{(a_{Mg}^{biot})(a_{Fe}^{cord})} = \frac{(\gamma_{Fe}^{biot}\ \gamma_{Mg}^{cord})(X_{Fe}^{biot}\ X_{Mg}^{cord})}{(\gamma_{Mg}^{biot}\ \gamma_{Fe}^{cord})(X_{Mg}^{biot}\ X_{Fe}^{cord})},$$

$$\frac{(X_{Fe}^{biot}\ X_{Mg}^{cord})}{(X_{Mg}^{biot}\ X_{Fe}^{cord})} = \frac{(\gamma_{Mg}^{biot}\ \gamma_{Fe}^{cord})}{(\gamma_{Fe}^{biot}\ \gamma_{Mg}^{cord})} \cdot \exp(-\Delta G^{o}/RT)$$

The left hand term is known as the distribution coefficient, K_D, and is usually expressed as follows:

$$K_D = \frac{(X_{Fe}^{biot})(1-X_{Fe}^{cord})}{(1-X_{Fe}^{biot})(X_{Fe}^{cord})} \qquad (1)$$

Both K and K_D, as defined here, refer only to the compositional relationships between $[Fe^{2+}, Mg]$ in cordierite and biotite. Other equilibrium constants and distribution coefficents can be derived from other

pairs of minerals and also for Fe-Mn or Na-K exchange relations. As it is, the expression derived here does not take into consideration the distribution of elements, in particular crystallographic sites. This sort of distribution can be important, as has been shown by Ghose (1962), Mueller (1962, 1969) and Grover and Orville (1968).

Expressions for the equilibrium constant with varying temperatures and pressures can be obtained as follows: the Van't Hoff equation $\frac{(d \ln K)}{(dT)}_P = -\frac{\Delta H^o}{RT^2}$ expresses the variaton of K with temperature. ΔH^o is the standard heat change of the reaction for pure end-members. If K_1 and K_2 are equilibrium constants at temperatures T_1 and T_2, integration of the Van't Hoff equation gives:

$$\ln K_1 - \ln K_2 = \frac{\Delta H^o}{R} (1/T_2 - 1/T_1), \text{ or },$$

$$K_2 = K_1 \exp \left(\frac{\Delta H^o}{R} (1/T_2 - 1/T_1)\right)$$

Keeping temperatue constant at a given pressure P_1, we have $\ln K_{P_1} = -\left(\frac{\Delta G_1^o}{RT}\right)$ (2)

and at pressure P_2, we have $\ln K_{P_2} = -\left(\frac{\Delta G_2^o}{RT}\right)$ (3)

From equations (2) and (3) we have,

$$K_{P_2} = K_{P_1} \exp \frac{(\Delta G_1^o - \Delta G_2^o)}{RT} \quad \text{where } (\Delta G_1^o - \Delta G_2^o)$$

is the standard energy difference caused by pressure difference $(P_2 - P_1)$. But $(G_1^o - G_2^o) = \Delta V^o (P_2 - P_1)$, where ΔV^o is the change in molar volume for the exchange reaction for pure end-members.

Hence $K_{P_2} = K_{P_1} \exp \left(\frac{\Delta V^o}{RT}(P_2 - P_1)\right)$

The term ΔV^o can be calculated for the exchange reaction and is equal to -1.07. In this calculation, the molar volumes (Table 21) of phlogopite, annite and Mg-cordierite were taken from Thompson (1955) and Evans (1964) while that of Fe-cordierite was calculated from its molecular weight and density.

Table 21

Molar Volumes of Fe and Mg End-Members of Biotite and Cordierite

Mineral	Molar Volume
Annite	154.28
Phlogopite	149.93
Fe-cordierite	241
Mg-cordierite	236

Knowing the ΔV value, it can be estimated whether pressure has a significant affect on the exchange reaction. For example, let us assume that $P_2 = 5kb$, $P_1 = 1atm$, $T = 500^0K$ and $R = 82.05atm\ cc/deg.$ Therefore, $K_{P_2} = K_{P_1} \exp(-1.07x5000/82.05x773) = 1.08xK_{P_1}$ which means that the effect of pressure on the equilibrium is very small. In general, the solid-solid reactions have a small ΔV (Thompson 1955) and therefore it can be generalized that the greatest variation in the distribution coefficient will be caused by temperature.

If the minerals behave as non-ideal solutions K_2 will be affected by the activity coefficients. However, adequate data are not available on the activity coefficients of most minerals in order to assess the influence of these terms on the distribution coefficients. Kretz (1961) considered that the activity coefficient ratios may be constant over a given temperature, composition and pressure range, i.e. $\frac{(\gamma_{Mg}^{biot}\ \gamma_{Fe}^{cord})}{(\gamma_{Fe}^{biot}\ \gamma_{Mg}^{cord})}$ will be constant in the present sample. If, in addition this term is close to unity the variation in K_D can be approximated by $\ln \frac{K_{D_2}}{K_{D_1}} = (\frac{-\Delta H^o}{R})\ (1/T_2 - 1/T_1)$.

If both solid solutions were ideal and devoid of ordering complications, the activity coefficients for all phases would be equal to unity. However, some mineral solid-solutions may not be ideal, and the ratio of activity coefficients may not be constant. The chief parameter that contributes to non-ideality is internal ordering between crystallographically distinct sites. Such an ordering is present in any of the minerals examined, solid-solutions will not be ideal and $K \neq K_D$. In the present case, ordering of elements has been positively recognized only in gedrite and cummingtonite (Chapter IV). Since insufficient data are available to evaluate the ideality of garnet, biotite and cordierite, we shall confine the discussion to an ideal solution model.

Distribution of Mg and Fe

The distribution of these two elements among the coexisting garnet, biotite, gedrite and cordierite was examined by plotting the atomic ratios Fe/Fe+Mg+Mn on a 'distribution diagram'. This ratio is generally represented by X^{α}_{Fe} where α is the mineral under consideration.

In view of the compositional zoning encountered in garnet crystals, the rim compositions of these

crystals were utilized in calculating the atomic ratios. Unfortunately, the number of garnetiferous rocks analysed in which the coexisting phases also were analysed are few in number. The atomic fractions of garnet and other coexisting phases as well as the distribution coefficients are listed in Table 22.

Some of the values in Table 22, when plotted on the distribution diagram show a scattered pattern which may be attributed to the failure of the minerals to attain exchange equilibrium or to the effect of other elements such as Mn and Ca. Kretz (1959) and Sen and Chakraborty (1968) showed the influence of Mn and Ca in garnet on the Fe-Mg distribution between garnet and biotite. In the present study, the observed scattering can be related to the CaO content in garnet. There appears to be a correlation between $K_D^{ged\text{-}gar}$ Fe and CaO content of garnet (Fig. 23), and some correlation in the case of cordierite-garnet, as well as biotite-garnet (Figs. 27 and 28). The influence of other compositional variables such as Ti and Al^{vi} in biotites was tested but no apparent correlation was obtained. Inspite of the scatter, the partition pattern between garnet and biotite compare with that of the other workers, as compiled by Albee (1965) and Sen and Chakraborty (1968).

Table 22: Mol. Fraction and K_D Values for Fe and Mg between Garnet and the Coexisting Phases

Sample No.	X_{Fe}^{gar}	X_{Fe}^{ged}	X_{Fe}^{biot}	X_{Fe}^{cord}	$K_D^{ged-gar}$ Fe	$K_D^{biot-gar}$ Fe	$K_D^{cord-gar}$ Fe
12	0.76		0.52	0.35		0.34	0.17
14	0.89	0.57	0.47	0.33	0.31	0.21	0.11
21	0.78	0.59	0.53	0.34	0.42	0.32	0.15
32	0.82	0.62	0.50	0.34	0.36	0.22	0.11
41	0.80	0.54	0.46	0.33	0.29	0.21	0.12

Figure 26. Figure showing the influence of Ca in garnet on the $K_{D\,(Fe-Mg)}$ between biotite and garnet.

Figure 27. Figure showing the influence of Ca in garnet on the $K_{D\,(Fe-Mg)}$ between gedrite and garnet.

Figure 28. Figure showing the influence of Ca in garnet on the $K_{D\,(Fe-Mg)}$ between cordierite and garnet.

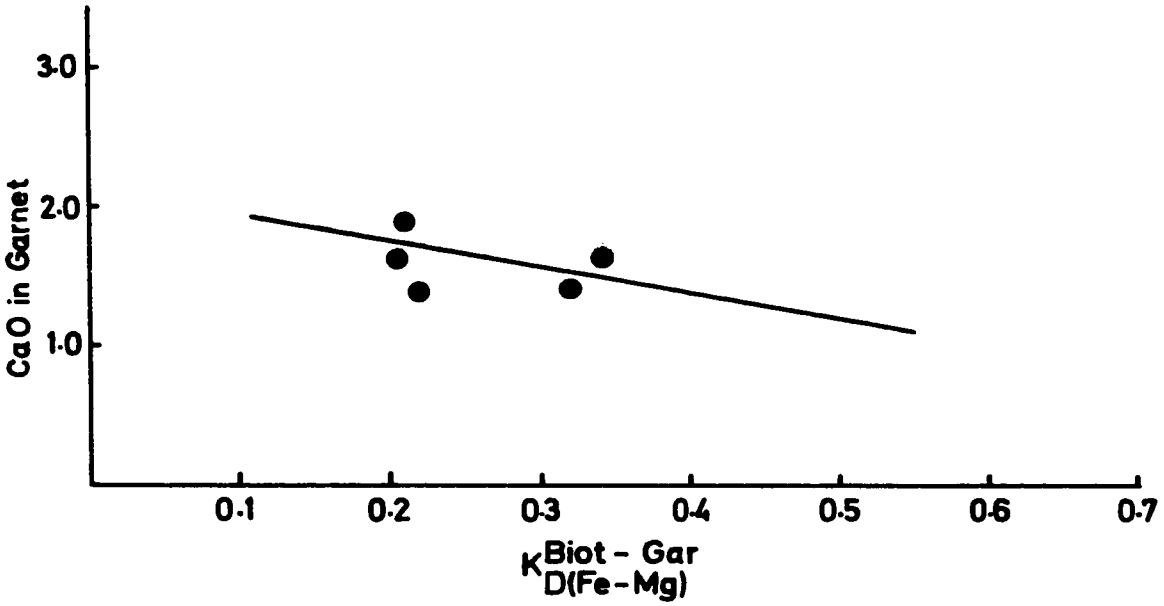
3·0
2·0
1·0
CaO in Garnet
0·1
0·2
0·3
0·4
0·5
0·6
0·7
$K^{Biot-Gar}_{D(Fe-Mg)}$

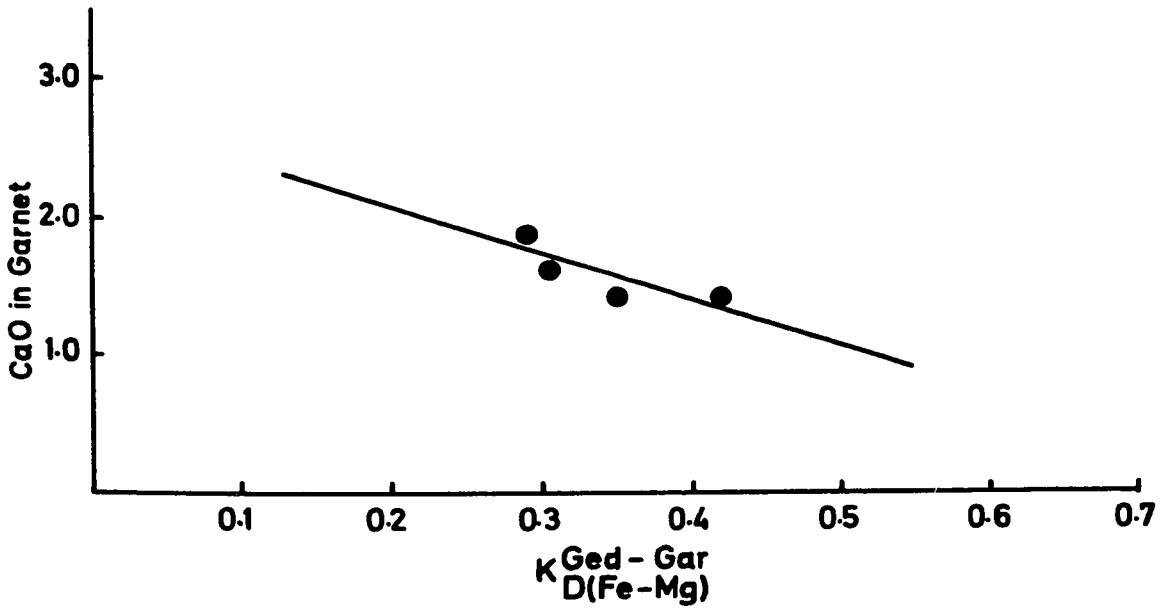
3·0
2·0
1·0
CaO in Garnet
0·1
0·2
0·3
0·4
0·5
0·6
0·7
$K^{Ged-Gar}_{D(Fe-Mg)}$

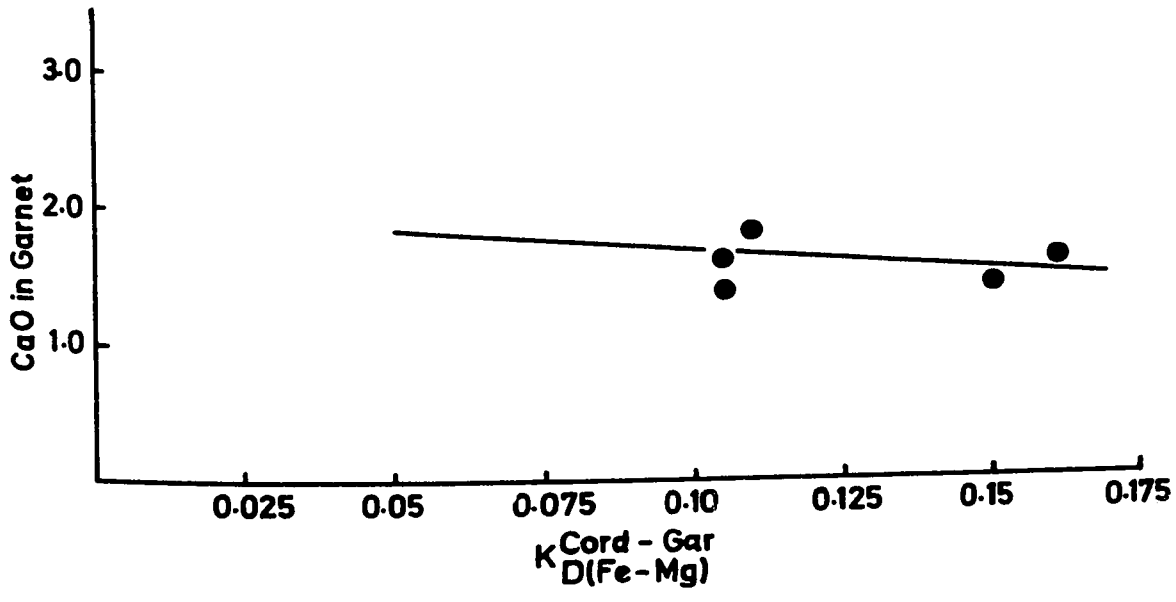
3·0
2·0
1·0
CaO in Garnet
0·025
0·05
0·075
0·10
0·125
0·15
0·175
$K^{Cord-Gar}_{D(Fe-Mg)}$

The distribution of Fe^{2+} and Mg between gedrite and biotite (Fig. 29) follows a distribution curve which has been calculated from the theoretical equation and an average K_D value. This indicates a close approach to equilibrium. The points fall in a small area indicating a limited compositional variation. Two analyses of coexisting gedrite and biotite from Fishtail Lake, Ontario (Lal and Moorhouse, 1969) fall very close to this distribution curve.

Points on the distribution diagram of Fe^{2+} between cummingtonite and biotite show considerable clustering. The distribution diagram is not presented but the data are given in Table 23. In spite of this, it can be concluded that equilibrium with respect to Fe^{2+} and Mg was closely approached. In the case of biotite-gedrite and biotite-cummingtonite the distribution patterns are different. A glance at the distribution diagram (Fig. 29) indicates that Fe^{2+} shows greater preference for gedrite than biotite. On the other hand, in the case of cummingtonite-biotite, iron is partitioned equally, or may show slight preference for biotite (Table 23).

The partition of Fe^{2+} between cordierite and gedrite indicates a close approach to equilibrium.

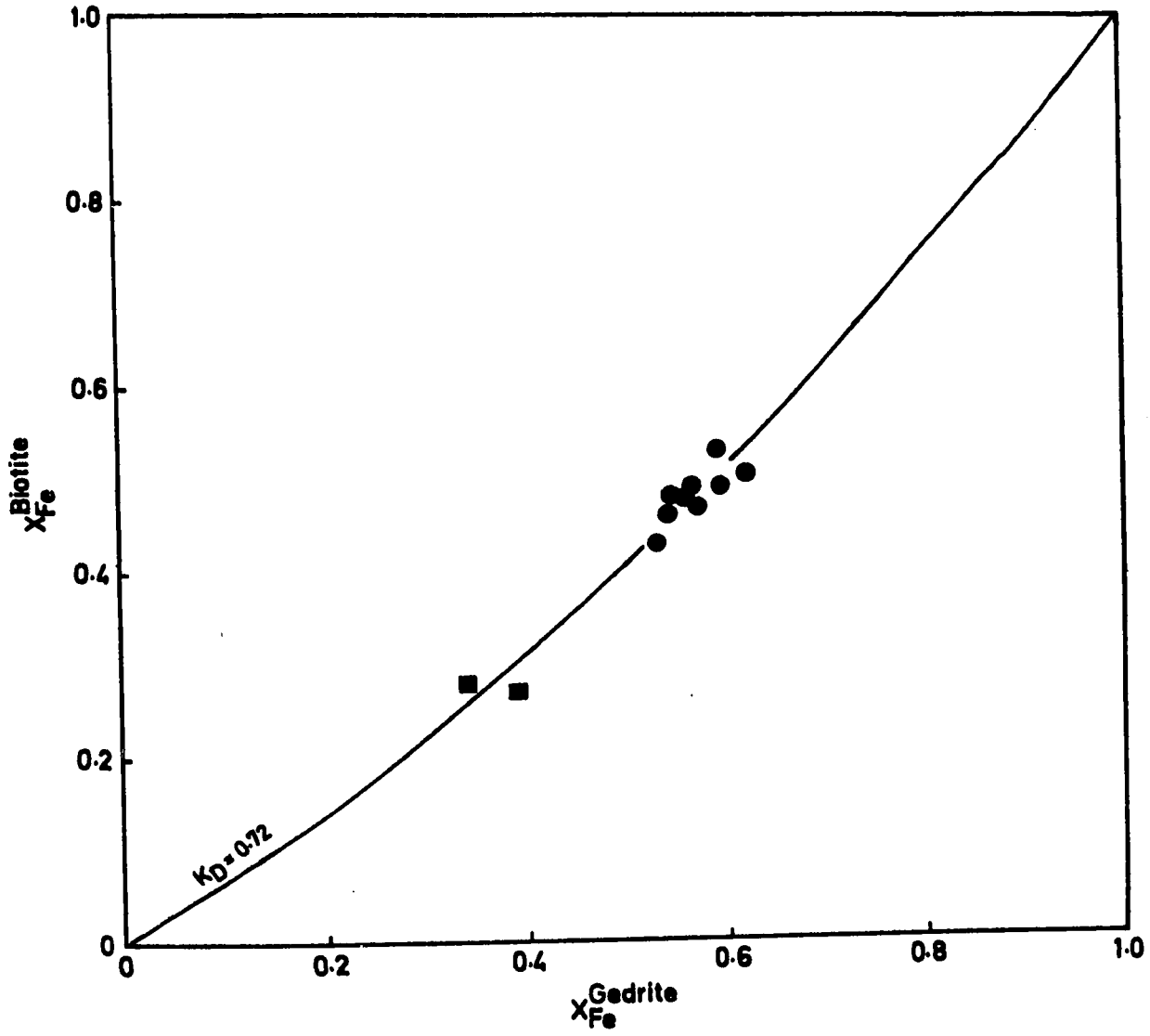

Figure 29. Distribution of Fe and Mg between biotite and gedrite.

Table 23: Mol. Fraction and K_D (Fe-Mg) for Cummingtonite and Biotite

Sample No.	X_{Fe}^{cumm}	X_{Fe}^{biot}	$K_D^{biot-cumm}$ Fe
24	0.49	0.50	1.04
84	0.49	0.48	0.96
107b	0.49	0.51	1.08
139b	0.47	0.52	1.21
143b	0.50	0.53	1.12
173b	0.52	0.51	0.96
284	0.50	0.52	1.08

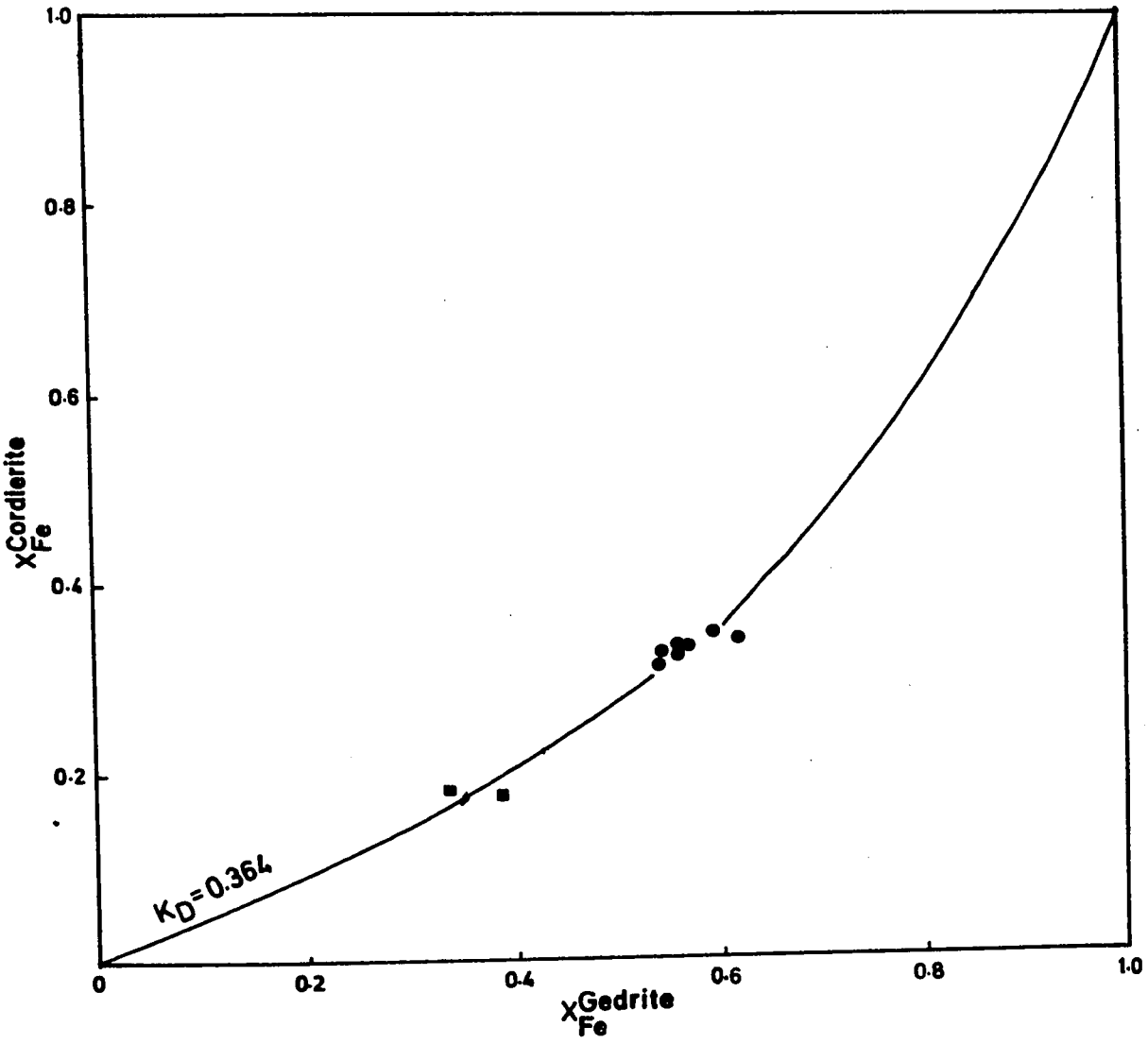

Figure 30. Distribution of Fe and Mg between cordierite and gedrite.

The compositional range in this pair is also limited as is evident from the clustering on the distribution diagram (Fig. 30). Samples from the Fishtail Lake area were also plotted on the diagram, and these fall along the distribution curve.

Figure 32 shows the distribution of Fe^{2+} between cordierite and biotite. The points fall near the distribution curve that has been located from the average K_D value and equation (1), indicating that these phases approached equilibrium with regard to Mg-Fe^{2+} exchange. However, there is a certain amount of deviation in pairs that come from the area below the garnet-gedrite zone.

An attempt is made here to analyse the reasons for the deviation of these points from the regular distribution pattern. On the theoretical grounds, a smooth distribution curve is proof that the phases considered have attained chemical equilibrium at constant temperature and pressures. In practice, by taking possible compositional variations into consideration the empirical characteristics of the distribution curve can be related to geological environment. This type of evaluation has been made for the partition of Fe^{2+}-Mg between orthopyroxene and clinopyroxene over much of their compositional range

(Kretz, 1961, 1963). It is obvious that the distribution coefficients are directly dependent on the temperature of equilibration both in the case of ideal and non-ideal solutions. In order to infer the possible influence of temperature on this double distribution, distribution coefficients were plotted against the distance from the granitic pluton (Fig. 32). This plot gives a negative slope with good correlation. It has been shown by Kretz (1963) that the distribution coefficients approach unity with increasing temperature. As is evident in the distribution diagram from the present study, the cordierite-biotite pairs that are close to the granite (and are supposed to have been equilibrated at a higher temperature) deviate more from unity, while the pairs below the garnet-gedrite zone that lie far from the granite (and thus have supposedly equilibrated at a lower temperature) are closer to unity. This is very surprising in view of the progressive nature of the metamorphism from the greenschist facies near the cordierite isograd to andalusite-sillimanite grade near the granite contact. From this it may be inferred that the cordierite-biotite pairs closer to the contact were not equilibrated during the peak period of metamorphism,

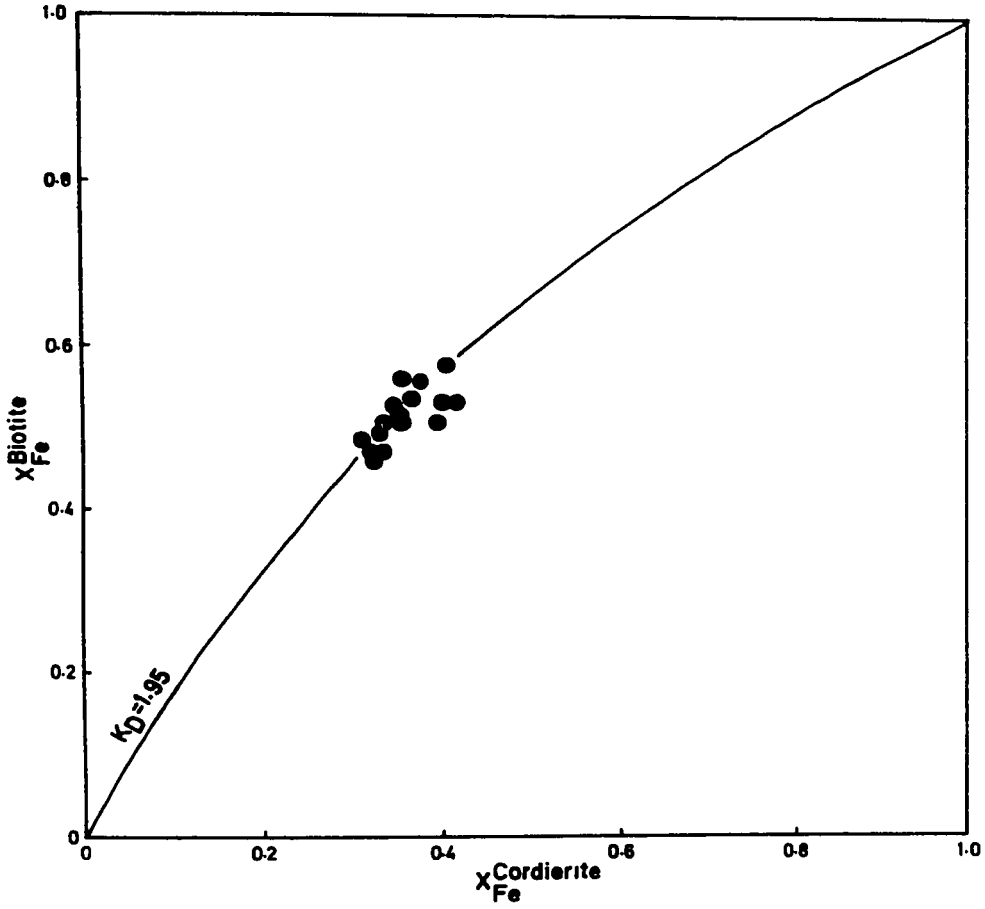

Figure 31. Distribution of Fe and Mg between cordierite and biotite.

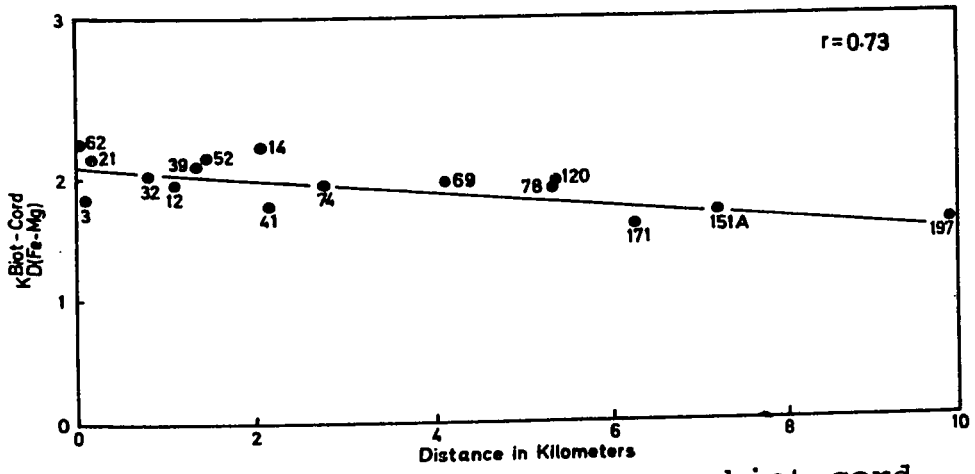

Figure 32. Relation between $K_{D\,(Fe-Mg)}^{biot-cord}$ and distance from the Sparrow Lake pluton.

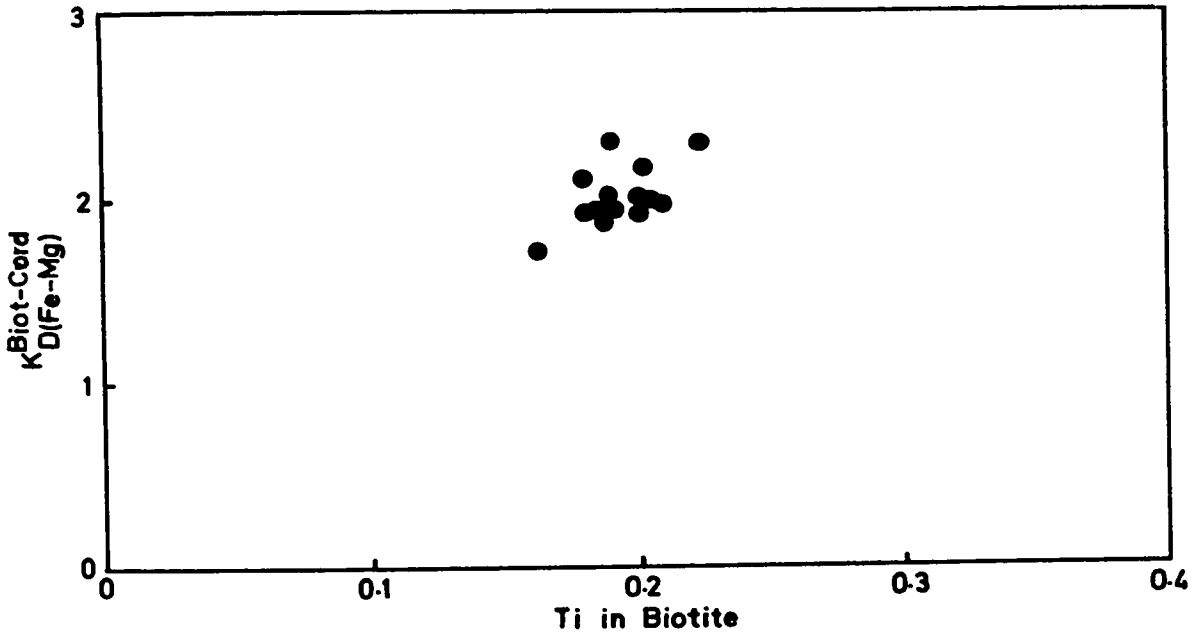

Figure 33. Plot of Ti in biotite against $K_{D\,(Fe-Mg)}^{biot-cord}$

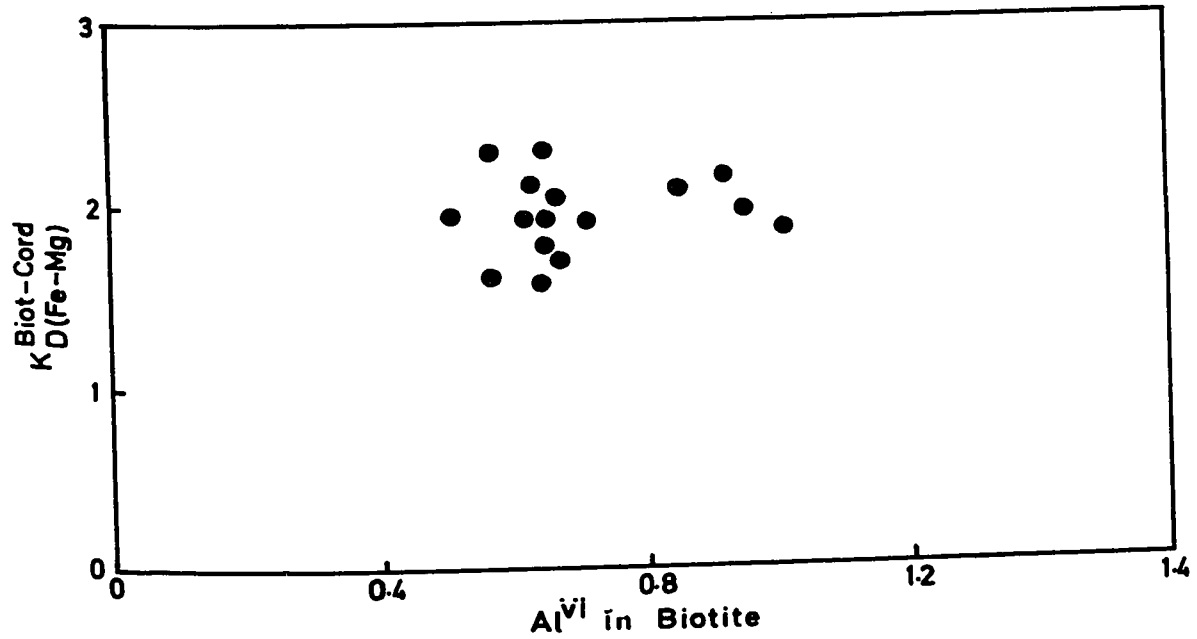

Figure 34. Plot of Al^{VI} in biotite against $K_{D\,(Fe-Mg)}^{biot-cord}$

that is, the intrusion of granite. Those cordierite-biotite pairs away from the granite which have a higher distribution coefficient values may be considered to have communicated chemically during the earlier period of regional metamorphism.

It is also possible that other variations such as mineral paragenesis and Al^{vi}, Fe^{3+} and Ti in biotite could produce the observed deviation in the distribution coefficient. However, it seems unreasonable to attribute this variation to mineral paragenesis, in view of the similarity of distribution coefficients with respect to distance from the granite in diverse assemblages (see for example, samples 120 and 78, 69 and 109 etc.). A plot of $K_D^{\text{biot-cord}}_{Fe}$ values against Ti and Al^{vi} concentrations in biotite shows that Ti has no influence and Al^{vi} has only slight influence on the Mg-Fe distribution (Figs. 33 and 34).

Chemical data of coexisting biotite and cordierite that have been published by other workers also plotted on the distribution diagram (Fig. 35). The distribution curve calculated from equation (1) and the average K_D value follow closely that of the Yellowknife trend. In this compilation samples of contact as well as regional metamorphic pairs are included. In spite

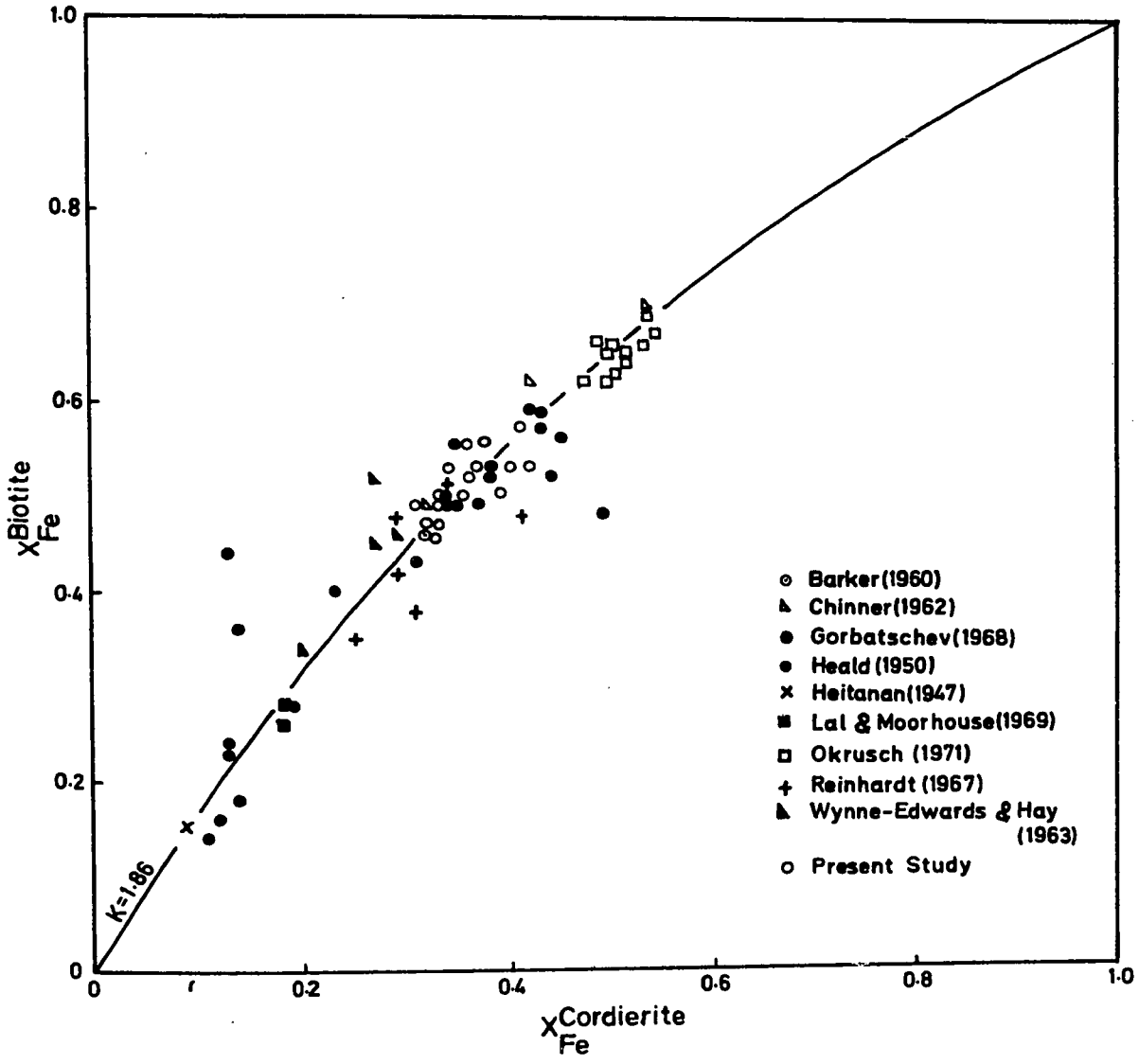

Figure 35. Distribution of Fe and Mg between cordierite and biotite in natural mineral assemblages.

of these contrasting metamorphic environments, particularly, with regards to pressure the distribution does not deviate greatly from the smooth curve which indicates that K_D is not notably pressure sensitive. This confirms the deductions obtained from the theoretical view point. However, some samples deviate from the distribution curve and this is considered to be due to the influence of oxidation and analytical error (Gorbatshev , 1968).

Distribution of Mn

Mn can be treated as a minor element in the minerals of the present study. Mn concentrations are expressed in terms of atomic ratios Mn/Fe+Mg+Mn, and in the case of garnet, the rim compositions were utilized. In most cases the distribution points show a considerable scattering especially those for garnet and other coexisting minerals. This may be due to zonation in garnet. As Mn is highly concentrated in garnet cores, and these crystals represent a non-equilibrium situation, the crystals may not have equilibrated with the coexisting phases. In addition to zonation other variables such as calcium content of garnet may cause the irregular distribution of Mn.

The distribution of Mn between cordierite and

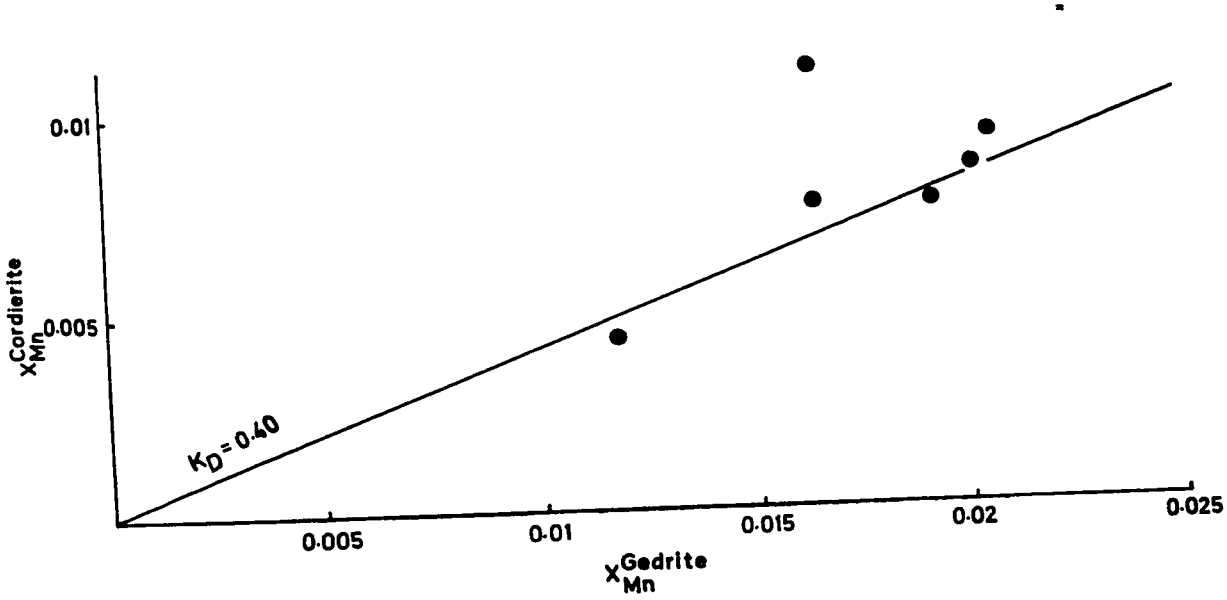

Figure 36. Distribution of Mn between gedrite and cordierite.

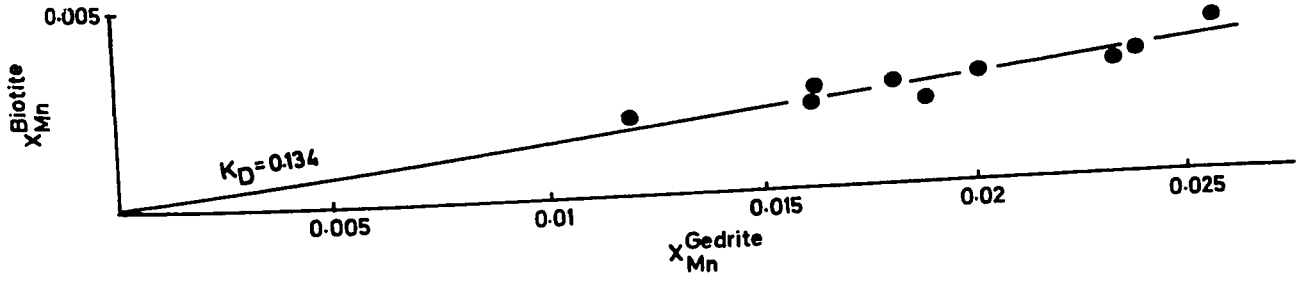

Figure 37. Distribution of Mn between gedrite and biotite.

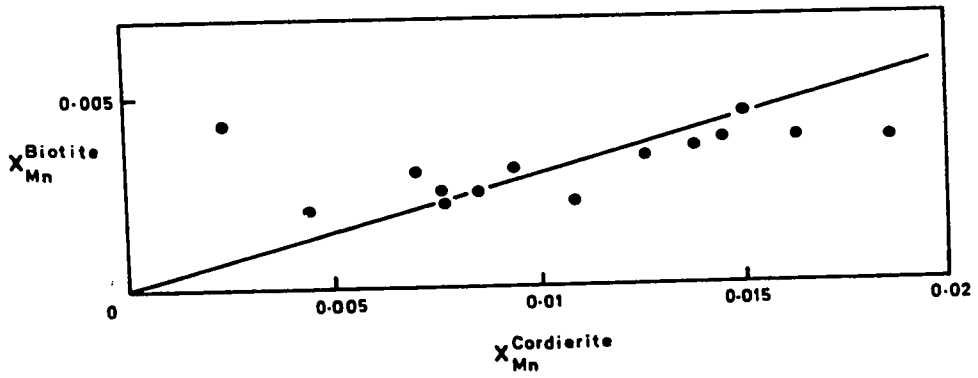

Figure 38. Distribution of Mn between cordierite and biotite.

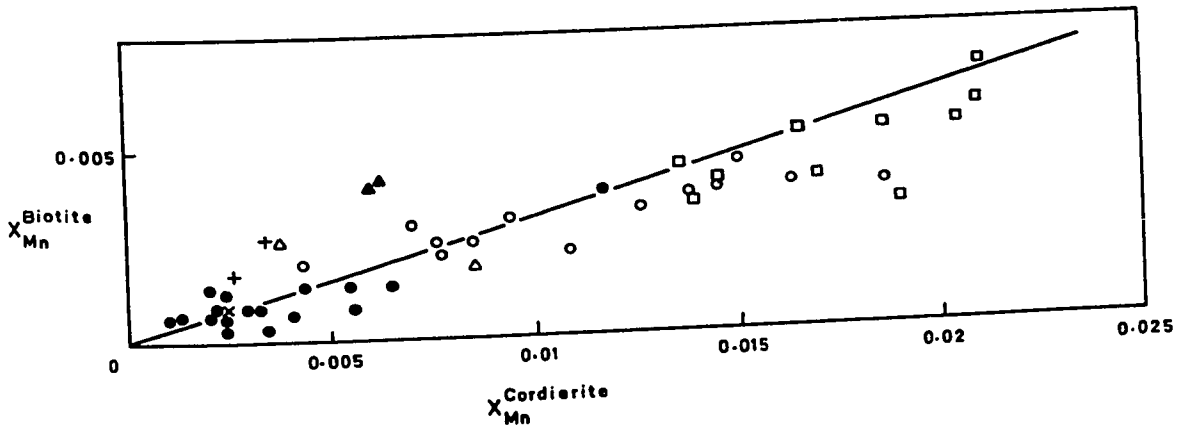

Figure 39. Distribution of Mn between cordierite and biotite in natural mineral assemblages.

gedrite is fairly regular (Fig. 36). Only samples 52 and 41 deviate from regularity, the reasons for which are not known.

The partitioning of Mn in gedrite-biotite and biotite-cordierite pairs shows a linear trend passing through the origin, except for a few points in the case of the latter pair (Figs 37 and 38). In the case of cordierite-biotite, with higher concentrations of Mn the distribution line seems to bend towards the cordierite axis, probably due to the fact that at these concentrations, Henry's law is not obeyed. This distribution pattern shows the same tendency even after the data of other workers was taken into consideration (Fig. 39).

The distribution of Mn between cummingtonite and biotite is near linear (Fig. 40), Mn showing a stronger affinity for cummingtonite than biotite.

Distribution of Na and K

The partition of Na between cordierite and biotite shows a considerable scatter, but the trend appears to be linear (Fig. 41). Clustering within this trend can be related to mineral paragenesis. For example, in rocks devoid of gedrite, the mineral pairs have a low X_{Na} value (Na/Na+K), while in rocks containing gedrite

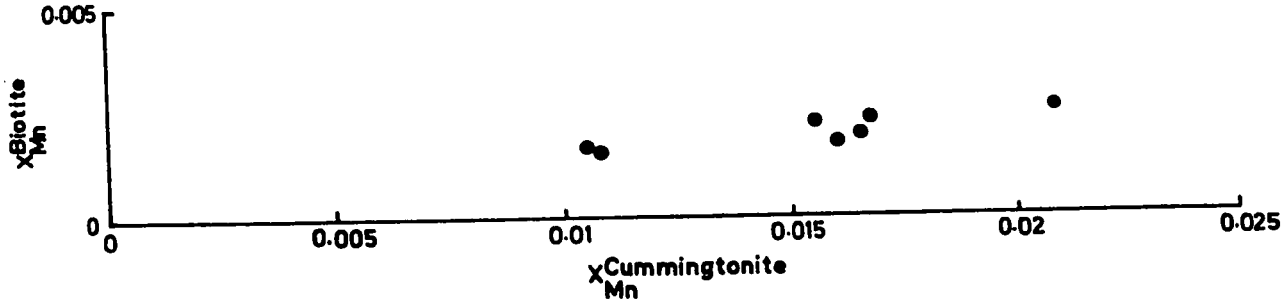

Figure 40. Distribution of Mn between cummingtonite and biotite.

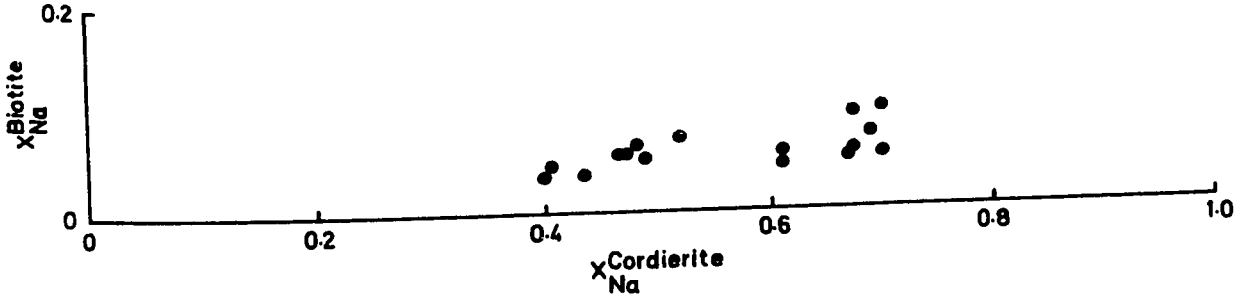

Figure 41. Distribution of Na between cordierite and gedrite.

they possess higher X_{Na} values. Both these groups contain coexisting oligoclase which is another Na-bearing mineral. Na is an essential element for the stability of the gedrite structure and it has been shown by Robinson et al. (1971) that the concentration of Na can be correlated with tetrahedral Al. Therefore, the presence of gedrite in which Na is an essential element for charge balance considerations, imposes restrictions on the partition of Na between cordierite and biotite.

The partition of Na between gedrite and biotite defines a straight line, only two points, 78 and 109, falling away from the distribution line. Reasons for the deviation of these two points are not clear, but biotite in these two samples contain high concentrations of Na. The X_{Na} values are given in Table 24.

The distribution of Na between gedrite and cordierite shows an irregular character. The Na concentration in cordierite varies over a considerable range, while in gedrite it shows only limited variation (Table 24). A more or less constant concentration of Na in gedrite indicates the importance of this element in the stability of the gedrite structure.

Table 24: Mol. Fraction Na/Na+K in Gedrite, Cordierite and Biotite

Sample No.	X_{Na}^{ged}	X_{Na}^{cord}	X_{Na}^{biot}
14	0.93	0.52	0.07
21	0.90	0.61	0.04
32	0.90	0.67	0.09
41	0.93	0.69	0.07
52	0.95	0.67	0.05
74	0.91	0.61	0.06
78	0.94	0.70	0.10

Distribution of Ca

The distribution of Ca among the coexisting phases cannot be related by a simple exchange reaction as this element occupies non-equivalent sites in the minerals under consideration. For example, in the case of biotite this element is concentrated in A sites along with alkalis while in others it goes to octahedral sites. Hence in minerals like biotite the occurrence of Ca is more dependent on charge balance requirements than any other control.

The partition of Ca between garnet and the coexisting phases shows a considerable scatter. This may perhaps be due to inequilibration of this element as a consequence of chemical zoning in garnets.

The distribution of Ca between gedrite and cordierite shows a wide scatter. This irregular distribution may be caused by the Mn concentration in gedrite. In this mineral Mn and Ca are both concentrated in the M_4 sites (Papike and Ross, 1970), and thus the concentration of one will influence the other. Therefore, this may be considered as one of the reasons, since the Mn concentration in gedrite does indeed show considerable variation.

Between biotite and gedrite, the Ca partition

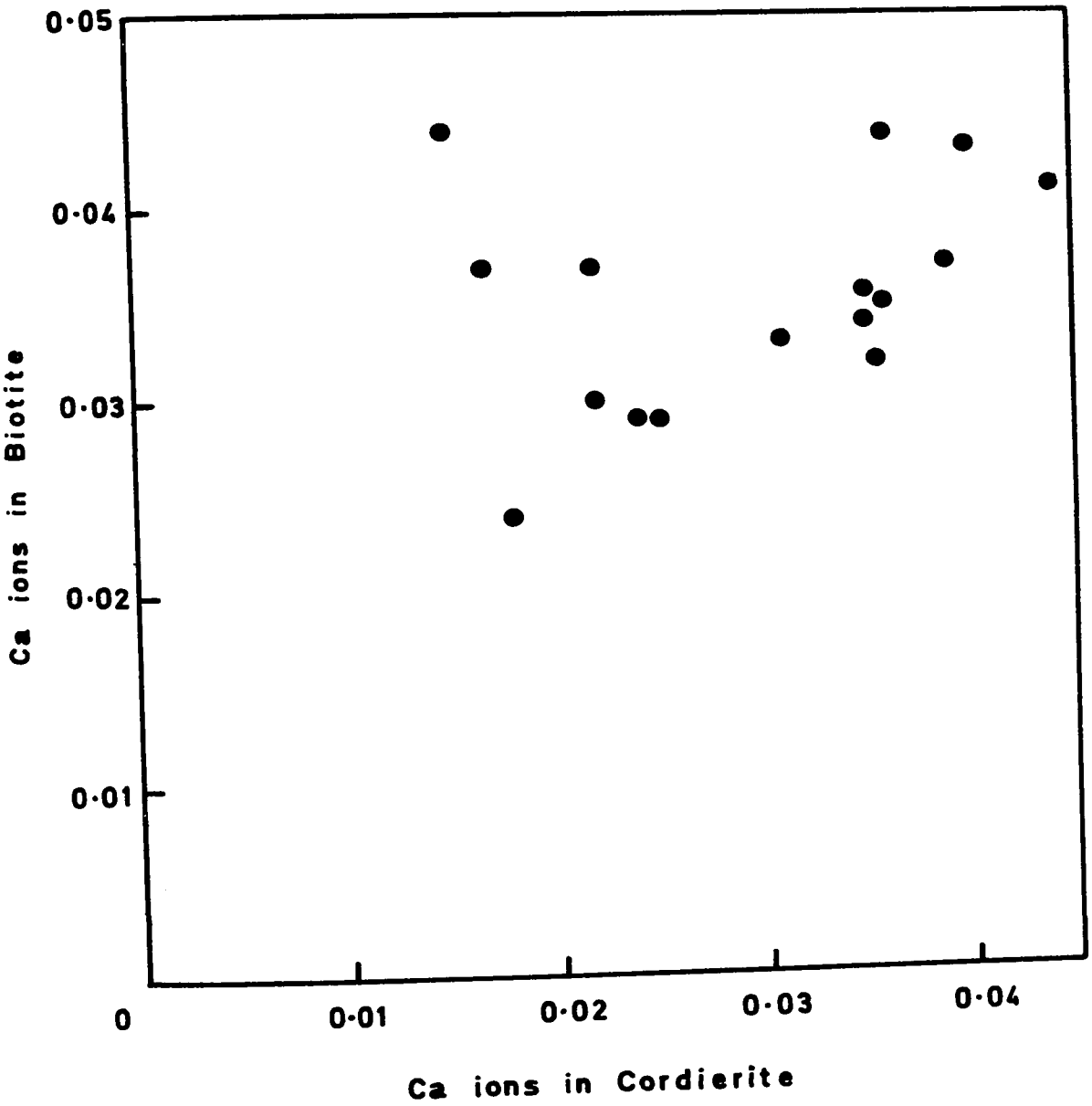

Figure 42. Distribution of Ca between cordierite and biotite.

shows two trends, which cannot be explained by mineral assemblages or metamorphic grade. This is due to non-equilibrium, since the element occupies nonequivalent sites in these minerals and hence cannot be related by an exchange reaction. Although the partition of Ca between cordierite and biotite cannot be related to a simple exchange reaction, the pattern is somewhat regular (Fig. 42), only a few points being scattered.

Distribution of Al between Gedrite and Biotite

No simple exchange reaction for the partitioning of Al can be written, except perhaps an exchange of the type $Al^{3+} \rightleftharpoons Fe^{3+}$. Al in these minerals occupies both the tetrahedral and octahedral positions. The tetrahedral Al substitutes for Si while the octahedral Al substitutes for Mg and Fe^{2+}. Thus the concentration of this element in either of the phases is to a large extent governed by charge balance requirements rather than an exchange reaction.

The partition of Al^{iv} in gedrite and biotite shows clustering and the amounts of tetrahedral Al in either of these phases remains fairly constant.

A plot of Al^{vi} in gedrite vs. Al^{vi} in biotite shows an irregular distribution. Examination of the values (Tables 9 and 12, Chapter IV, page 91)

reveals that this is mainly due to the variation of this element in gedrite over a considerable compositional range, although it is fairly constant in case of biotite. Analysis of the crystallochemical aspects of gedrite furnishes information that may account for the variation of Al^{iv} in gedrite. Papike and Ross (1970) showed that Al in six-fold coordination is essentially concentrated in M_2 site. On the basis of size, Mg, Fe^{3+}, and Ti may also be expected to occupy the same site. Hence, the concentration of these elements could influence the Al^{vi}, as all these elements are in competition for the same site. Mössbauer spectral study and chemical analysis of gedrite showed negligible amounts of oxidized iron, so the possible influence of this element can be disregarded. Similarly, as the Ti concentration is too low to affect the Al concentration, the possible influence of this element may also be ruled out. The remaining possible variable is the concentration of Mg in gedrite, which shows significant variation. In order to ascertain the influence of this element on the Al^{vi} partition in gedrite and biotite, the distribution coefficent (Al^{vi} gedrite/Al^{vi} biotite) is plotted against Mg ions in gedrite (Fig. 43). The

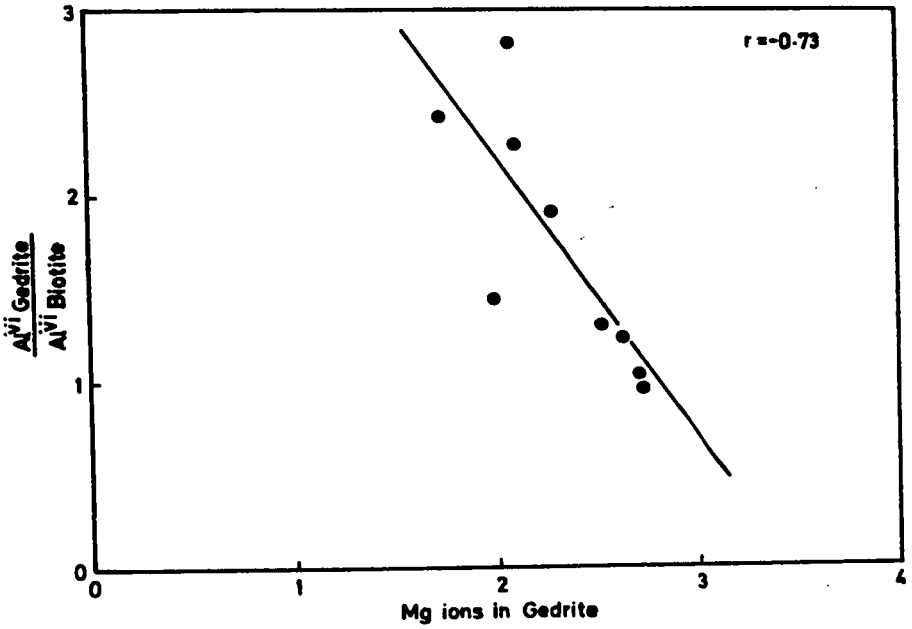

Figure 43. Plot showing the relation between Mg ions in gedrite against Al^{VI} gedrite/Al^{VI} biotite.

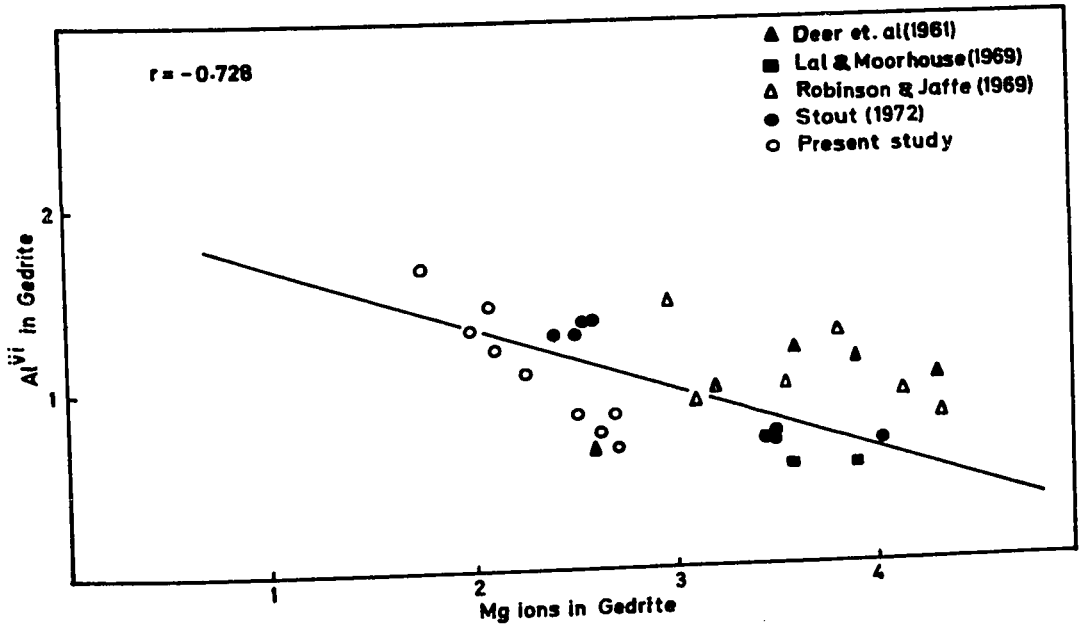

Figure 44. Plot showing relation between Mg ions versus Al^{VI} in gedrite.

negative slope of the resultant trend shows a good correlation between the variables suggesting that the distribution coefficient is indeed influenced by the Mg ion concentration in gedrite.

A correlation of this kind indicates that in gedrite a substitution of the type $(Mg,Si) \rightleftharpoons Al.Al$ is more pronounced than the $(Mg,Fe^{2+},Si) \rightleftharpoons Al.Al$ that has been proposed by Deer et al. (1961) and Robinson et al. (1971). To further test the validity of this statement, Al^{vi} was plotted against Mg. For this purpose, comparison was made with gedrite analyses reported in the literature. As predicted, a strong negative correlation was obtained (Fig. 44).

Distribution of Zn

Zn shows a fairly regular distribution between gedrite-biotite and cummingtonite-biotite (Figs 45 and 46).

Zn is almost equally partitioned between biotite and gedrite, and only at lower concentrations does the element show a slight preference for gedrite. On the other hand it shows a definite preference for cummingtonite relative to biotite. Tentatively, it may be suggested that in the Fe-Mg minerals, higher concentrations of Zn are associated with higher

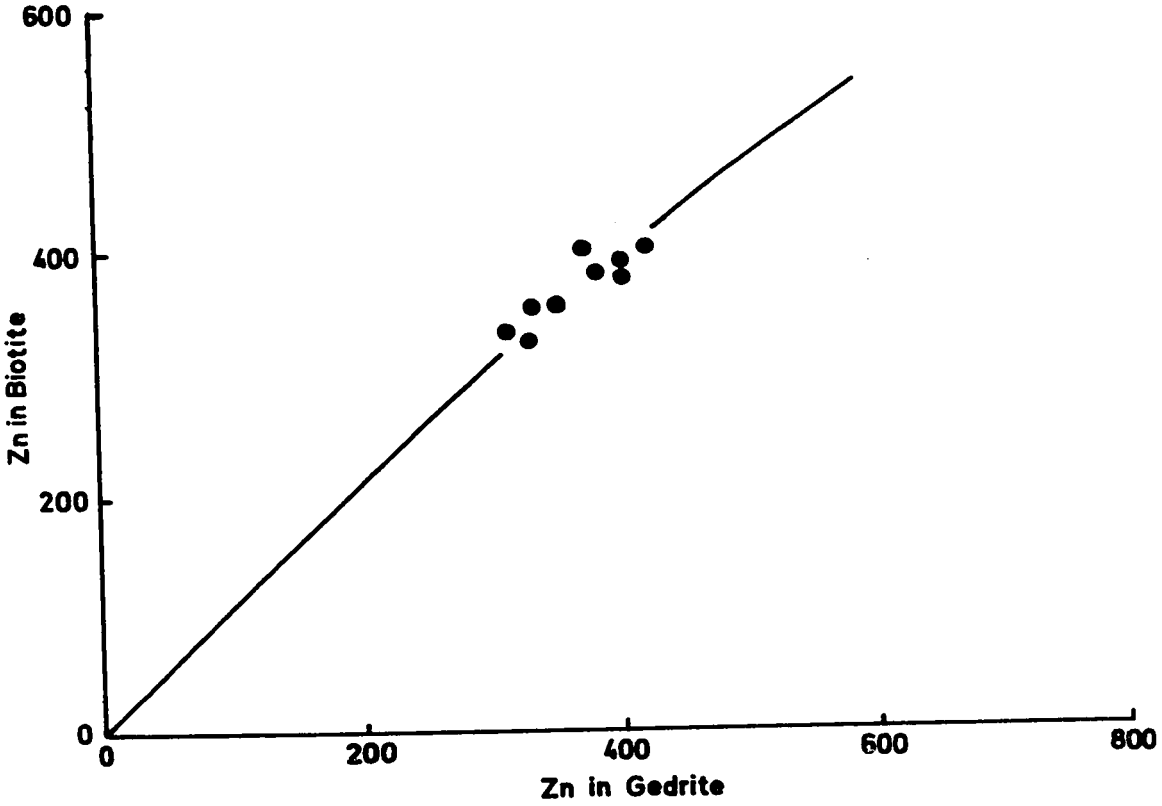

Figure 45. Distribution of Zn in gedrite and biotite.

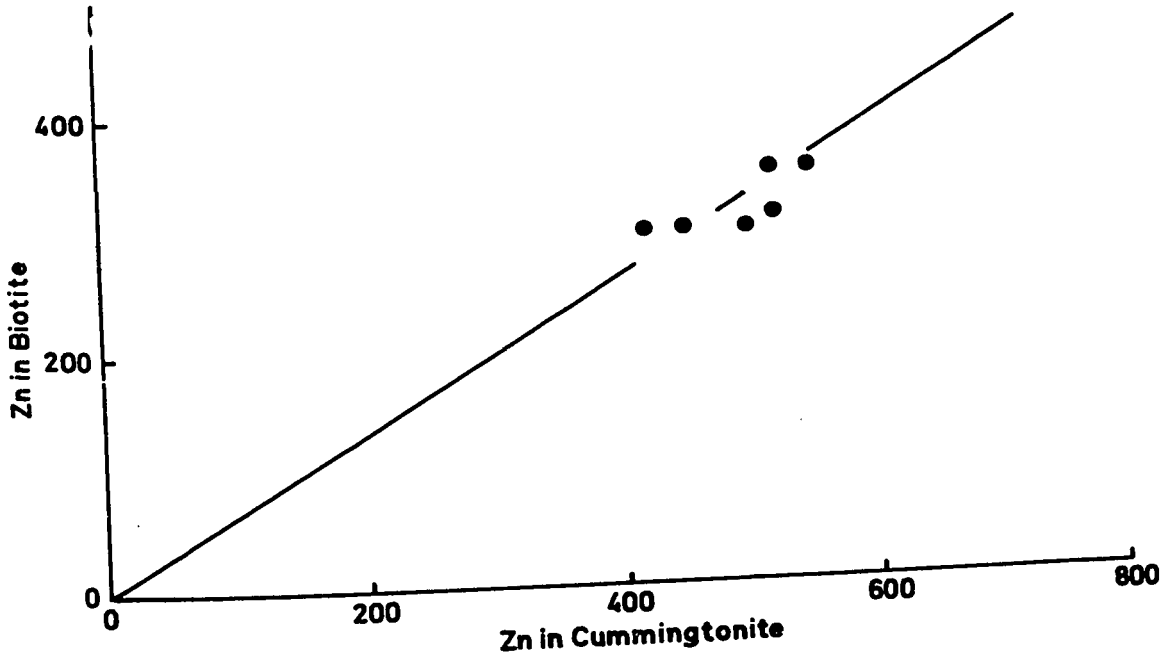

Figure 46. Distribution of Zn in cummingtonite and biotite.

concentrations of Mg.

Summary of Element Distribution

1. The distribution of Fe-Mg between the coexisting phases shows a regular pattern indicating a close approach to equilibrium. Deviations from regularity can sometimes be explained as a result of the influence of other elements, as has been shown by Kretz (1959) in case of other minerals. This feature is best illustrated by garnet where concentration of Ca in garnet influences the Mg-Fe distribution as well as the Mn distribution.

The distribution pattern of Mg-Fe between cordierite and biotite shows some ambiguous relations. The cordierite-biotite pairs from specimens away from the granite contact have a K_D value relatively close to unity, while those pairs near the contact have a K_D value that deviates more from unity. Field and petrographic data suggest that the cordierite-biotite pairs near the contact were probably not equilibrated during the peak period of metamorphism.

2. In almost all cases the Mn partitioning between coexisting phases shows a close approach to equilibrium. Within the range of concentrations encountered, the distribution curves are linear.

On the basis of distribution diagrams for Mg-Fe and Mn,-(Mg,Fe) certain conclusions regarding the enrichment of these elements amongst the coexisting phases can be drawn. In the case of coexisting garnet, gedrite, cordierite and biotite the Fe/Mg ratios are as follows:

garnet>gedrite>biotite>cordierite

With a certain range of concentrations this trend is also followed by Mn. However Mn is slightly concentrated in cordierite relative to biotite, i.e.

garnet>gedrite>cordierite>biotite

Thus with the exception of cordierite and biotite, high Mn concentrations are associated with high Fe concentrations.

3. The distribution of Ca shows a somewhat irregular pattern, and in some case this can be explained as the influence of other elements. In general, the scattering may be attributed to the concentration of this element in nonequivalent sites among the coexisting phases. However, the relative enrichment of Ca among the coexisting phases follows the trend:

plagioclase>garnet>gedrite>cordierite>biotite

4. The distribution of Na is somewhat irregular. In a few cases it can be explained in terms of the

influence of a third element, while in other cases reasons are unknown.

5. The partition of Al^{iv} among the minerals does not define any distribution trend; however, the partitioning of Al^{vi} between gedrite and biotite is strongly dependent on the Mg concentration of gedrite. This is due to substitution of the type $(Mg,Si) \rightleftharpoons Al.Al$.

The regular distribution of certain elements among coexisting phases in these Archean metamorphic rocks demonstrates that the chemical equilibrium attained during recrystallization can be preserved for long periods of time in geological history.

Some correlations between distribution coefficients and metamorphic grade have been attempted. The relations are obscured either due to the influence of concentration of a third element or due to lack of equilibration at the peak period of metamorphism as is the case of the cordierite-biotite pairs.

DISCUSSION AND CONCLUSIONS

Field and petrographic studies reveal that metamorphic grade in the study area varies from greenschist facies to hornblende-hornfels facies. The physical conditions of metamorphism, inferred from published experimental data, from the thickness of the supracrustal rocks and from the typical mineral assemblages can be inferred to be the low pressure-high temperature type defined by Miyashiro (1961, 1972). However, a slight deviation from the metamorphic path drawn by Miyashiro (1972) is noted; slightly higher pressures are suggested (Fig. 9).

The common occurrence of low pressure metamorphism in Archean terranes (de Roever, 1956, 1965; Miyashiro, 1972) suggests that high thermal gradients were characteristic during the early Precambrian times. This may be an indication that the crust was thinner at that time. This early stage of crustal evolution may be inferred from 1) absence of glaucophane schist facies metamorphism (de Roever, 1956, 1965); 2) telescoped nature of the metamorphic isograds around plutons suggesting high level intrusion (Anhaeusser et al. 1969), and 3) occurrence of low potash tholeites indicating little contamination of magma on ascent

(Baragar, 1966; Glikson, 1970).

Textural studies on the metasediments reveal a sequence of 'imprints' due to metamorphism, deformation and intrusion. The effects of two major deformational phases (D_1 and D_2) are recorded, associated with which were developed two intersecting schistosities (S_1 and S_2). Almost all the metamorphic mineral growth in the lower grade rocks occurred during these two phases of deformation. For example, flattened cordierite crystals in S_2 foliation indicate growth during the D_2 phase. However, contact metamorphic effects complicate this picture; sillimanite, gedrite and cordierite in the aureole of the Sparrow Lake pluton have random orientation, and it is thought that they grew during a quiescent late stage of the D_2 phase. This is supported by the proximity and parallelism of the sillimanite isograd and the edge of the Sparrow Lake pluton; and by the size distribution of cordierite crystals with reference to their distance from the pluton.

The temperature in the rocks had dropped considerably when the final deformation (D_3) caused biotite crystals to be kinked and bent without any recrystallization. The time at which biotite, lying

in S_2, altered to chlorite cannot be dated with reference to D_3.

Thus, there was a progressive rise in temperature during the first two deformational events. Following low grade regional metamorphism in D_1, the temperature in the metasediments rose to a maximum when the Sparrow Lake pluton was intruded during late D_2, causing further growth of high grade minerals. During the cooling of rocks after the D_2 phase, retrogressive metamorphism affected the metasediments.

Such a sequence of deformation, metamorphism and magmatic events appears to be common in other Archean terranes. For example, Anhaeusser et al. (1969) report that there exists "an intimate relation between metamorphism and deformation, and the sequence is usually of two or more periods of mineral development and deformation, followed by widespread post-tectonic crystallization and late stage retrogression in the waning stages of metamorphism". However, there is a slight difference between the Yellowknife rocks and the 'norm' reported above (see also Glikson, 1970, 1972). In the latter, the high grade metamorphism is attributed solely to the late synkinematic granite, which is not the case in the study area. Thus,

either the Yellowknife-Beaulieu region represents a unique area of Archean medium-grade regional metamorphism, or the metamorphism in the other regions has not been fully described.

In low pressure metamorphic terrains, it is difficult to isolate the extent of the relative influences of regional and contact metamorphism. Exactly the same mineral assemblages can be produced by low pressure metamorphism, and at the contacts of high level intrusions. Textural studies such as the one conducted in the present case are helpful in distinguishing the influence of the two phenomena.

The transition of greenschist facies metamorphism to cordierite-bearing assemblages towards the granite has been recorded in other parts of the Slave Province (Jolliffe, 1938, 1946; Jolliffe and Henderson, 1942; Henderson et al. 1971). The mineral assemblages of the study area were also observed in the Hearne Lake and Yellowknife Mapsheets (see Henderson et al. 1971), where however, staurolite occurs locally. The restricted occurrence of this mineral in certain layers, analogous to gedrite, indicates that bulk compositional differences played a prominent role in its development. Mineral assemblages similar to those

in the study area (though without gedrite) were reported by Davidson (1967) about 70 miles to the east, near Benjamin Lake. Evidently, the nature of metamorphism in many parts of the Slave Province is much the same as that of the area around Sparrow Lake.

The different mineral assemblages observed can be related primarily to original bulk composition. The zonal arrangement of some minerals around the Sparrow Lake pluton suggests that physical conditions also played a significant role.

The cordierite-gedrite-bearing rocks were originally greywackes, poor in potash. The composition of the rocks is not restricted to the system SiO_2-Al_2O_3-FeO-MgO, as was supposed by previous workers. The field, petrographic and chemical data suggest that these rocks experienced isochemical metamorphism; hence the chemical composition of the ancient sediments was probably very similar to that of the present day metasediments. In Archean greenstone belts, analysis of the greenstones compare very favourably with fresh lavas (Wilson et al. 1965; Baragar, 1966, 1968; Glikson, 1970; Hallberg, 1972), indicating that isochemical metamorphism is not an isolated phenomenon. The small difference in composition between lowest

grade and highest grade rocks in the study area also suggests this. However, metasomatic effects are not entirely absent, and are present at the contacts of granite and pegmatite bodies.

The chemistry of the minerals shows a small variation, perhaps due to small differences in original bulk composition. On the basis of the present study the following conclusions can be drawn:

1) the compositional variation in biotite reflects differences in mineral paragenesis rather than metamorphic grade.

2) variation in cordierite composition can be related to mineral paragenesis; but some variability may be due to metamorphic grade, and to differences in water pressure etc.

3) the compositional data for orthoamphiboles shows that they are enriched in Na and Al and are gedritic in composition.

4) the CaO content of cummingtonite is lower than 0.4%, at least in some cases, suggesting that contrary to works by Layton and Phillips (1961) and Schürmann (1966) this constituent is not essential for its stability.

5) the garnets are chemically zoned, having Mn rich

cores and Fe rich rims. The degree of zonation can be related to size, larger garnets being more zoned. In general, the composition profiles may be considered in relation to the depletion models of Hollister (1966) and Atherton (1968), but several factors can influence the degree of zonation. Kretz (1966) has shown that nucleation of crystals in metamorphic rocks is not instantaneous, and this factor may be an important parameter that can give rise to different degrees of zoning.

The chemical studies have shown that equilibrium was attained during rock metamorphism. In general, equilibrium in metamorphic rocks can be examined in relation to 1) textures; 2) phase rule considerations and 3) the partition of elements among coexisting phases. Textural equilibrium may give clues to the establishment of chemical equilibrium; but lack of textural equilibrium does not imply lack of chemical equilibrium (Zen, 1963), but only suggests that chemical equilibrium has not been attained. Further evidence may be obtained from the phase rule considerations. The major components of the rocks are SiO_2, Al_2O_3, Fe_2O_3, FeO, MgO, MnO, TiO_2, K_2O, CaO, Na_2O and H_2O. The other components such as C, S, B and P are

strongly fractionated in graphite, sulfides, tourmaline and apatite, respectively. The accessory phases may be considered not to have a significant effect on the phase relations. Consistent differences in opaque mineralogy suggest that the chemical potential of oxygen may be treated as fixed (Thompson, 1955, Zen, 1963). The restricted mobility of oxygen in metasedimentary sequences has been commonly noted (Chinner, 1960; Mueller, 1961, 1967; Zen, 1963; Peikert, 1963; Guidotti, 1970). Therefore, local fugacity of oxygen was probably largely controlled by the initial bulk composition. Water may be treated as a mobile component (Thompson, 1957), and the ten major components represent the 'fixed components'. As no more than ten phases are encountered in any of the assemblages studied, the phase rule is not violated.

A more rigorous measure of equilibrium is found in the regular distribution of elements in the coexisting phases. The distribution of Fe and Mg between biotite, cordierite and gedrite shows a regular trend, indicating that exchange equilibrium was attained. In the case of garnets, the outer rims are evidently equilibrated with the coexisting phases;

however, the partition of Fe and Mg is also influenced by the Ca in the garnet rims. Mn and Na also show a regular trend among coexisting phases. In summary, the distribution of elements among coexisting phases demonstrates that exchange equilibrium, within volumes of a few cubic centimeters, was generally attained.

Archean metamorphic rocks are after all perhaps not such a poor subject for textural and chemical studies in spite of their antiquity!

REFERENCES

Albee, A.L., 1965, Distribution of Fe, Mg and Mn between garnet and biotite in natural mineral assemblages: J. Geol., 73, 155-164.

Akella, J. and Winkler, H.G.F., 1966, Orthorhombic amphiboles in some metamorphic reactions: Contri. Min. Pet., 12, 1-12.

Anhaeusser, C.R., Mason, R., Viljoen, M.J., and Viljoen, R.P., 1969, A reappraisal of some aspects of Precambrian Shield geology: Geol. Soc. Am. Bull., 80, 2175-2200.

Atherton, M.P., 1968, The variation of garnet, biotite and chlorite composition in medium grade pelitic rocks from the Dalradian, Scotland, with particular reference to zonation in garnet: Contri. Min. Pet., 18, 347-371.

Baragar, W.R.A., 1966, Geochemistry of the Yellowknife volcanic rocks: Can. J. Earth Sci., 3, 9-30.

_____, 1968, Major element geochemistry of the Noranda volcanic belt, Quebec-Ontario: Can. J. Earth Sci., 4, 773-790.

Barker, F., 1962, Cordierite-garnet gneiss and associated microcline rich pegmatite at Sturbridge, Massachusetts and Union,

Connecticut: Am. Min., 47, 907-918.

Barth, T.F.W., 1936, Structural and petrological studies in Dutchess County, New York, Part II, Petrology and metamorphism of palaeozoic rocks: Geol. Soc. Am. Bull., 47, 775-850.

Best, M.G., and Weiss, L.E., 1964, Mineralogical relations in some pelitic hornfelses from Southern Sierra Nevada, California: Am. Min., 49, 1240-1266.

Billings, M.P., 1937, Regional metamorphism in the Littleton-Moosibauke Area, New Hampshire: Geol. Soc. Am. Bull., 48, 463-566.

Boldizsar, T., 1964, Terrestrial heat flow in the Carpathians: J. Geophy. Res., 69, 5269-5275.

Boyle, R.W., 1961, Geology, geochemistry and origin of the gold deposits of the Yellowknife District, N.W.T.: G.S.C. Memoir. 310, 193p.

Brown, E.H., 1967, The greenschist facies of eastern Otago, New Zealand: Contri. Min. Pet., 14, 259-292.

Bugge, J.A.W., 1943, Geological and petrographical investigations in the Kongsberg-Bamble Formation: Norg. Geol. Undersökelse No. 160, 150p.

Butler, B.C.M., 1967, Chemical study of minerals from

the Moine schists of the Ardanamurchan Area, Argyllshire, Scotland: J. Pet., 8, 233-267.

Burwash, R.A., Campbell, F.A., Cumming, G.L., and Folinsbee, R.A., 1963, Potassium-argon dates of diabase dyke systems, District of Mackenzie, N.W.T.,: Trans. Can. Inst. Mining Metall., 67, 303-307.

Carmichael, D.M., 1969, On the mechanism of prograde metamorphic reactions in quartz-bearing pelitic rocks: Contri. Min. Pet., 20, 244-267.

Chinner, G.A., 1959, Garnet-cordierite paragenesis: Carnegie Inst. Wash. Yearb., 58, 112-114.

_____ , 1960, Pelitic gneisses with varying ferrous/ferric ratios from Glen Clova, Angus, Scotland: J. Pet., 1, 178-217.

_____ , 1961, The origin of sillimanite in Glen Clova, Angus: J. Pet., 2, 312-323.

_____ , 1962, Almandine in thermal aureoles: J. Pet., 3, 316-340.

Compton, R.R., 1960, Contact metamorphism in Santa Rosa Range, Nevada: Geol. Soc. Am. Bull., 71, 1383-1416.

Condie, K.C., 1967, Geochemistry of Early Precambrian rocks from Wyoming: Geochim. Cosmochim. Acta, 31, 2135-2149.

Davidson, A., 1967, Metamorphism and intrusion in the Benjamin Lake map-area, Northwest Territories: Ph.D. Thesis, Univ. of British Columbia, Vancouver, 204p.

_____ , 1971, Granite studies in the Slave Province: G.S.C., Paper 72-1A, Part A, 109-115.

Deer, W.A., Howie, R.A. and Zussman, J., 1961, Rock-forming minerals, I-IV, Longmans, New York.

Drake, J.C., 1968, The composition of almandine and coexisting minerals in mica schists of the Errol quadrangle, New Hampshire-Maine: Ph.D. Thesis, Harvard Univ., Massachusetts, 220p.

Ernst, W.G., 1963, Significance of phengitic micas from low grade schists: Am. Min., 48, 1357-1373.

Eskola, P., 1914, On the petrology of the Orijarvi region in southwestern Finland: Bull. Comm. Geol. Fin., No. 40, 277p.

_____, 1915, On the relations between the chemical and mineralogical composition on the meta-

morphic rocks of the Orijarvi region: Bull. Comm. Geol. Fin., 44, 109-143.

Eskola, P., 1920, The mineralogical facies of rocks: Norsk Geol. Tidsskr., 6, 143-194.

_____, 1933, On the differential anatexis of rocks: Bull. Comm. Geol. Fin., 103, 12-25.

Eugster, H.P., and Wones, D.R., 1962, Stability relations of ferruginous biotite, annite: J. Pet., 3, 82-125.

Evans, B.W., 1964, Coexisting albite and oligoclase in some schists from New Zealand: Am. Min., 49, 173-179.

_____, 1965, Pyrope garnet-piezometer or thermometer ?: Geol. Soc. Am. Bull., 76, 1295-1300.

_____, 1965, Application of reaction-rate method to the breakdown equilibria of muscovite and muscovite plus quartz: Am. J. Sci., 263, 647-667.

Fawcett, J.J., and Yoder, H.S., 1962, Quartz-chlorite assemblages in the system $MgO-Al_2O_3-SiO_2-H_2O$: Carnegie Inst. Wash. Yearb., 62, 140-143.

_____, 1966, Phase relations of chlorites in the system $MgO-Al_2O_3-SiO_2-H_2O$: Am. Min., 51, 353-380.

Folinsbee, R.E., 1941, Optic properties of cordierite in relation to alkalies in the cordierite-beryl structure: Am. Min., 216, 485-500.

_____, 1942, Metamorphism and ore deposits of the Yellowknife-Beaulieu Area: Ph.D. Thesis, Univ. of Minnesota, Minneapolis.

_____, Baadsgaard, H., Cumming, G.L., and Green, D.C., 1968, A very ancient island arc. In the crust and upper mantle of the Pacific Area: Geophy. Monogr., 12, 441-448.

Fortier, Y.O., 1946, Yellowknife-Beaulieu region, Northwest Territories: G.S.C., Prel. Ser. Map 46-23.

_____, 1947, Ross Lake, Northwest Territories: G.S.C. Prel. Ser. Map 47-16.

Froese, E., 1963, Structural geology and metamorphic petrology of the Coronation Mine Area, Saskatchewan: Ph.D. Thesis, Queen's Univ., Kingston, Ont.

Garlick, G.D., and Epstein, S., 1967, Oxygen isotopic ratios in coexisting minerals of regionally metamorphosed rocks: Geochim. Cosmochim. Acta, 31, 181-214.

Geijer, S., 1963, On the association of magnesia and sulphide ores in metasomatic mineralization:

Arkiv. Min. Geol., 2, 153-164.

Gelman, M.L., 1963, A new occurrence of gedrite in the U.S.S.R.: Dokl. Akad. Nauk. SSSR, 141, 1281-1284.

Ghose, S., 1961, The crystal structure of a cummingtonite: Acta Cryst., 14, 622-627

Gibbs, G.V., 1966, The polymorphism of cordierite: I The crystal structure of low cordierite: Am. Min., 51, 380-388.

_____ , and Smith, J.V., 1965, Refinement of the crystal structure of pyrope: Am. Min., 50, 2023-2039.

Glikson, A.Y., 1970, Geosynclinal evolution and geochemical affinities of Early Precambrian systems: Tectnophy., 9, 397-433.

_____ , 1972, Early Precambrian evidence of a primi-ocean crust and island nucleii of sodic granite: Geol. Soc. Am. Bull., 83, 3323-3344.

Gorbatschev, R., 1968, Distribution of elements between cordierite, biotite, and garnet: Neues Jahrb. Min. Abhand., 110, 57-80.

Grant, J.A., 1968, Partial melting of common rocks as a possible source of cordierite-antho-

phyllite-bearing assemblages: Am. J. Sci., 266, 908-931.

Green, D.C., and Baadsgaard, H., 1971, Temporal evolution and petrogenesis of an Archean crustal segment at Yellowknife, N.W.T., Canada: J. Pet., 12, 177-217.

Green, J.C., 1963, High level metamorphism of pelitic rocks in northern New Hampshire: Am. Min., 48, 991-1023.

Grover, J.E., and Oraville, P.M., 1969, The partitioning of cations between coexisting single and multi-site phases with application to the assemblages: orthopyroxene-clinopyroxene and orthopyroxene-olivine: Geochim. Cosmochim. Acta, 33, 773-785.

Guidotti, C.V., 1970, The mineralogy and petrology of the transition from the upper sillimanite zone in Quossoc Area, Maine: J. Pet., 11, 410-425.

Hallberg, J.A., 1972, Geochemistry of the Archean volcanic belts in eastern goldfields of Western Australia: J. Pet., 13, 45-56.

Harker, A., 1939, Metamorphism, Methuen and Co., Ltd, London, England, 362p.

Harwood, D.S., and Larson, R.R., 1969, Variations in the delta-index of cordierite around the Cuspitic pluton, West-central Maine: Am. Min., 54, 896-908.

Heald, M.T., 1950, Structure and petrology of the Lovewell Mountain quadrangle, New Hampshire: Geol. Soc. Am. Bull., 61, 43-89.

Heitanan, A., 1956, Kyanite, andalusite and sillimanite in the schists in Boehls Butte quadrangle, Idaho: Am. Min., 41, 1-27.

_____, 1959, Kyanite-garnet and gedritite from Orfino, Idaho: Am. Min., 44, 539-564.

Henderson, J.B., 1970a, Stratigraphy of the Archean Yellowknife Supergroup, Yellowknife Bay-Prosperous Lake Area, District of Mackenzie: G.S.C. Paper 70-26, 12p.

_____, 1970b, Petrology and origin of the sediments of the Yellowknife Supergroup (Archean), Yellowknife, District of Mackenzie: Ph.D. Thesis, The John's Hopkins Univ., Baltimore, 263p.

_____, 1972, Sedimentology of Archean turbidites at Yellowknife, Northwest Territories: Can. J. Earth Sci., 9, 882-902.

Henderson, J.B., Cecile, M.P., and Kamineni, D.C., 1971, Yellowknife and Hearne Lake Map-Areas, District of Mackenzie, with emphasis on the Yellowknife Supergroup (Archean): G.S.C., Paper 72-1A, 117-119.

Henderson, J.F., 1938, Beaulieu River, Northwest Territories: G.S.C. Prel. Ser. 38-1.

_____, 1943, Structure and metamorphism of Early Precambrian rocks between Gordon and Great Slave Lakes, N.W.T.: Am. J. Sci., 241, 430-446.

_____, and Jolliffe, A.W., 1941, Beaulieu River, District of Mackenzie, Northwest Territories: G.S.C. Map 581A.

_____, and Brown, I.C., 1952, The Yellowknife greenstone belt, Northwest Territories: G.S.C. Prel. Ser. 52-28.

Hess, P.C., 1969, The metamorphic paragenesis of cordierite in pelitic rocks: Contri. Min. Pet., 24, 191-207.

Heywood, W.W. and Davidson, A., 1969, Geology of Benjamin Lake Map-Area, District of Mackenzie: G.S.C. Memoir 361, 35p.

Hirchberg, A., and Winkler, H.G.F., 1968, Stability

relations between chlorite, cordierite and almandine during metamorphism: Contri. Min. Pet., 18, 17-42.

Holdaway, M.J., 1971, Stability of andalusite and the aluminosilicate phase diagram: Am. J. Sci., 271, 97-131.

Hollister, L.S., 1966, Garnet zoning: an interpretation based on the Rayleigh fractionation model: Sci., 154, 1647-1651.

Hsu, L.C., 1968, Selected phase relationships in the system Al-Mn-Fe-Si-O-H: A model for garnet equilibria: J. Pet., 9, 40-83.

Hutchinson, R.W., 1955, Regional zonation of pegmatites near Ross Lake, District of Mackenzie, Northwest Territories: G.S.C. Bull. 34p.

Iyama, T., 1955, Optical properties and unit cell dimensions of cordierite and indialite: Min. Jour., 1, 372-394.

Johnson, M.R.W., 1961, Polymetamorphism in movement zones in the Caledonian thrust belts of Northern Scotland: J. Geol., 69, 417-432.

_____, 1962, Relations of movements and metamorphism in the Dalradians of

Banfshire: Trans. Edin. Geol. Soc., 19, 26-64.

Jolliffe, A.W., 1938, Yellowknife Bay-Prosperous Lake Area, N.W.T.: G.S.C. Paper 38-21, 41p.

_____, 1942, Yellowknife Bay, Northwest Territories: G.S.C. Map 868A.

_____, 1946, Prosperous Lake, District of Mackenzie, N.W.T.: G.S.C. Map 668A.

Kamineni, D.C., and Wong, A.S., 1973, Gedrite from Yellowknife-Beaulieu region, District of Mackenzie, N.W.T. : Can. Min., 11, 1012-1015.

_____,and Carrara, A., 1973, Comparison of the composition of porphyroblastic and fabric-forming biotite in two metamorphic rocks: Can. J. Earth Sci., (In press).

Kennedy, G.C., 1959, Phase relations in the system Al_2O_3-H_2O at high temperatures and pressures: Am. J. Sci., 257, 563-573.

Kerrick, D.M., 1968, Experiments on the stability limits of pyrophyllite at 1.8Kb and 3.9Kb water pressure: Am. J. Sci., 266, 204-214.

Klein, C., 1964, Cummingtonite-grunerite series: A chemical, optical and X-ray study: Am.

Min., 49, 963-982.

Kracek, F.C., 1948, Phase transformations in one-compoment silicate systems (Symposium at Cornell Univ.,), John Wiley and Sons, New York.

Kretz, R., 1959, Chemical study of garnet, biotite and hornblende from gneisses of southwestern Quebec, with the emphasis on the distribution of elements among coexisting minerals: J. Geol., 67, 371-402.

_____, 1960, The distribution of certain elements among coexisting calcic pyroxenes, calcic amphiboles and biotites in skarns: Geochim. Cosmochim. Acta, 20, 161-191.

_____, 1961, Some applications of thermodynamics to coexisting minerals of variable composition: examples, orthopyroxene-clinopyroxene and orthopyroxene-garnet: J. Geol., 69, 361-387.

_____, 1963, Distribution of magnesium and iron between orthopyroxene and calcic pyroxene in natural mineral assemblages: J. Geol., 71, 773-785.

_____, 1966, Grain size distribution for certain metamorphic minerals in relation to

nucleation and growth: J. Geol., 74, 147-174.

Kretz, R., 1967, Study of pegmatite bodies and enclosing rocks, Yellowknife-Beaulieu Region, District of Mackenzie: G.S.C., Bull., 159, 109p.

_____, 1970, Variation in the composition of muscovite and albite in a pegmatite dyke near Yellowknife: Can. J. Earth Sci., 7, 1219-1235.

Kuroda, Y., 1954, On some metasomatic phenomenon in the quartz-diorite of the Hitachi Mine (English abstract): Sci. Rept. Tokyo Edu. Univ., 3, 185-195.

Kwak, T.A.P., 1970, An attempt to correlate non-predicted variations of distribution coefficients with mineral grain inhomogeneity using a field example studied near Sudbury, Ontario: Contri. Min. Pet., 26, 199-224.

Lal, R.K., and Moorhouse, W.W., 1969, Cordierite-gedrite rocks and associated gneisses of Fishtail Lake, Harcourt Township, Ontario: Can. J. Earth Sci., 6, 145-165.

Lambert, R. St. J., 1959, The mineralogy and metamorphism of the Moine schists of the Morar and Knoydart Districts of Inverness-shire: Trans. Roy. Soc. Edin., 63, 553p.

Layton, W., and Phillips, R., 1960, The cummingtonite problem: Min. Mag., 32, 659-663.

Leech, A.P., 1966, Potassium-argon dates of basic intrusive rocks of the District of Mackenzie, N.W.T. : Can. J. Earth Sci., 3, 389-412.

Lord, C.S., 1939, Snare River, Northwest Territories: G.S.C. Paper 39-5, 17p.

Lyons, J.B., 1955, Geology of the Hanover quadrangle, New Hampshire-Vermont: Geol. Soc. Am. Bull., 66, 105-146.

McGlynn, J.C., and Henderson, J.B., 1970, Archean volcanism and sedimentation in the Slave Structural Province, In Baer, A.J., (editor), Symposium on basins and geosynclines of the Canadian Shield: G.S.C., Paper 70-40, 31-44.

McNamara, M.J., 1965, The lower greenschist facies in Scottish Highlands: Geol. Fören.

Stockholm Forh., 87, 347-389.

McNamara, M.J., 1966, Chlorite-biotite equilibrium reactions in a carbonate free system: J. Pet., 7, 404-413.

Meagher, E.P., and Gibbs, G.V., 1965, Crystal structure and polymorphism of cordierite: Geol. Soc. Am. Spec. Paper 87, p. 107.

Menzer, G., 1928, Die krystall struktur der granate: Zeit. Krist., 69, p. 300.

Miyashiro, A., 1953, Calcium-poor garnet in relation to metamorphism: Geochim. Cosmochim. Acta, 4, 179-208.

_____, 1957, Cordierite-indialite relations: Am. J. Sci., 255, 43-62.

_____, 1961, Evolution of metamorphic belts: J. Pet., 2, 277-311.

_____, 1964, Oxidation and reduction in the earth's crust with special reference to role of graphite: Geochim. Cosmochim. Acta, 28, 717-729.

_____, 1972, Pressure and temperature conditions and tectonic significance of regional and ocean-floor metamorphism: Tectnophy., 13, 141-159.

Mueller, R.F., 1960, Compositional characteristics and equilibrium relations in mineral assemblages of a metamorphosed iron formation: Am. J. Sci., 258, 449-497.

_____, 1961a, Analysis of relations among Mg, Fe, and Mn in certain metamorphic minerals: Geochim. Cosmochim. Acta, 25, 267-296.

_____, 1961b, Oxidation in high temperature petrogenesis: Am. J. Sci., 259, 460-480.

_____, 1962, Energetics of certain silicate solid-solutions: Geochim. Cosmochim. Acta, 26, 581-598.

_____ , 1967, Mobility of elements in metamorphism: J. Geol., 75, 565-582.

_____ , 1969, Kinetics and thermodynamics of intracrystalline distributions: Min. Soc. Am. Spec. Paper 2, 83-93.

Nelston, B.W., and Roy, R., 1958, Synthesis of the chlorites and their structural and chemical constitution: Am. Min., 43, 707-725.

Newton, R.C., 1966, BeO in pegmatitic cordierite: Min. Mag., 35, 920-927.

Okrusch, M., 1971, Garnet-cordierite-biotite equilibria in the Steinach Aureole, Bavaria: Contri.

Min. Pet., 32, 1-23.

Okrusch, M., and Evans, B.W., 1970, Minor element relationships in coexisting andalusite and sillimanite: Lithos, 3, 261-268.

Osborne, E.F., 1939, The Montauban mineralized zone, Quebec: Econ. Geol., 34, 712-726.

Papike, J.J., and Ross, M., 1970, Gedrites; crystal structures and intracrystalline cation distributions: Am. Min., 55, 1945-1972.

Peikert, E.W., 1963, Biotite variation as a guide to petrogenesis of granitic rocks in the Precambrian of northern Alberta: J. Pet., 4, 432-459.

Pettijohn, F.J., 1963, Chemical composition of sandstone exclusive of carbonates and volcanic sands: J. Geol., 69, 84-100.

Prider, R.T., 1940, Cordierite-anthophyllite rocks associated with spinel-hypersthenite from Tooday, Western Australia: Geol. Mag., 77, 364-382.

Pye, E.G., 1957, Geology of the Manitouwadge Area: Ont. Dept. Mines, Rept. 66, Part 8.

Ramberg, H., 1952, The origin of metamorphic and metasomatic rocks: The Univ. of Chicago Press, Chicago, 317p.

Ramberg, H., and DeVore, G., 1951, The distribution of Fe and Mg in coexisting olivines and pyroxenes: J. Geol., 59, 193-210.

Read, H.H., 1952, Metamorphism and migmatization in the Ythan Valley, Aberdeenshire: Trans. Edin. Geol. Soc., 15, 265-279.

Reinhardt, E.W., 1968, Phase relations in cordierite-bearing gneisses from Gananoque Area, Ontario: Can. J. Earth Sci., 5, 455-482.

Reynolds, D.L., 1947, Hercynian Fe-Mg metasomatism in Cornwall, a reinterpretation: Geol. Mag., 84, 29-50.

Richardson, S.W., 1968, Staurolite stability in a part of the system Fe-Al-Si-O-H: J. Pet., 9, 467-488.

_____, Gilbert, M.C., and Bell, P.M. 1969, Experimental determination of the kyanite-andalusite-sillimanite equilibria, the aluminosilicate triple point: Am. J. Sci., 267, 259-272.

Robinson, P., and Jaffe, H.W., 1969, Chemographic exploration of amphibole assemblages from central Massachusetts and southwestern New Hampshire: Min. Soc. Am. Spec. Paper 2,

251-274.

Robinson, P., Ross, M., and Jaffe, H.W., 1971, Compositions of gedrite and hornblende, and anthophyllite-gedrite solvus: Am. Min., 56, 1005-1041.

Roever, W.P. de, 1956, Some differences between post-palaeozoic and older regional metamorphism: Geol. en. Mijn., 18, 123-127.

_____, 1965, On the cause of the preferential distribution of certain metamorphic minerals in orogenic belts of different age: Geol. Rund., 54, 933-943.

Salotti, C.A., 1962, Anthophyllite within the albite-epidote hornfels facies, Fremont County, Colorado: Am. Min. 47, 1055-1066.

Saxena, S.K. and Hollander, N.J., 1969, Distribution of iron and magnesium in coexisting biotite, garnet and cordierite: Am. J. Sci., 267, 210-216.

Schreyer, W., and Schairer, J.F., 1961, Compositions and structural states of anhydrous Mg-cordierite: A reinvestigation of the central part of the system $MgO-Al_2O_3-SiO_2$: J. Pet., 2, 324-406.

Schreyer, W., and Yoder, H.S., 1964, The system Mg-cordierite-H_2O and related rocks: Neues Jahrb. Min., 101, 271-342.

Schürmann, K., 1966, Synthesis and stability of cummingtonite: Min. Soc. Am. Spec. Paper 1, 255-260.

Segnit, E.R., 1963, Synthesis of clinochlore at high pressures: Am. Min., 48, 1080-1089.

_____ , and Kennedy, G.C., 1961, Reactions and melting relations in the system muscovite-quartz at high pressures: Am. J. Sci., 259, 280-287.

Seifert, F., 1970, Low temperature compatibility relations of cordierite-haplopelites of the system K_2O-MgO-Al_2O_3-SiO_2-H_2O: J. Pet., 11, 73-99.

Sen, S., and Chakraborty, K.R., 1968, Magnesium-iron exchange equilibrium in garnet-biotite and metamorphic grade: Naues Jahrb. Min. Abh., 108, 108-207.

Seki, Y., 1957, Petrological study of hornfelses in the central part of the median zone of Kitakami Mountainland: Saitama Univ. Sci. Repts. Ser. B, 2, 307-361.

Simonen, A., 1948, On the petrology of the Aulanko Area in southwest Finland: Bull. Comm. Geol. Fin., 143, 38-47.

Sims, P.K., and Gable, D.J., 1963, Cordierite-bearing mineral assemblages in Precambrian rocks, Central City quadrangle, Colorado: U.S.G.S. Prof. Paper 475-B, 1135-1337.

Slany, V.R., 1971, Colour aerial photography of the Yellowknife District, N.W.T. (85I,J): G.S.C. Paper 72-1A, 61p.

Sorby, R.C., 1964, Anthophyllite-cordierite gneiss in the basal rock complex of the Hagesund Peninsula, western Norway: Norsk. Geol. Tidsskr., 44, 323-340.

Spry, A., 1969, Metamorphic textures, Pergaman Press, 150p.

Stewart, F.H., 1942, Chemical data on a silica-poor argillaceous hornfels and its minerals: Min. Mag., 26, 260-266.

Stockwell, C.H., 1933, Great Slave Lake-Coppermine River Area, Northwest Territories: G.S.C. Summer Rept. 1931, Pt. C, 37-63.

_____, 1964, Fourth report on Structural Provinces, orogenics, and time-classification of rocks of the Canadian Precambrian Shield:

G.S.C. Paper 64-17, 1-21.

Stout, J.H., 1972, Phase petrology and mineral chemistry of coexisting amphiboles from Telemark, Norway: J. Pet., 13, 99-145.

Strens, R.G., 1968, Stability of Al_2SiO_5 solid-solutions: Min. Mag., 36, 839-849.

Sundius, N., 1935, On the origin of late magmatic solutions containing magnesia, iron and silica: Sverges Geol. Undersokn, Ser. C. 392, Arsbok 29.

Tilley, C.E., 1935, Metasomatism associated with greenstone-hornfels of Kenidjack, Cornwall: Min. Mag., 24, 181-202.

_____, 1937, Anthophyllite-cordierite granulites of Lizard: Geol. Mag., 74, 300-308.

_____, and Flett, J., 1930, Hornfels from Kenidjack, Cornwall: Summ. Prog. Geol. Great Bri., Part II, 24-41.

Thompson, J.B., Jr., 1955, The thermodynamic basis for the mineral facies concept: Am. J. Sci., 253, 65-103.

_____, 1957, The graphical analysis of mineral assemblages in pelitic schists: Am. Min. 42, 842-858.

Tozer, C.F., 1955, The mode of occurrence of sillimanite in Glen District, County Donegal: Geol. Mag., 92, 310-320.

Tuminen, H.V., and Mikkola, T., 1950, Metamorphic Mg-Fe enrichment in the Orijarvi Region as related to folding: Comp. Rend. Soc. Geol. Fin., 23, 67-92.

Turner, F.J., 1948, Mineralogical and structural evolution of metamorphic rocks: Geol. Soc. Am. Mem. 30, 342p.

_____ , 1968, Metamorphic petrology, mineralogical and field aspects, McGraw Hill, New York, 403p.

_____ , and Verhoogen, J., 1960, Igneous and metamorphic petrology, McGraw Hill, New York, 694p.

Turnock, A.C., 1960, The stability of Fe chlorites: Carnegie Inst. Wash. Yearb., 59, 98-104.

Vallance, R.G., 1967, Mafic rock alteration and isochemical development of some cordierite-anthophyllite rocks: J. Pet., 8, 84-96.

Velde, B., 1966, The upper stability of muscovite: Am. Min., 51, 924-929.

Wenk, E., 1962, Plagioklas als index mineral in den zertralpen: Schw. Min. Pet. Mitt., 42,

139-152.

White, W.S. and Billings, M.P., 1951, Geology of the Woodsville quadrangle, Vermont-New Hampshire: Geol. Soc. Am. Bull., 62, 647-696.

Wilson, M.E., 1935, Rock alteration at the Amulet Mine, Noranda District, Quebec: Econ. Geol., 30, 478-492.

Wilson, H.D.B., Andrews, P., Moxham, R.L., and Ramlal, K., 1965, Archean volcanism in the Canadian Shield: Can. J. Earth Sci., 2, 161-175.

Winkler, H.G.F., 1967, Petrogenesis of metamorphic rocks, second edition, Springer-Verlag, New York, 237p.

Winchell, A.N., and Winchell, H., 1951, Elements of optical mineralogy, Part II: John Wiley and Sons, Inc., New York.

Wones, D.R., and Eugster, H.P., 1965, Stability of biotite: experiment, theory and application: Am. Min., 50, 1228-1272.

Wynne-Edwards, H.R., and Hay, P., 1963, Coexisting cordierite and garnet in regionally metamorphosed rocks from the Westport Area, Ontario: Can. Min., 71, 453-478.

Yoder, H.S. Jr., 1952, The $MgO-Al_2O_3-SiO_2-H_2O$ System and the related metamorphic facies: Am.

J. Sci., Bowen volume, 569-627.

Yoder, H.S. Jr., and Eugster, H.P., 1955, Synthetic and natural muscovites: Geochim. Cosmochim. Acta, 8, 225-280.

_____, and Chinner, G.A., 1960a, Almandite-pyrope-water system at 10,000 bars: Carnegie Inst. Wash. Yearb., 59, 81-84.

_____, 1960b, Grossularite-pyrope-water system at 10,000 bars: Carnegie Inst. Wash. Yearb., 59, 78-81.

Zen, E.-AN, 1963, Components, phases and criteria of chemical equilibrium in rocks: Am. J. Sci., 261, 929-942.

Zwart, H.J., 1960, Relations between folding and metamorphism in the Central Pyrenees and their chronological succesion: Geol. Mijnb., 22, 163-180.

_____, 1963, Some examples of the relations between deformation and metamorphism from the Central Pyrenees: Geol. Mijnb., 42, 143-154.

Appendix I

Mineral Separation

The samples selected were cut with a diamond saw, and the slices were then crushed in a porcelain mortar. In almost all instances powdered fractions of -230 to 325 mesh size were chosen for separation as this size proved to be relatively free from inclusions. The scheme adopted in mineral separation is given in Fig. 48.

Biotite, amphibole and garnet separated by this method is estimated to be 95 to 98% pure by weight and a further purity up to 99% and better was achieved by hand picking under a binocular microscope. It was not possible to separate the coexisting cummingtonite and gedrite due to overlap in the properties of magnetic susceptibility and density. Cordierite concentrated by this process was used for the distortion index determination.

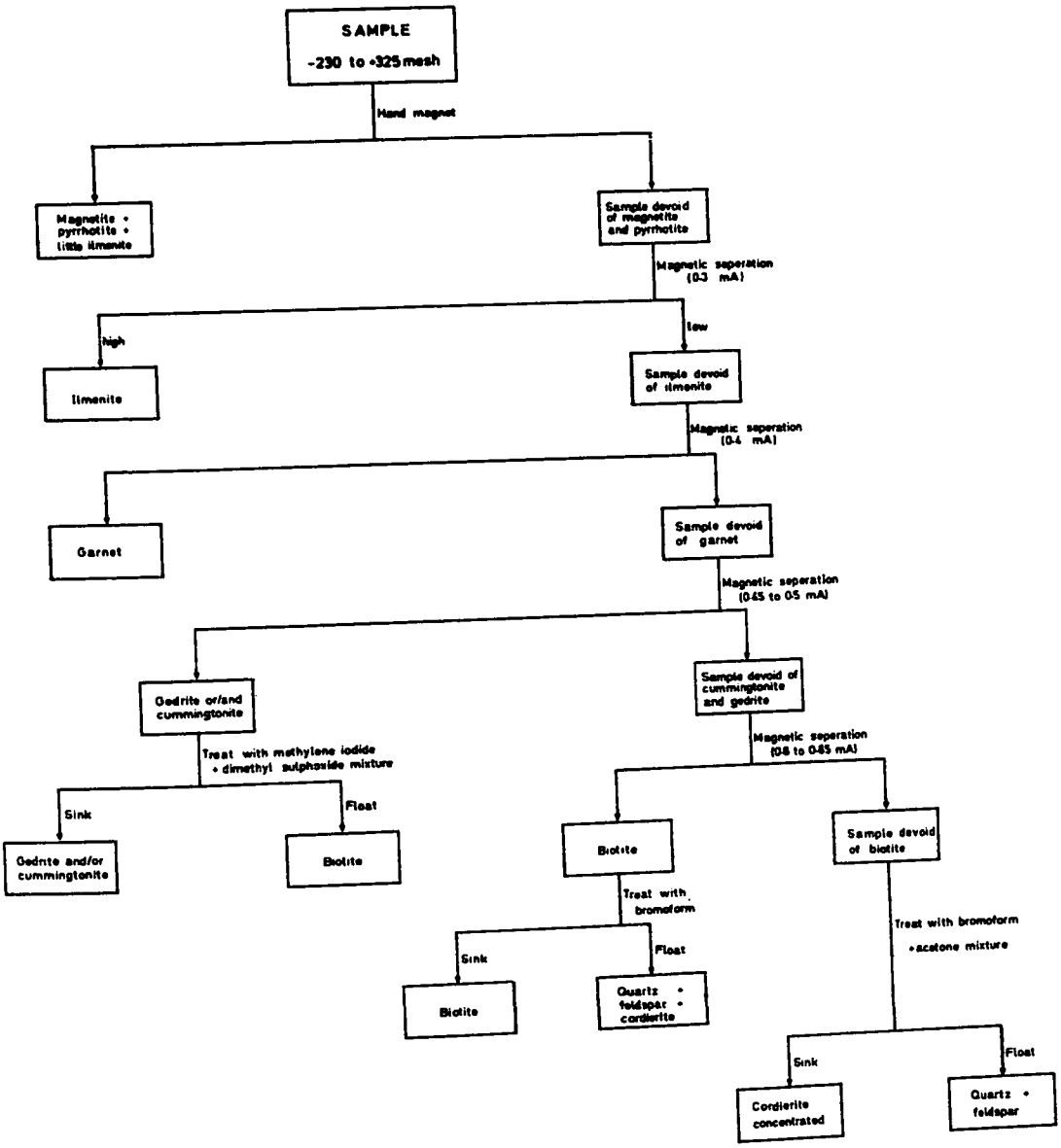

Figure 47. Flow-sheet discribing the mineral separation technique.

Appendix II

Chemical Analysis

1. Atomic Absorption Spectrometric Method

Biotite, gedrite, cummingtonite and some garnet were analysed on a Techtron AA4 model atomic absorption spectrophotometer. The procedure adapted is that described by Kretz (1970).

The purified mineral samples were ground to fine powder in an agate mortar, heated in an oven for one hour at 110°C to drive off the moisture, and then placed in a dessicator for about 10 minutes. 100 mg. of the sample were weighed into a teflon crucible, moistered with a drop or two of distilled water, and 1 ml. of perchloric acid and 10 ml. of hydrofluoric acid were added, finally it was heated on a hot plate at 70°C to 80°C until completely evaporated. The process of dissolving is repeated two to three times, depending on the nature of the mineral, until it is completely dissolved. Then, it is evaporated to complete dryness, 1 ml. of perchloric acid and 10 to 15 ml. of distilled water are added, and it is warmed on a hot plate until a clear solution is formed. The solution was made up to 100 ml. in a volumetric flask and used to determine Fe (total),

Mg, Mn, Na, K, Ca, Li and Zn. Reference solutions were prepared for each of the elements from Fisher's standard solutions. To estimate the accuracy of the analysis standard solutions of basalt (BCR 1) and andesite (AGV 1) supplied by the U.S.G.S. and biotite standard (K 35-1), analysed by Dr. J.A. Maxwell of the G.S.C. were run side by side. All the unknown samples were duplicated and the average of the analysis is presented.

The 100 mg. sample in 100 ml. solution had to be diluted in some cases for some elements in order to bring the concentration of a particular element to the detection range of the instrument. For Mg and Ca determination, 2 ml. of 7.3% La solution was added to 10 ml. of the unknown solutions to suppress the interference of Al. The La solution was also added to the same volume of Fisher's standard solutions to bring the dilution to the same level as that of the unknown solutions. The dilution scheme is presented in Fig. 2.

From Table 25, the accuracy and precision of the analytical procedure is within quite acceptable limits.

SiO_2, Al_2O_3, TiO_2 and FeO in the rocks (except

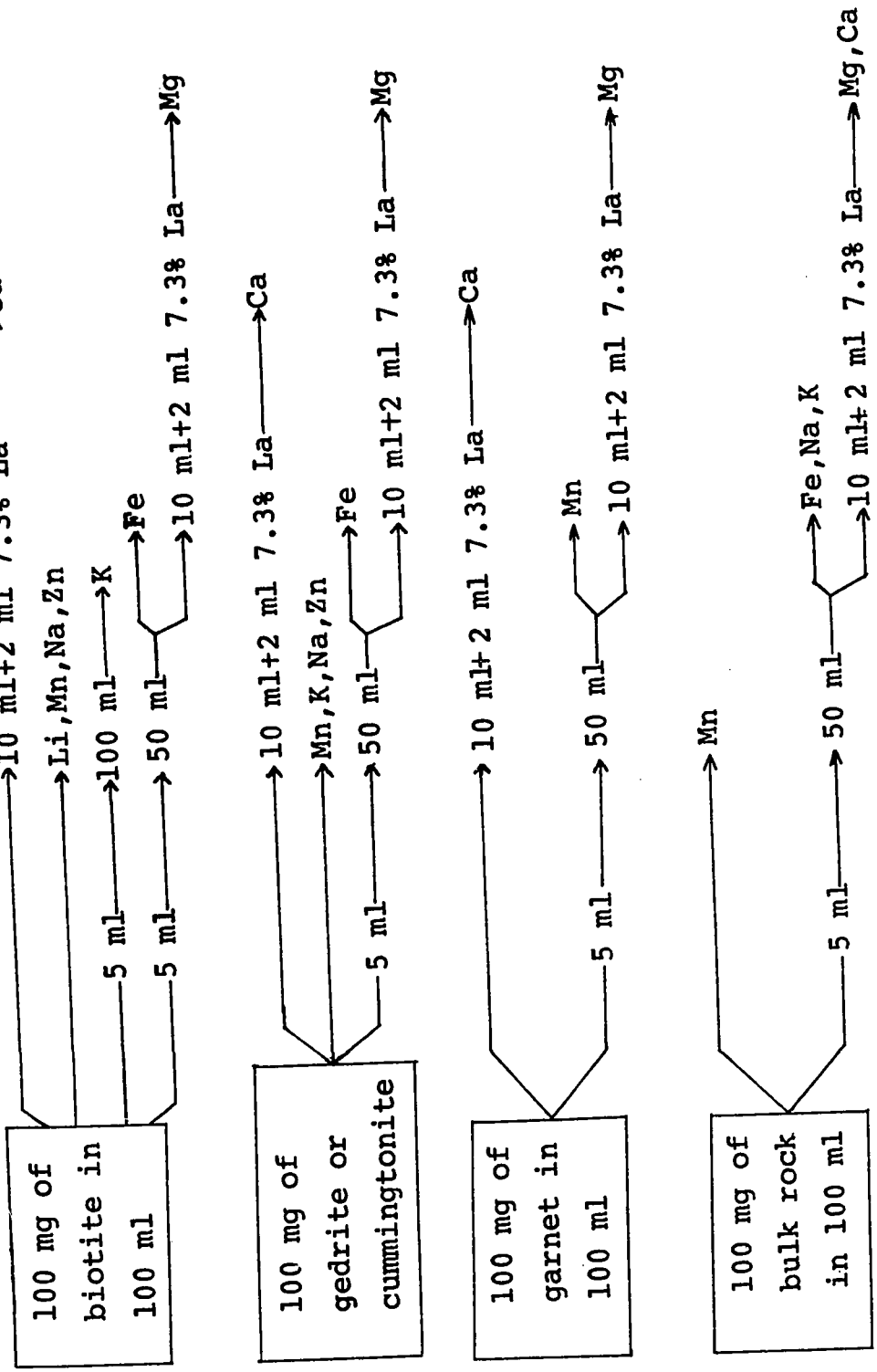

Figure 48: Scheme Adopted in Atomic Absorption Analyses

Table 25: Reproducibility of Analyses on the Atomic Absorption Spectrophotometer

Element	BCR 1			AGV 1			K35-1		
	U.S.G.S. results	1st run	2nd run at later date	U.S.G.S. results	1st run	2nd run at later date	G.S.C. results	1st run	2nd run at later date
Fe(total)	9.30	9.25	9.22	4.66	4.65	4.65	16.14	16.05	16.00
MgO	3.49	3.50	3.50	1.50	1.52	1.55	10.35	10.22	10.30
MnO	0.19	0.20	0.20	0.10	0.10	0.10	0.49	0.47	0.48
CaO	6.91	6.85	6.80	4.90	4.84	4.85	----	----	----
Na_2O	3.29	3.35	3.35	4.23	4.33	4.33	0.18	0.17	0.17
K_2O	1.69	1.61	1.60	2.86	2.80	2.80	9.37	9.20	9.20

cummingtonite-bearing rocks) was determined by Dr. N. Suhr of the Pennsylvania State University. SiO_2, Al_2O_3 and TiO_2 were determined by atomic absorption spectrophotometer, while FeO was determined by titrimetric methods. In the cummingtonite-bearing rocks, SiO_2, Al_2O_3 and TiO_2 were determined by Mr. P.S. Rao of the Institute für Mineralogie, Darmstadt, West Germany by X-ray fluorescence technique.

2. Electron Microprobe analysis

Cordierite was analysed on an ARL electron microprobe at Queen's University. For this purpose, polished thin sections were prepared and carbon-coated. Experimental conditions were: electron accelerating potential 15 kv, sample current 0.05-0.07 μa, beam size 3-5 μm, integration to 20 seconds. The following standards were used in the analysis:

SiO_2----quartz	Al_2O_3----Spinel, Bayer's Al_2O_3
Fe(total)-Fe metal	MgO----Spinel
MnO----Mn metal	CaO----synthetic anorthite
Na_2O----Dagfesthian albite	K_2O----synthetic potash feldspar

The cordierite was located by optical methods, by the use of polaroid photographs and also with

the help of frequency meters for certain elements such as Mg, Fe and Al. At least, 20 points were analysed in each section and the data was averaged. The data was processed on a computer programme available at Queen's University in which corrections for dead time (dead time assumed to be 2.5×10^{-6}s.), drift from standard to standard, background, absorption (Frazier's computer fit for absorption coefficients, Philbert's absorption correction), Heinrich's sigma value, fluorescence correction from Reed and finally the atomic number effects from Duncan and Reed.

SiO_2, Al_2O_3 and TiO_2 in biotite and gedrite were also determined on the microprobe. A biotite standard, K 37-1, the same biotite as was used in the atomic absorption spectrometric method) and a hornblende standard (E 31-63 of Kretz) were used in these determinations. The experimental conditions were accelerating potential 15 kv, sample curent 0.05-0.1 u, integration time 20 s, and a beam size of 5μm. About 15 spots were analysed in each sample and the counts were averaged. Since there was not much difference between standards used and the unknowns, correction procedures were relatively simple; only those for drift and background were employed. Accuracy

of the analysis is estimated to be $SiO_2 \pm 5\%$, $Al_2O_3 \pm 5\%$ and $TiO_2 \pm 10\%$.

The biotite crystals that were analysed on the atomic absorption were also analysed on the probe to compare accuracy and precision. The results are listed in Table 26.

Table 26

Sample No.	Element	Atomic Absorption	Probe
12	Fe (total)	15.22	15.45
	MgO	11.42	11.85
32	Fe (total)	15.12	15.66
	MgO	10.69	10.22
69	Fe (total)	14.50	14.20
	MgO	9.06	9.58

Plagioclase crystals in fourteen samples were analysed on the probe for Na_2O and CaO. Dagfesthian albite for Na and anorthite for Ca were used as standards. The experimental conditions were same as for in the previous cases. About 20 points were analysed and the counts were averaged. Corrections for drift and background were applied.

Garnet crystals were analysed on the microprobe. Ca, Mn, Mg and Fe were analysed for all the garnets, at the core and rim, and Al and Si were analysed in

a few cases. Carbon-coated thin sections were prepared for this purpose and garnet crystals of largest size were selected in each case. In a few cases where there is a considerable difference in size, both the biggest and the smallest crystals were analysed. Two to four points were analysed in the core and rim positions of each crystal and averaged.

A complete zoning profile was obtained for garnet crystals in sample 39A for Ca, Mg, Mn and Fe. For this purpose large garnet crystals isolated from the sample and polished to the center, mounted on an ebonite holder and carbon-coated. The crystals were scanned from edge to edge at fairly regular intervals.

Experimental conditions used in the analysis were: electron accelerated potential 15 kv, sample current 0.05-0.1 μa beam size 3-4 μm, integration time 20 s. Standards used in this analysis were garnets (360-55, 217-55), supplied by Dr. Kretz.

A complete analysis of three andalusite crystals was performed on the electron microprobe. Experimental conditions and standards used were same as those of cordierite. The data was processed on the computer using the same corrections as for cordierite.

Appendix III

X-Ray Diffraction Powder Data of Gedrite and Cummingtonite

X-ray powder diffraction work was performed on gedrite and cummingtonite from the study area. This work was undertaken essentially to confirm the identification of these two amphiboles.

Powder photographs were taken by exposing the sample (24 hours) to Mn-filtered, Fe-radition, on a large camera (114.6 mm) and corrections for film shrinkage were applied by means of an internal standard (quartz). The purity of the amphiboles used in taking the powder photographs is extremely high. Handpicking was repeated several times to get a pure sample. The photographs were measured by means of a high precision contact vernier, and the data processed on a least-square refinement program, designed by Dr. D.B. Stewart of the U.S.G.S. The d-values and the corresponding indices obtained by the least-square refinement program are presented in Appendix III.

The cell parameters obtained for gedrite and cummingtonite are given in Tables 10 and 11 respectively. Cell parameters of gedrite and cummingtonite reported by other workers are also presented for comparison.

There are only a few such values for gedrite in the literature. In the case of cummingtonites only two sets of values reported by Klein (1964) are taken into account and these are shown for comparison. As has been reported by other workers, gedrite in the present study also satisfies an orthorhombic symmetry with pnma space group, whilst cummingtonite satisfies monoclinic symmetry with a C_2/m space group. The cell parameters calculated for gedrite and cummingtonite compare favourably with those of other workers.

Table 27: Unit Cell Parameters of Gedrite

	Present Work	Milton and Ito (1961)	Papike and Ross (1970)		Stout (1971)
a Å	18.557±0.0041	18.594	18.531	18.601	18.58
b Å	17.873±0.0036	17.890	17.741	17.839	17.89
c Å	5.283±0.0030	5.304	5.249	5.284	5.30

Table 28: Unit Cell Parameters of Cummingtonite

	Present Work	Klein (1964)	
a Å	9.525±0.0034	9.562±0.002	9.534±0.0019
b Å	18.202±0.0040	18.324±0.007	18.231±0.0047
c Å	5.313±0.0032	5.338±0.0035	5.322±0.0044
β	101.83 ± 0.40	101.86	101.97 ± 0.33

Table 29: X-ray Diffraction Data of Gedrite

hKl	d(Calc. Å)	d(Obser. Å)	I/Io
020	8.94	8.98	65
210	8.24	8.25	100
230	5.01	----	----
111	4.89	----	----
400	4.64	4.64	5
040	4.47	4.47	10
420	4.12	4.13	10
131	3.87	3.88	5
231	3.64	3.64	10
331	3.33	3.34	10
440	3.22	3.22	90
610	3.05	3.06	100
341	2.988	----	----
521	2.876	2.878	20
260	2.836	----	----
251	2.821	2.823	40
630 441	2.745	2.750	40
531	2.706	----	----
351	2.671	2.674	40
161	2.570	2.571	30
202	2.541	2.543	10
451	2.496	2.502	40
302	2.429	2.433	5
650	2.339	2.341	5
551	2.315	2.314	5
271	2.231	2.230	8
502	2.152	2.152	10
561	2.127	2.127	10
821	2.067	2.067	8
480	2.013	----	----
661	1.988	1.987	5
750	1.976	----	----
702 940	1.873	1.873	5
931	1.828	1.826	20
0.10.0	1.787	1.788	5
10. 3.0	1.772	1.773	10
961	1.615	1.616	30
2.11.0	1.601	1.600	20
922	1.599	1.599	30
11. 2.1	1.582	1.582	10
6.10.0 12. 0.0	1.547	1.547	30
10. 6.1	1.511	1.511	10
0.12.0	1.489	1.489	20
553	1.454	1.452	10
10. 4.2 6.11.0	1.438	1.438	10

Table 30: X-ray Diffraction Data of Cummingtonite

hKl	d(Calc. Å)	d(Obser. Å)	I/Io
020	9.101	9.082	40
110	8.297	8.259	100
$11\bar{1}$	4.820	4.810	<5
040	4.550	4.538	35
220	4.149	4.145	40
$13\bar{1}$	3.858	3.861	35
131	3.448	3.444	5
240	3.256	3.253	90
060	3.034	3.060	100
310	3.063	3.058	<5
221	2.998	2.985	<10
151	2.748	2.741	90b
061	2.620	2.623	40
$20\bar{2}$	2.499	2.503	40b
350	2.363	2.366	20
080 $35\bar{1}$	2.290	2.294	35
$42\bar{1}$	2.240	2.245	<10
261 $24\bar{2}$	2.190	2.190	90
081 202	2.095	2.092	<10
351	2.035	2.038	<20f
370 190	1.994	1.997	<5f
$40\bar{2}$	1.945	1.965	<5
$19\bar{1}$	1.874	1.877	<10
460	1.848	1.851	10
371	1.785	1.7849	20b
461	1.658	1.658	80
1.11.0	1.629	1.629	80
2.10.1	1.578	1.579	15
600	1.556	1.555	40
0.12.0	1.517	1.517	70
3.11.0	1.460	1.460	30
$4.10.\bar{1}$	1.430	1.434	25
512 $46\bar{3}$	1.383	1.381	60 <10
$66\bar{2}$	1.325	1.325	30
$2.12.\bar{2}$	1.297	1.296	40
4.12.0	1.271	1.270	30

b = broad f = faint

Appendix IV

Table 31: Mössbauer Characteristics of Cummingtonite and Gedrite

Sample No.	Sites Assigned	Chemical isomer shift	Kuadrapole shift	Width at half-peak height	Area	Distribution of Fe^{2+}
Cummingtonite	M_4	1.27	2.87	T_1=0.40 T_4=0.38	A_1=0.37 A_4=0.32	1.693
	M_1,M_2 & M_3	1.21	1.67	T_2=0.37 T_3=0.36	A_2=0.36 A_3=0.30	1.619
	Average Mean Square Residual			611		
	Chi-squared			549		
Gedrite	M_4	1.27	2.66	T_1=0.39 T_4=0.48	A_1=0.26 A_4=0.36	1.34
	M_1,M_2 & M_3	1.24	1.87	T_3=0.59 T_5=0.44	A_3=0.54 A_4=0.24	1.74
	Average Mean Square Residual			675		
	Chi-squared			549		

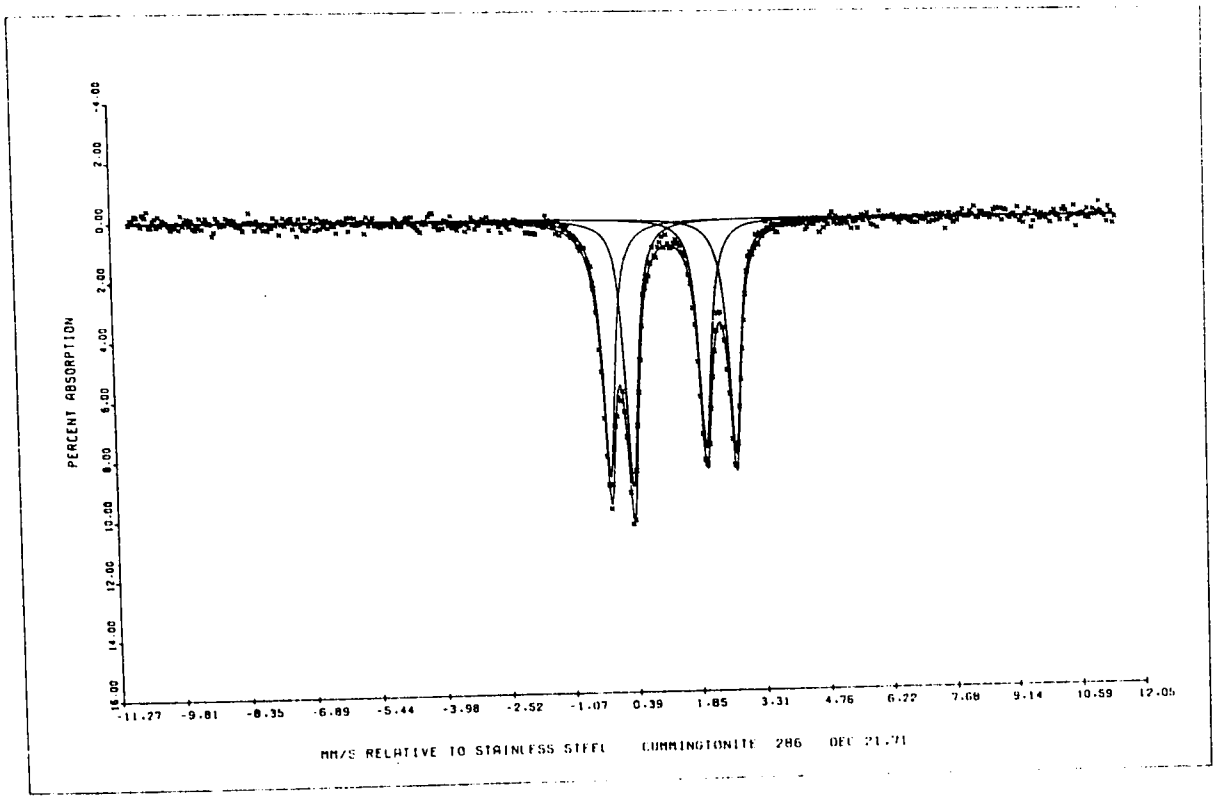

Figure 49. Mössbauer spectra of cummingtonite.

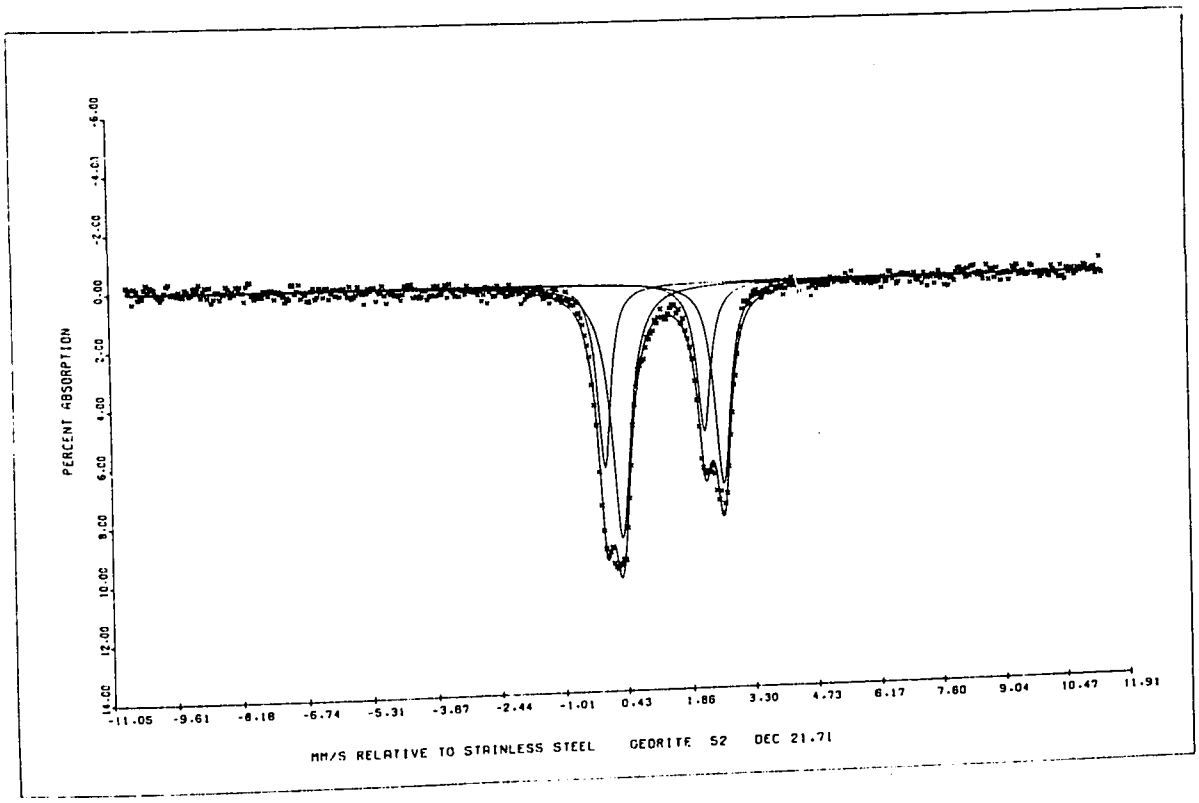

Figure 50. Mössbauer spectra of gedrite.

Appendix V

Approximate Modal Analyses of Cummingtonite Rocks

	107a	107b	173A	173A,b
Quartz	52	59	51	57
Plagioclase	12	10	12	14
Cummingtonite	28	22	31	20
Biotite	<1	6	0	5
Apatite	3	1	2	1
Ilmenite	4	2	4	3

APPENDIX VI

Table 33: List of Mineral Assemblages in the Samples Selected for Chemical Study

Sample Numbers	Mineral Assemblage
2, 4, 7	Garnet+biotite+oligoclase+ilmenite±magnetite+pyrrhotite+apatite+tourmaline±chlorite*
12, 19, 43, 89, 115	Garnet+cordierite+biotite+oligoclase+pyrrhotite+ilmenite+apatite+tourmaline±chlorite*
14, 21, 27, 32, 39A 41, 52, 74, 78, 142A & 109	Cordierite+gedrite+biotite+garnet+ilmenite±magnetite pyrrhotite+apatite+tourmaline+oligoclase+chlorite*
39, 120, 151A, 69, 171 & 197	Cordierite+biotite+pyrrhotite+ilmenite+tourmaline+apatite
3, 62, 445, 450 & SL1	Andalusite+cordierite+biotite+ilmenite+pyrrhotite+sillimanite+oligoclase+muscovite±chlorite*
24, 107A, 139A, 143A, 173A & 286	Cummingtonite+ilmenite+oligoclase±biotite±epidote+apatite±magnetite

* Retrograde Product

Table 34. Modal Composition of the Samples

	Qtz	Feld	Gar	Bio	Mus	Cor	Ged	And	Sill	Ilm	Mag	Phyr	Tour	Apt	Chlo
2	20	20	2	20	---	---	---	---	----	2	0.1	2	0.1	2	0.1
3	20	15	---	20	---	2	---	2	2	2	---	0.1	0.1	0.1	0.1
4	10	20	2	30	---	---	---	---	----	2	---	2	---	0.1	2
12	20	20	2	20	---	10	---	---	----	2	0.1	0.1	0.1	0.1	---
14	20	20	0.1	10	---	10	10	---	----	2	---	0.1	0.1	0.1	2
19	20	20	2	10	---	10	10	---	----	2	---	0.1	0.1	0.1	0.1
27	20	20	0.1	10	---	10	5	---	----	2	---	0.1	0.1	0.1	2
32	20	20	2	10	---	10	10	---	----	2	---	2	0.1	0.1	0.1
40	10	20	2	30	---	---	---	---	----	2	---	2	---	0.1	---
41	20	20	0.1	10	---	2	10	---	----	2	0.1	2	0.1	0.1	0.1
43	20	30	2	20	---	10	---	---	----	2	---	0.1	0.1	2	2
52	20	20	0.1	10	---	2	10	---	----	2	---	2	0.1	0.1	2
69	10	30	---	30	---	10	---	---	----	2	0.1	2	0.1	0.1	0.1
74	20	20	0.1	10	---	2	10	---	----	0.1	---	0.1	0.1	0.1	0.1
78	20	20	0.1	10	---	10	10	---	----	2	---	0.1	0.1	0.1	2
89	20	20	2	10	---	2	---	---	----	2	---	0.1	0.1	0.1	2

Table 34. Modal Composition of the Samples (continued)

	Quz	Feld	Gar	Bio	Mus	Cor	Ged	Amd	Sill	Ilm	Mag	Phyr	Tour	Apt	Chlo
109	20	20	0.1	10	---	10	10	---	----	2	---	2	0.1	0.1	2
115															
120	10	30	---	30	2	10	---	---	----	2	0.1	0.1	0.1	0.1	0.1
142A	20	20	2	10	---	2	2	---	----	2	0.1	0.1	0.1	0.1	0.1
143															
151A	20	20	---	30	---	20	---	---	----	2	---	0.1	0.1	0.1	2
171	10	30	---	30	---	10	---	---	----	2	---	0.1	0.1	0.1	0.1
197	10	30	---	30	---	10	---	---	----	2	---	0.1	0.1	0.1	0.1
446	10	20	---	30	2	2	---	10	2	2	---	0.1	0.1	0.1	0.1
450	10	20	---	30	10	10	---	10	2	2	---	2	0.1	0.1	0.1
SL1	10	20	---	30	2	10	---	10	2	2	---	0.1	0.1	0.1	0.1

0.1 = 0.5, 2 = 0.5-5, 10 = 5-15, 20 = 15-25, 30 = 25-35, 40 = 35-45, 50=45-55, 60=55-65

70=65-75, 80=75-85, 90=85-95, 98=95-100.

Plate 1. S_2 biotite schistosity at acute angle to S_1 (parallel to S_o)'stratiform foliation' in pelitic rocks at locality 69.

Plate 2. S_2 biotite schistosity at high angle to S_1 (parallel to S_o)'stratiform foliation' in semipelitic rocks. Locality: 1.5 Km west of Thompson Lake.

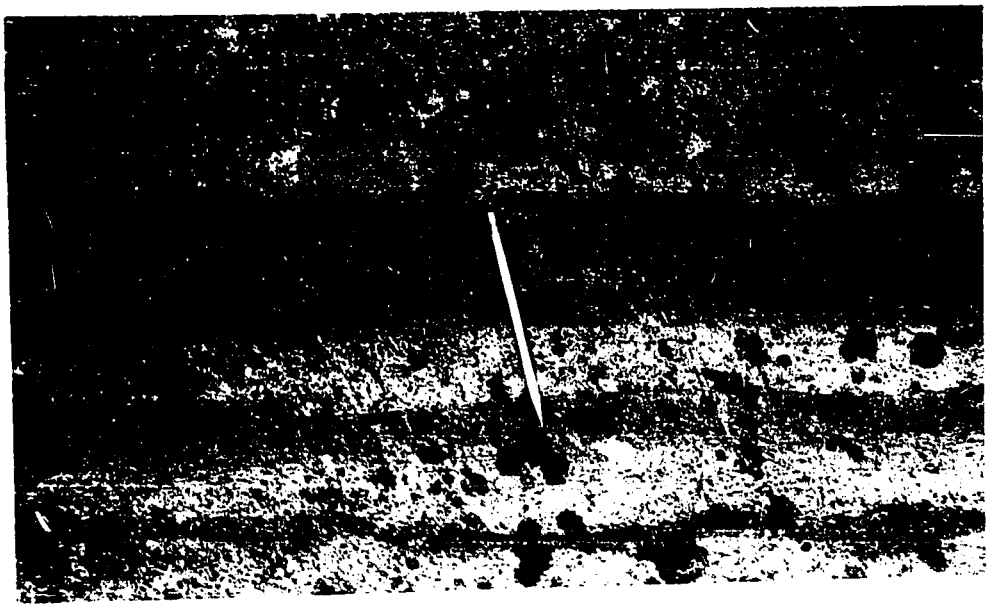

Plate 3. Zoned boudin containing cummingtonite-rich core in siliceous layer in the metasediments at locality 12.

Plate 4. Typical banding (also bedding) in the metasediments at locality 39. Dark layers are pelitic and lighter layers are psammitic.

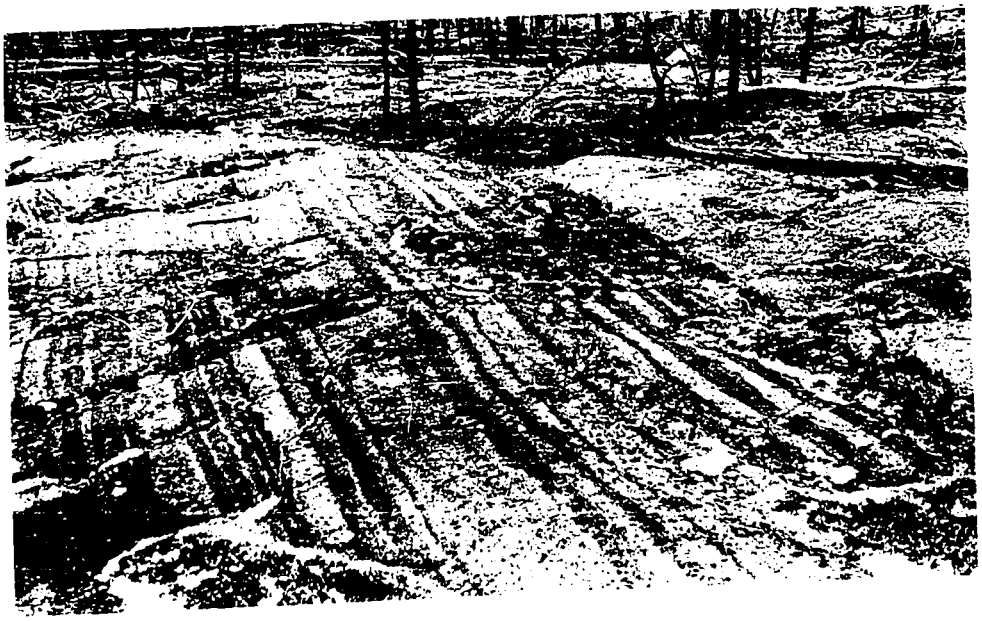

Plate 5. Gedrite crystal (Ge) partially replaced by biotite (Bi); polarized light, x 50; locality 32.

Plate 6. Random gedrite needles across S_2 schistosity (alignment of small biotite crystals); also note replacement texture in gedrite by biotite; locality 78; polarized light, x 40.

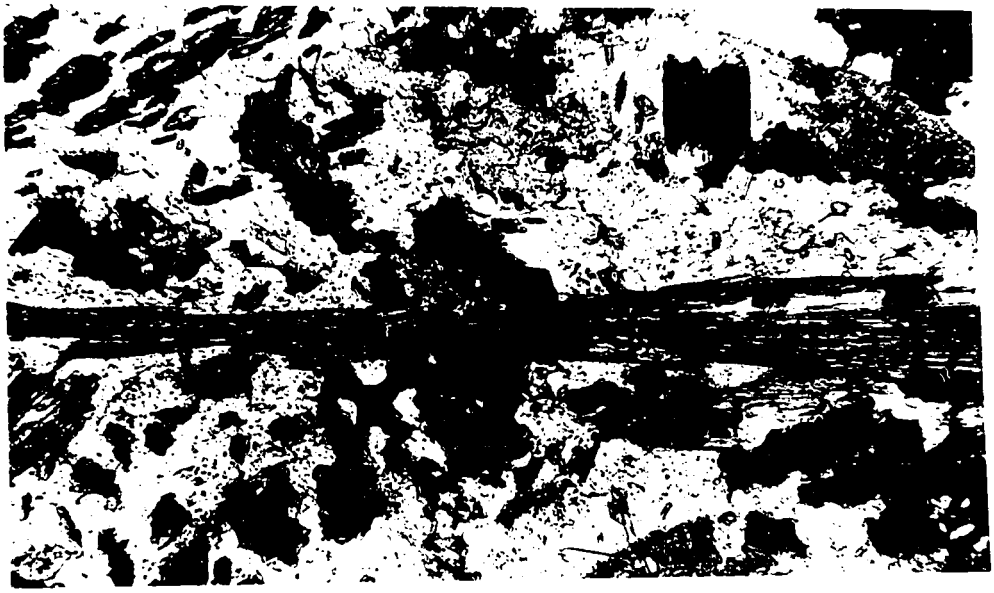


G
S2

Plate 7. Pre- or early- D_2 biotite porphyroblast flattened in S_2 biotite schistosity; polarized light, x 65; locality 286.

Plate 8. Pre- or early- D_2 cordierite porphyroblast flattened in S_2 biotite schistosity; polarized light, x 10; locality 151A.

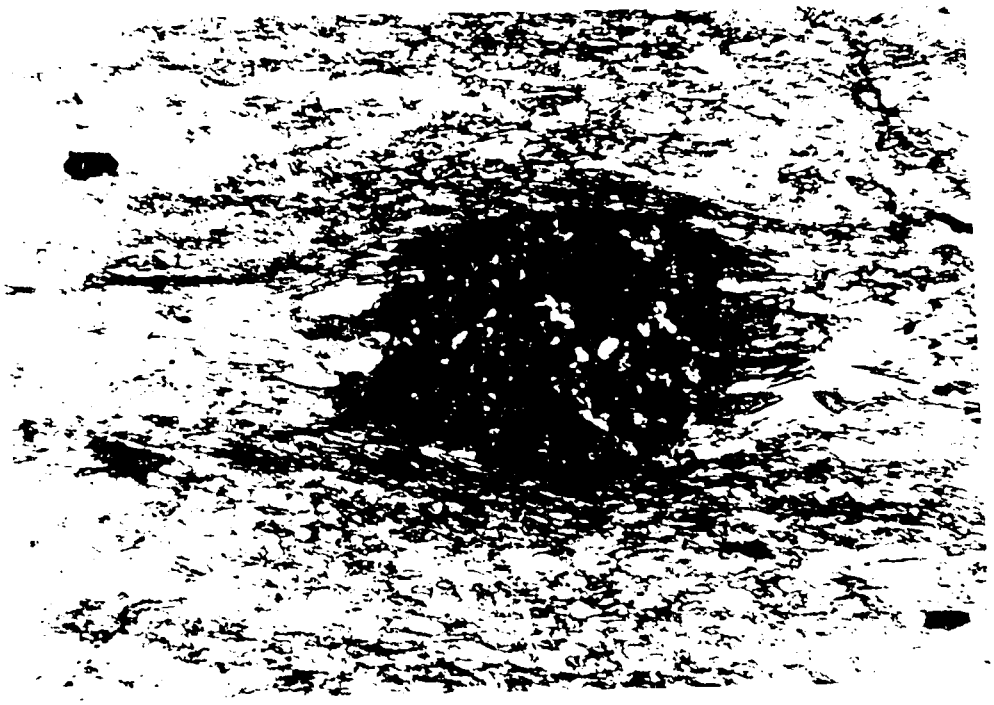

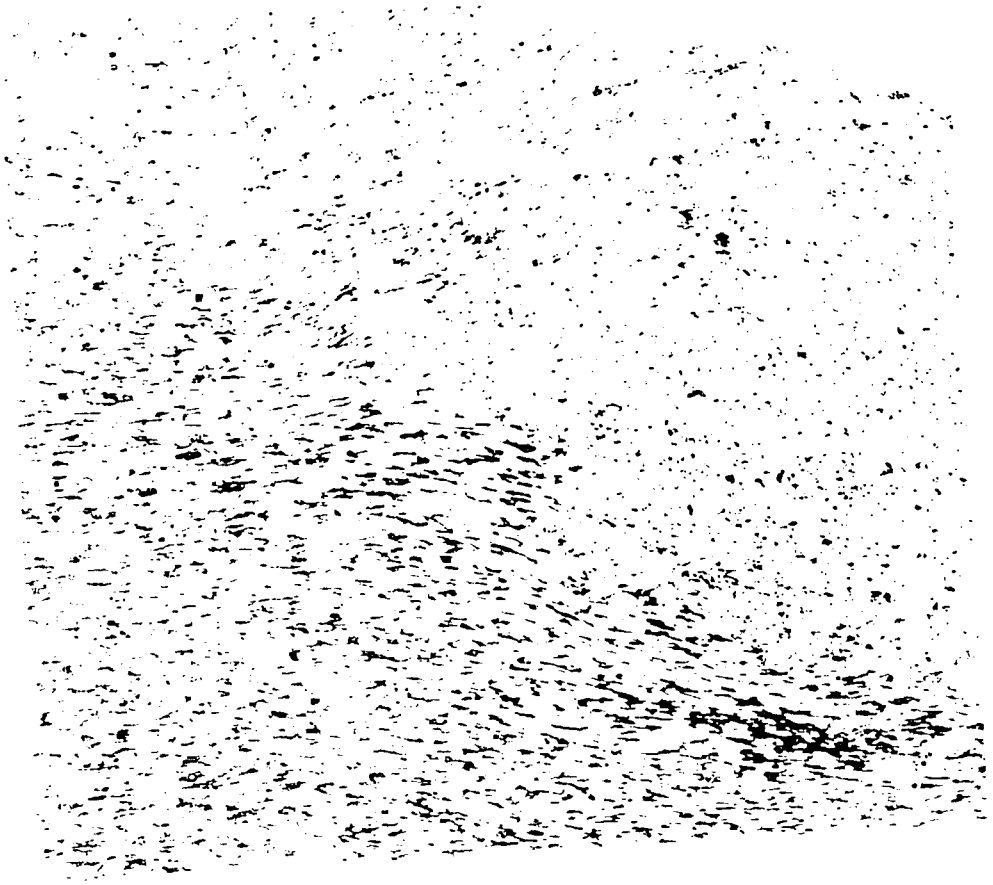

Plate 9. Cordierite (c), garnet (g), gedrite (Ge) and biotite schist; polarized light, x 40; locality 32.

Plate 10. Random cummingtonite crystals across weak S_2 biotite schistosity in siliceous concretion; polarized light, x 25; locality 143A.

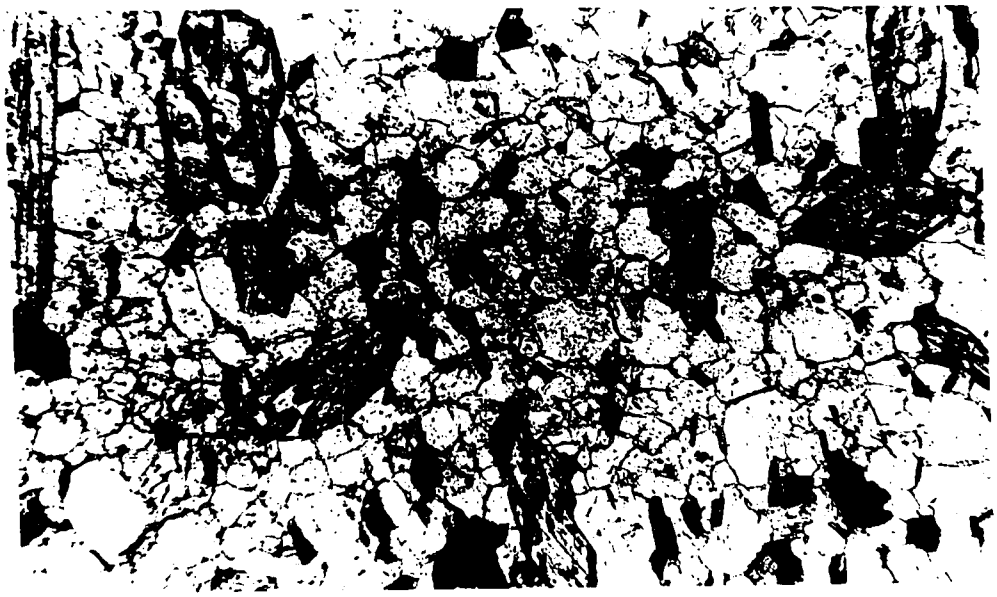

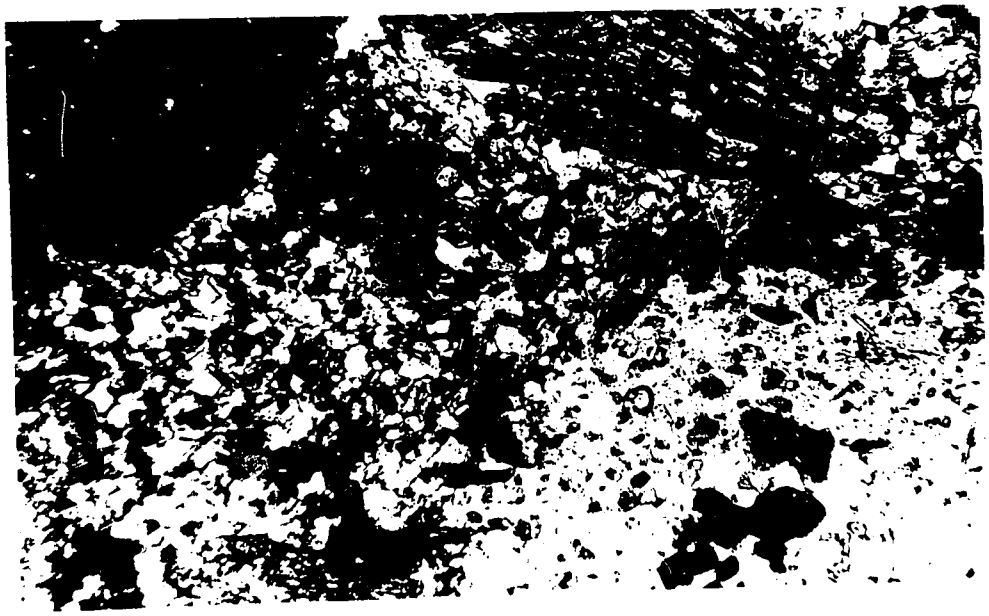

UNIVERSITE D'OTTAWA / UNIVERSITY OF OTTAWA
École des études supérieures/School of Graduate Studies

Title of thesis PETROLOGY AND GEOCHEMISTRY OF SOME ARCHEAN METAMORPHIC ROCKS NEAR YELLOWKNIFE DISTRICT OF MACKENZIE

Name of candidate KAMINENI, Dayananda Choudari

Degree Ph.D. Department Geology

Date of defence June 13th, 1973

We, the undersigned, certify that we have approved this thesis and that the candidate has defended it successfully.

W.K. Fyson (Signature of Examiners)

D.D. Hogarth

A. Miyashiro (not present at the defence)

A.J. Baer

R. Kretz (Thesis Supervisor)

(Dean of Graduate Studies)

UNIVERSITÉ D'OTTAWA / UNIVERSITY OF OTTAWA
École des études supérieures/School of Graduate Studies

NAME OF AUTHOR KAMINENI, Dayananda Choudari

TITLE OF THESIS PETROLOGY AND GEOCHEMISTRY OF SOME ARCHEAN METAMORPHIC ROCKS NEAR YELLOWKNIFE DISTRICT OF MACKENZIE

DEGREE Ph.D. (Geology) YEAR GRANTED 1973

D C Kamineni
(Signed) (Author)

Date: June 13th, 1973

Permanent Address:
80 Manor Ave
#4 ottawa K1N6Y5
ont. Canada